

AD-299033

**ACOUSTIC NOISE AND VIBRATION STUDIES  
AT  
CAPE CANAVERAL MISSILE TEST ANNEX**

**VOLUME II, VIBRATION**

Robert P. Boyd

TECHNICAL REPORT NO. ASD-TR-61-608, VOLUME II

January 1963

Deputy Commander/Test and Support  
Aeronautical Systems Division  
Air Force Systems Command  
Wright-Patterson Air Force Base, Ohio

Project No. 1309, Task No. 130905

20070919070

## NOTICES

When Government drawings, specifications, or other data are used for any purpose other than in connection with a definitely related Government procurement operation, the United States Government thereby incurs no responsibility nor any obligation whatsoever; and the fact that the Government may have formulated, furnished, or in any way supplied the said drawings, specifications, or other data, is not to be regarded by implication or otherwise as in any manner licensing the holder or any other person or corporation, or conveying any rights or permission to manufacture, use, or sell any patented invention that may in any way be related thereto.

Qualified requesters may obtain copies of this report from the Armed Services Technical Information Agency, (ASTIA), Arlington Hall Station, Arlington 12, Virginia.

This report has been released to the Office of Technical Services, U.S. Department of Commerce, Washington 25, D.C., in stock quantities for sale to the general public.

Copies of this report should not be returned to the Aeronautical Systems Division unless return is required by security considerations, contractual obligations, or notice on a specific document.

## FOREWORD

This report, Volume II of "Acoustic Noise and Vibration Studies at Cape Canaveral, Florida," pertaining to the Vibration Study was prepared by the Environmental Criteria Branch, Environmental Division, Directorate of Engineering Test, Deputy for Test and Support, Wright-Patterson AFB, Ohio. The work was performed under AFSC Task 723104 entitled "Biodynamic Environments of Aerospace Flight Operations" and AFSC Task 130905 entitled "Measurement and Analysis of Induced Environments." The data presented was measured by the Aeronautical Systems Division Survey team at the request of the Directorate of Range Development (MTL), Cape Canaveral Missile Test Annex, Air Force Missile Test Center, Patrick AFB, Florida. The project was supported under Atlantic Missile Range Operations Directive 058.

Field measurements were conducted during the period of 7 July 1961 through 17 November 1961. ASD personnel who participated in this survey are J. N. Cole, R. T. England, H. K. Hille, and R. G. Powell of the Bio-acoustic Branch, Aerospace Medical Research Laboratories (conducting the acoustic portion of the studies) and R. P. Boyd, G. A. Plzak, H. K. Reich, and C. E. Thomas of the Environmental Criteria Branch, Directorate of Engineering Test (conducting the vibration portion of the studies).

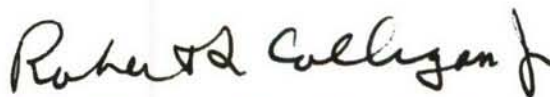
Appreciation is expressed to the many organizations that supported this survey program, including: the Directorates of Range Development (MTL) and Range Operations (MTR), the Air Force Missile Test Center, Patrick AFB, Florida; Pan American Airways Inc.; and the Radio Corporation of America.



## ABSTRACT

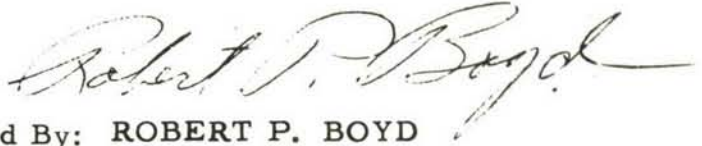
Acoustic-noise-induced vibrational effects upon seven antenna structures were recorded during fourteen missile launches at Cape Canaveral Missile Test Annex (CCMTA). Vibrational effects were recorded within the frequency range between 3 and 2000 cycles per second. Maximum vibrations encountered per one-third octave frequency band are presented in this report along with findings on the relationship of vibration levels to acoustic noise. All vibration levels measured in this test series were relatively low, changed in direct proportion to sound-pressure levels, and provided experimental substantiation for predicting increases in structural acceleration levels based on predicted increases in acoustic levels resulting from more powerful rocket engines.

This technical documentary report has been reviewed and is approved.



ROBERT L. COLLIGAN, JR.  
Colonel, USAF  
Deputy for Test and Support





Prepared By: ROBERT P. BOYD  
Project Engineer



Concurred in: <sup>for</sup> LOUIS SCHAFFER  
Colonel, USAF  
Director of Engineering Test  
Deputy for Test and Support



Concurred in: HUGH S. LIPPMAN  
Technical Director  
Deputy for Test and Support



Approved by: ROBERT L. COLLIGAN, JR.  
Colonel, USAF  
Deputy for Test and Support

## TABLE OF CONTENTS

<u>Section</u>		<u>Page</u>
I	Introduction .....	1
II	Discussion .....	1
	A. Test Procedure .....	1
	B. Test Instrumentation .....	5
	C. Presentation of Data .....	9
	D. Analysis of Data .....	10
III	Test Results .....	11
IV	Conclusions .....	14
	Appendix: Graphic Presentation of Data .....	15

## LIST OF ILLUSTRATIONS

<u>Figure</u>		<u>Page</u>
1	Cape Canaveral Test Site showing location of three test areas with respect to launch complexes .....	2
2	Accelerometer installation on 80-Foot Communications Antenna .....	3
3	Accelerometer installation on Tri-Helix No. 4 Antenna ...	3
4	Tel-2 Area showing general view of (1) 80-Foot Communications Antenna, (2) Tri-Helix No. 4 Antenna, and (3) TLM 18 Antenna.....	3
5	Accelerometer Installation on TLM 18 Antenna Dish.....	3
6	Accelerometer Installation on TLM 18 Antenna Pod .....	3
7	Accelerometer Installation on NASA Steerable Helix Array .....	4
8	Accelerometer Installation on Gabriel Antenna .....	4
9	Command Destruct Area showing general view of (1) NASA Steerable Helix Array, (2) Gabriel Antenna, and (3) RCA Tx Steerable Antenna .....	4
10	Accelerometer Installation on RCA Tx Steerable Antenna Dish.....	4
11	Accelerometer Installation on RCA Tx Steerable Antenna Pod .....	4
12	Azusa MK I Area showing X <sub>C</sub> Receiving Antenna .....	5
13	Accelerometer Installation on X <sub>C</sub> Receiving Antenna Dish	5
14	Accelerometer Installation on X <sub>C</sub> Receiving Antenna Pedestal	5
15	Schematic Diagram of Vibration Sensing and Recording Instrumentation .....	7
16	Schematic Diagram of Vibration Playback and Analyzing Instrumentation .....	8



# LIST OF ILLUSTRATIONS

<u>Figure</u>		<u>Page</u>
	<u>Summary Plots for Individual Vibration Pickups</u>	
17	Test No: 1251. Location: Tel-2, On 80-Foot Communication Antenna, Vertical Axis.....	16
18	Test No: 1251. Location: Tel-2, On 80-Foot Communication Antenna, Lateral Axis .....	16
19	Test No: 1251. Location: Tel-2, On 80-Foot Communication Antenna, Fore/Aft Axis .....	16
20	Test No: 1251. Location: Tel-2, On Tri-Helix No. 4, Vertical Axis.....	17
21	Test No: 1251. Location: Tel-2, On Tri-Helix No. 4, Lateral Axis .....	17
22	Test No: 1251. Location: Tel-2, On Tri-Helix No. 4, Fore/Aft Axis .....	17
23	Test No: 1251. Location: Tel-2, On TLM-18 Antenna Dish, Vertical Axis .....	18
24	Test No: 1251. Location: Tel-2, On TLM-18 Antenna Dish, Lateral Axis.....	18
25	Test No: 1251. Location: Tel-2, On TLM-18 Antenna Dish, Fore/Aft Axis .....	18
26	Test No: 1251. Location: Tel-2, On TLM-18 Antenna Pod, Vertical Axis.....	19
27	Test No: 1251. Location: Tel-2, On TLM-18 Antenna Pod, Lateral Axis .....	19
28	Test No: 1251. Location: Tel-2, On TLM-18 Antenna Pod, Fore/Aft Axis .....	19
29	Test No: 3211. Location: Tel-2, On 80-Foot Communication Antenna, Vertical Axis .....	20
30	Test No: 3211. Location: Tel-2, On 80-Foot Communication Antenna, Lateral Axis .....	20
31	Test No: 3211. Location: Tel-2, On 80-Foot Communication Antenna, Fore/Aft Axis .....	20

# LIST OF ILLUSTRATIONS

<u>Figure</u>		<u>Page</u>
32	Test No: 3211. Location: Tel-2, On Tri-Helix No. 4, Vertical Axis.....	21
33	Test No: 3211. Location: Tel-2, On Tri-Helix No. 4, Lateral Axis .....	21
34	Test No: 3211. Location: Tel-2, On Tri-Helix No. 4, Fore/Aft Axis .....	21
35	Test No: 3211. Location: Tel-2, On TLM-18 Antenna Dish Vertical Axis .....	22
36	Test No: 3211. Location: Tel-2, On TLM-18 Antenna Dish Lateral Axis .....	22
37	Test No: 3211. Location: Tel-2, On TLM-18 Antenna Dish Fore/Aft Axis .....	22
38	Test No: 3211. Location: Tel-2, On TLM-18 Antenna Pod Vertical Axis.....	23
39	Test No: 3211. Location: Tel-2, On TLM-18 Antenna Pod Lateral Axis .....	23
40	Test No: 3211. Location: Tel-2, On TLM-18 Antenna Pod Fore/Aft Axis .....	23
41	Test No: 5454. Location: Tel-2, On Tri-Helix No. 4, Vertical Axis.....	24
42	Test No: 5454. Location: Tel-2, On Tri-Helix No. 4, Lateral Axis .....	24
43	Test No: 5454. Location: Tel-2, On Tri-Helix No. 4, Fore/Aft Axis .....	24
44	Test No: 5454. Location: Tel-2, On TLM-18 Antenna Dish, Vertical Axis .....	25
45	Test No: 5454. Location: Tel-2, On TLM-18 Antenna Dish, Lateral Axis.....	25
46	Test No: 5454. Location: Tel-2, On TLM-18 Antenna Dish, Fore/Aft Axis .....	25

# LIST OF ILLUSTRATIONS

<u>Figure</u>		<u>Page</u>
47	Test No: 5454. Location: Tel-2, On TLM-18 Antenna Pod, Vertical Axis .....	26
48	Test No: 5454. Location: Tel-2, On TLM-18 Antenna Pod, Lateral Axis .....	26
49	Test No: 5454. Location: Tel-2, On TLM-18 Antenna Pod, Fore/Aft Axis.....	26
50	Test No: 4508. Location: Tel-2, On Tri-Helix No. 4, Vertical Axis .....	27
51	Test No: 4508. Location: Tel-2, On Tri-Helix No. 4, Lateral Axis .....	27
52	Test No: 4508. Location: Tel-2, On Tri-Helix No. 4, Fore/Aft Axis.....	27
53	Test No: 4508. Location: Tel-2, On Spar Attachment Point of TLM-18, Vertical Axis.....	28
54	Test No: 4508. Location: Tel-2, On Spar Attachment Point of TLM-18, Lateral Axis.....	28
55	Test No: 4508. Location: Tel-2, On Spar Attachment Point of TLM-18, Fore/Aft Axis .....	28
56	Test No: 4508. Location: Tel-2, On TLM-18 Antenna Pod, Vertical Axis.....	29
57	Test No: 4508. Location: Tel-2, On TLM-18 Antenna Pod, Lateral Axis .....	29
58	Test No: 4508. Location: Tel-2, On TLM-18 Antenna Pod, Fore/Aft Axis .....	29
59	Test No: 1805. Location: Command Destruct, At Base of Gabriel Antenna, Vertical Axis .....	30
60	Test No: 1805. Location: Command Destruct, At Base of Gabriel Antenna, Lateral Axis .....	30
61	Test No: 1805. Location: Command Destruct, at Base of Gabriel Antenna, Fore/Aft Axis.....	30



# LIST OF ILLUSTRATIONS

<u>Figure</u>		<u>Page</u>
62	Test No: 1805. Location: Command Destruct, On Dish of RCA Tx. Steerable Antenna, Vertical Axis .....	31
63	Test No: 1805. Location: Command Destruct, On Dish of RCA Tx. Steerable Antenna, Lateral Axis.....	31
64	Test No: 1805. Location: Command Destruct, On Dish of RCA Tx. Steerable Antenna, Fore/Aft Axis.....	31
65	Test No: 1805. Location: Command Destruct, On Pod of RCA Tx. Steerable Antenna, Vertical Axis .....	32
66	Test No: 1805. Location: Command Destruct, On Pod of RCA Tx. Steerable Antenna, Lateral Axis .....	32
67	Test No: 1805. Location: Command Destruct, On Pod of RCA Tx. Steerable Antenna, Fore/Aft Axis .....	32
68	Test No: 1811. Location: Command Destruct, On Steerable Helix Array, Vertical Axis .....	33
69	Test No: 1811. Location: Command Destruct, On Steerable Helix Array, Lateral Axis.....	33
70	Test No: 1811. Location: Command Destruct, On Steerable Helix Array, Fore/Aft Axis .....	33
71	Test No: 1811. Location: Command Destruct, On Base of Gabriel Antenna, Vertical Axis .....	34
72	Test No: 1811. Location: Command Destruct, On Base of Gabriel Antenna, Lateral Axis .....	34
73	Test No: 1811. Location: Command Destruct, On Base of Gabriel Antenna, Fore/Aft Axis .....	34
74	Test No: 1811. Location: Command Destruct, On Dish of RCA Tx. Steerable Antenna, Vertical Axis .....	35
75	Test No: 1811. Location: Command Destruct, On Dish of RCA Tx. Steerable Antenna, Lateral Axis.....	35
76	Test No: 1811. Location: Command Destruct, On Dish of RCA Tx. Steerable Antenna, Fore/Aft Axis.....	35

# LIST OF ILLUSTRATIONS

<u>Figure</u>		<u>Page</u>
77	Test No: 1811. Location: Command Destruct, On Pod of RCA Tx. Steerable Antenna, Vertical Axis .....	36
78	Test No: 1811. Location: Command Destruct, On Pod of RCA Tx. Steerable Antenna, Lateral Axis.....	36
79	Test No: 1811. Location: Command Destruct, On Pod of RCA Tx. Steerable Antenna, Fore/Aft Axis .....	36
80	Test No: 5050. Location: Command Destruct, On Steerable Helix Array, Vertical Axis .....	37
81	Test No: 5050. Location: Command Destruct, On Steerable Helix Array, Lateral Axis.....	37
82	Test No: 5050. Location: Command Destruct, On Steerable Helix Array, Fore/Aft Axis .....	37
83	Test No: 5050. Location: Command Destruct, at Base of Gabriel Antenna, Vertical Axis.....	38
84	Test No: 5050. Location: Command Destruct, at Base of Gabriel Antenna, Lateral Axis .....	38
85	Test No: 5050. Location: Command Destruct, at Base of Gabriel Antenna, Fore/Aft Axis .....	38
86	Test No: 5050. Location: Command Destruct, On Dish of RCA Tx. Steerable Antenna, Vertical Axis .....	39
87	Test No: 5050. Location: Command Destruct, On Dish of RCA Tx. Steerable Antenna, Lateral Axis.....	39
88	Test No: 5050. Location: Command Destruct, On Dish of RCA Tx. Steerable Antenna, Fore/Aft Axis .....	39
89	Test No: 5050. Location: Command Destruct, On Pod of RCA Tx. Steerable Antenna, Vertical Axis .....	40
90	Test No: 5050. Location: Command Destruct, On Pod of RCA Tx. Steerable Antenna, Lateral Axis .....	40
91	Test No: 5050. Location: Command Destruct, On Pod of RCA Tx. Steerable Antenna, Fore/Aft Axis .....	40

# LIST OF ILLUSTRATIONS

<u>Figure</u>		<u>Page</u>
92	Test No: 1262. Location: Command Destruct, On Steerable Helix Array, Vertical Axis .....	41
93	Test No: 1262. Location: Command Destruct, On Steerable Helix Array, Lateral Axis.....	41
94	Test No: 1262. Location: Command Destruct, On Steerable Helix Array, Fore/Aft Axis .....	41
95	Test No: 1262. Location: Command Destruct, At Base of Gabriel Antenna, Vertical Axis .....	42
96	Test No: 1262. Location: Command Destruct, At Base of Gabriel Antenna, Lateral Axis .....	42
97	Test No: 1262. Location: Command Destruct, At Base of Gabriel Antenna, Fore/Aft Axis .....	42
98	Test No: 1262. Location: Command Destruct, On Dish of Steerable Tx. Antenna, Vertical Axis .....	43
99	Test No: 1262. Location: Command Destruct, On Dish of Steerable Tx. Antenna, Lateral Axis.....	43
100	Test No: 1262. Location: Command Destruct, On Dish of Steerable Tx. Antenna, Fore/Aft Axis .....	43
101	Test No: 1262. Location: Command Destruct, On Pod of RCA Steerable Tx. Antenna, Vertical Axis .....	44
102	Test No: 1262. Location: Command Destruct, On Pod of RCA Steerable Tx. Antenna, Lateral Axis .....	44
103	Test No: 1262. Location: Command Destruct, On Pod of RCA Steerable Tx. Antenna, Fore/Aft Axis .....	44
104	Test No: 3212. Location: Command Destruct, On Steerable Helix Array, Vertical Axis .....	45
105	Test No: 3212. Location: Command Destruct, On Steerable Helix Array, Lateral Axis.....	45
106	Test No: 3212. Location: Command Destruct, On Steerable Helix Array, Fore/Aft Axis.....	45



# LIST OF ILLUSTRATIONS

<u>Figure</u>		<u>Page</u>
107	Test No: 3212. Location: Command Destruct, On Base of Gabriel Antenna, Vertical Axis .....	46
108	Test No: 3212. Location: Command Destruct, On Base of Gabriel Antenna, Lateral Axis .....	46
109	Test No: 3212. Location: Command Destruct, On Base of Gabriel Antenna, Fore/Aft Axis .....	46
110	Test No: 3212. Location: Command Destruct, On Dish of RCA Steerable Tx. Antenna, Vertical Axis .....	47
111	Test No: 3212. Location: Command Destruct, On Dish of RCA Steerable Tx. Antenna, Lateral Axis .....	47
112	Test No: 3212. Location: Command Destruct, On Dish of RCA Steerable Tx. Antenna, Fore/Aft Axis .....	47
113	Test No: 3212. Location: Command Destruct, On Pod of RCA Steerable Tx. Antenna, Vertical Axis .....	48
114	Test No: 3212. Location: Command Destruct, On Pod of RCA Steerable Tx. Antenna, Lateral Axis .....	48
115	Test No: 3212. Location: Command Destruct, On Pod of RCA Steerable Tx. Antenna, Fore/Aft Axis .....	48
116	Test No: 1803. Location: Command Destruct, On Steerable Helix Array, Vertical Axis .....	49
117	Test No: 1803. Location: Command Destruct, On Steerable Helix Array, Lateral Axis .....	49
118	Test No: 1803. Location: Command Destruct, On Steerable Helix Array, Fore/Aft Axis .....	49
119	Test No: 1803. Location: Command Destruct, On Base of Gabriel Antenna, Vertical Axis .....	50
120	Test No: 1803. Location: Command Destruct, On Base of Gabriel Antenna, Lateral Axis .....	50
121	Test No: 1803. Location: Command Destruct, On Base of Gabriel Antenna, Fore/Aft Axis .....	50

## LIST OF ILLUSTRATIONS

<u>Figure</u>		<u>Page</u>
122	Test No: 1803. Location: Command Destruct, On Dish of RCA Steerable Tx. Antenna, Vertical Axis .....	51
123	Test No: 1803. Location: Command Destruct, On Dish of RCA Steerable Tx. Antenna, Lateral Axis.....	51
124	Test No: 1803. Location: Command Destruct, On Dish of RCA Steerable Tx. Antenna, Fore/Aft Axis .....	51
125	Test No: 1803. Location: Command Destruct, On Pod of RCA Steerable Tx. Antenna, Vertical Axis .....	52
126	Test No: 1803. Location: Command Destruct, On Pod of RCA Steerable Tx. Antenna, Lateral Axis.....	52
127	Test No: 1803. Location: Command Destruct, On Pod of RCA Steerable Tx. Antenna, Fore/Aft Axis .....	52
128	Test No: 3765. Location: Azusa MKI, On Pedestal of X <sub>C</sub> Receiving Antenna, Vertical Axis.....	53
129	Test No: 3765. Location: Azusa MKI, On Pedestal of X <sub>C</sub> Receiving Antenna, Lateral Axis .....	53
130	Test No: 3765. Location: Azusa MKI, On Pedestal of X <sub>C</sub> Receiving Antenna, Fore/Aft Axis .....	53
131	Test No: 3765. Location: Azusa MKI, On Dish of X <sub>C</sub> Receiving Antenna, Vertical Axis .....	54
132	Test No: 3765. Location: Azusa MKI, On Dish of X <sub>C</sub> Receiving Antenna, Lateral Axis .....	54
133	Test No: 3765. Location: Azusa MKI, On Dish of X <sub>C</sub> Receiving Antenna, Fore/Aft Axis .....	54
134	Test No: 1252. Location: Azusa MKI, On Pedestal of X <sub>C</sub> Receiving Antenna, Vertical Axis .....	55
135	Test No: 1252. Location: Azusa MKI, On Pedestal of X <sub>C</sub> Receiving Antenna, Lateral Axis .....	55
136	Test No: 1252. Location: Azusa MKI, On Pedestal of X <sub>C</sub> Receiving Antenna, Fore/Aft Axis .....	55

# LIST OF ILLUSTRATIONS

<u>Figure</u>		<u>Page</u>
137	Test No: 1252. Location: Azusa MKI, On Dish of $X_c$ Receiving Antenna, Vertical Axis .....	56
138	Test No: 1252. Location: Azusa MKI, On Dish of $X_c$ Receiving Antenna, Lateral Axis .....	56
139	Test No: 1252. Location: Azusa MKI, On Dish of $X_c$ Receiving Antenna, Fore/Aft Axis .....	56
140	Test No: 1804. Location: Azusa MKI, On Pedestal of $X_c$ Receiving Antenna, Vertical Axis .....	57
141	Test No: 1804. Location: Azusa MKI, On Pedestal of $X_c$ Receiving Antenna, Lateral Axis.....	57
142	Test No: 1804. Location: Azusa MKI, On Pedestal of $X_c$ Receiving Antenna, Fore/Aft Axis .....	57
143	Test No: 1804. Location: Azusa MKI, On Dish of $X_c$ Receiving Antenna, Vertical Axis .....	58
144	Test No: 1804. Location: Azusa MKI, On Dish of $X_c$ Receiving Antenna, Lateral Axis :.....	58
145	Test No: 1804. Location: Azusa MKI, On Dish of $X_c$ Receiving Antenna, Fore/Aft Axis .....	58
146	Test No: 3764. Location: Azusa MKI, On Pedestal of $X_c$ Receiving Antenna, Vertical Axis .....	59
147	Test No: 3764. Location: Azusa MKI, On Pedestal of $X_c$ Receiving Antenna, Lateral Axis.....	59
148	Test No: 3764. Location: Azusa MKI, On Pedestal of $X_c$ Receiving Antenna, Fore/Aft Axis.....	59
149	Test No: 3764. Location: Azusa MKI, On Dish of $X_c$ Receiving Antenna, Vertical Axis .....	60
150	Test No: 3764. Location: Azusa MKI, On Dish of $X_c$ Receiving Antenna, Lateral Axis .....	60
151	Test No: 3764. Location: Azusa MKI, On Dish of $X_c$ Receiving Antenna, Fore/Aft Axis .....	60



## LIST OF ILLUSTRATIONS

<u>Figure</u>		<u>Page</u>
	<u>Special Study Plots</u>	
152	Maximum Vibration Level vs Maximum Sound Pressure Level, Steerable Tx Antenna Dish, 200 cycle 1/3 Octave Center Frequency Band, Fore/Aft Direction.....	61
153	Maximum Vibration Level vs Maximum Sound Pressure Level, TLM 18 Antenna Dish, 100 cycle 1/3 Octave Center Frequency Band, Lateral Direction.....	62
154	DB Vibration Change per db Noise change: Results of 136 measurements of the Maximum Vibration and Noise Produced at a Measurement Point during various Missile Launches .....	63
155	Test No. 4508, Tel-2, Tri-Helix No. 4, Sound Pressure Level vs Time, 300-600 CPS .....	64
156	Test No. 4508, Tel-2, Tri-Helix No. 4, Sound Pressure Level vs Time, 600-1200 CPS .....	64
157	Test No. 4508, Tel-2, Tri-Helix No. 4, Vibration Level vs Time, 282-565 CPS .....	64
158	Test No. 4508, Tel-2, Tri-Helix No. 4, Vibration Level vs Time, 565-1125 CPS .....	64
159	DB Vibration Decay per db Noise Decay: Results of 198 Measurements During Missile Launch .....	65
160	DB Vibration Level change per db Noise Level Change: Accumulative Results of 334 Measurements showing percentage of instances in indicated ranges .....	66

## SECTION I

### INTRODUCTION

The Directorate of Range Development at Cape Canaveral Missile Test Annex was concerned about community response to the acoustic noise generated during missile launches and about the possible destructive vibrational effects upon antenna and other structures at the Missile Test Annex. Concern extended beyond current missiles to the potential effects of more powerful missiles of the future. For these reasons this series of acoustic and vibration studies were conducted.

The objectives of the vibration portion of the study were to survey selected ground-support facilities at Cape Canaveral to determine two sets of facts: first, the magnitude of vibrational effects upon representative tracking and telemetry antennas acoustically induced during present-day missile launching; and second, a means of predicting the vibration resulting from higher acoustic noise levels occurring during launching of larger missiles of the future. In this second objective, predicted vibration levels are based upon predicted acoustic noise levels and prediction procedures outlined in Volume I of this report.

## SECTION II

### DISCUSSION

#### A. Test Procedure

Seven representative far-field antenna structures were selected for the measurement of noise-induced vibration produced by the acoustical noise generated during the launching of several types of missiles from various locations on the Cape Canaveral Missile Test Annex (CCMTA).

Vibration measurement areas selected were Tel-2, Command Destruct, and Azusa MK I. The relative position of the areas with respect to missile launch pads is portrayed in Figure 1.

Vibration measurements at the Tel-2 area were made on three antennas: (1) 80' communications, (2) Tri-Helix #4 and (3) TLM-18, identified in Figure 4. Figures 2, 3, 5 and 6 show the test point locations and method of installing the vibration sensing accelerometers. At each test point three accelerometers were mounted on a rigid insulating block attachment with their axes of sensitivity aligned in three mutually perpendicular directions: vertical, lateral, and fore/aft. In general, the fore/aft direction was horizontal in line with the direction of missile sound propagation at missile launch time (T-O). In cases of missile-tracking antennas, such as the TLM-18, the defined fore/aft direction follows the direction of sound propagation.

At the Command Destruct Area vibration measurements were made on three (3) antennas: (1) NASA Steerable Helix Array, (2) Gabriel and (3) RCA Tx Steerable. Figures 7 to 11 portray a general view of the three

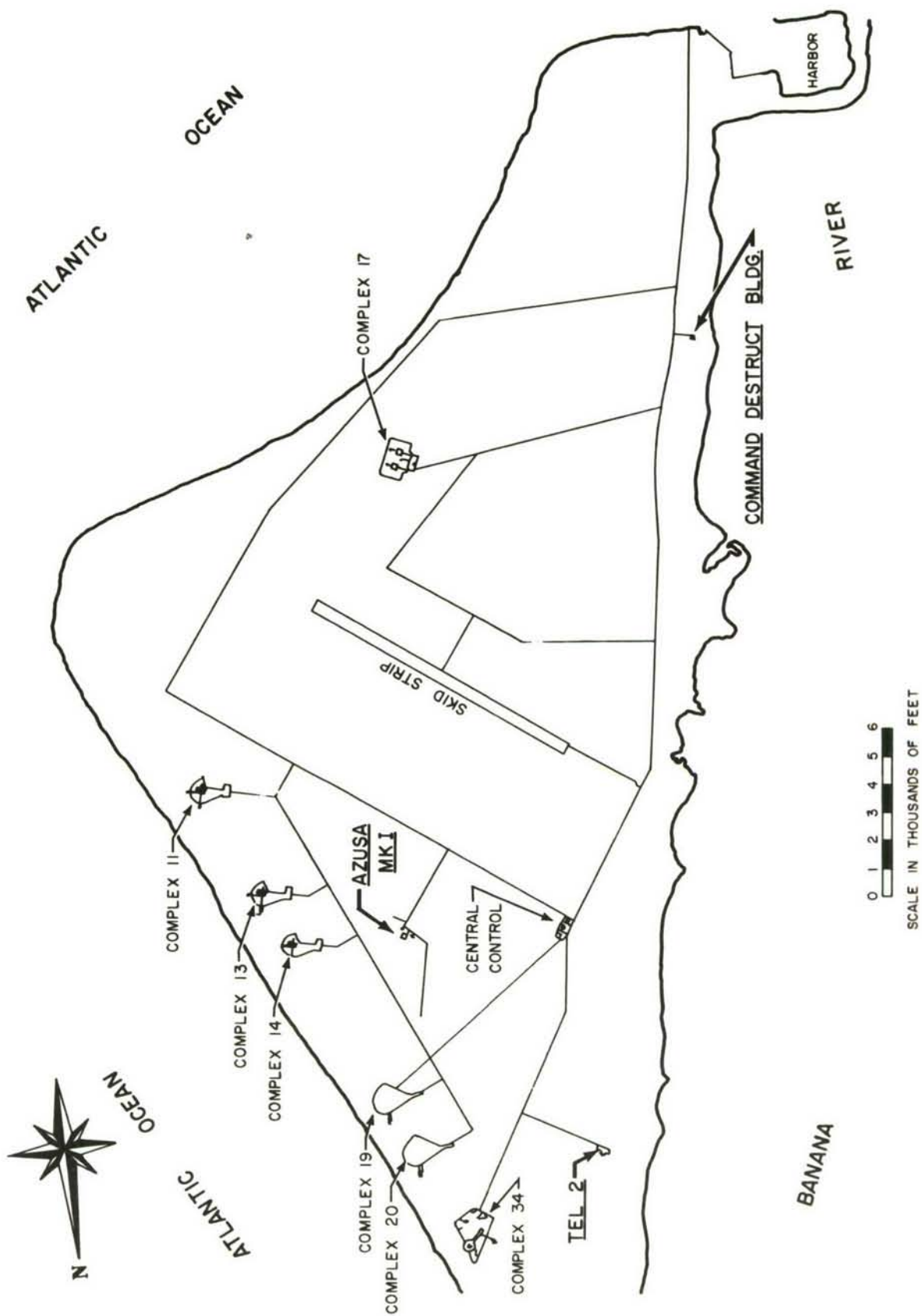


Figure 1. Cape Canaveral Test Site Showing Location of Three Test Areas with Respect to Launch Complexes.



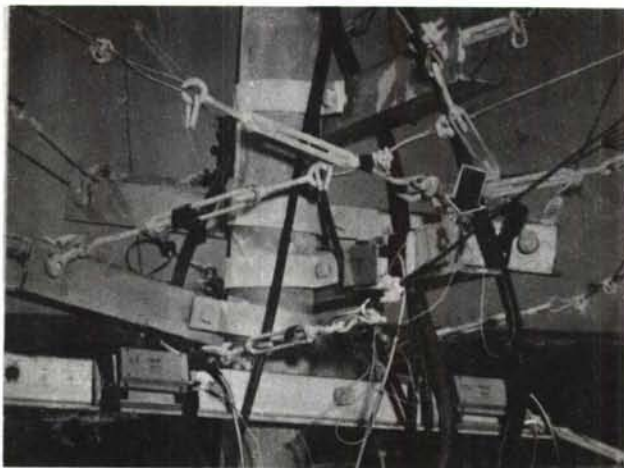


Figure 2. Accelerometer Installation  
80-Ft. Communications Antenna.



Figure 3. Accelerometer Installation  
Tri-Helix No. 4 Antenna



Figure 4.

Tel-2 Area Showing  
general view of  
(1) 80-Ft. Communication  
Antenna,  
(2) Tri-Helix No. 4  
Antenna, and  
(3) TLM 18 Antenna.

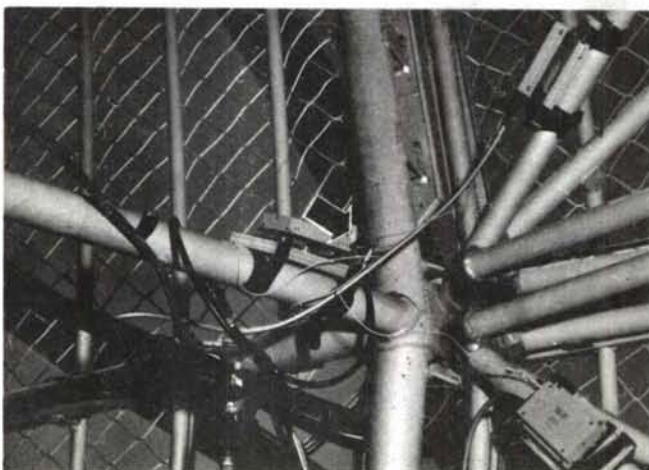


Figure 5. Accelerometer Installation  
TLM 18 Antenna Dish.

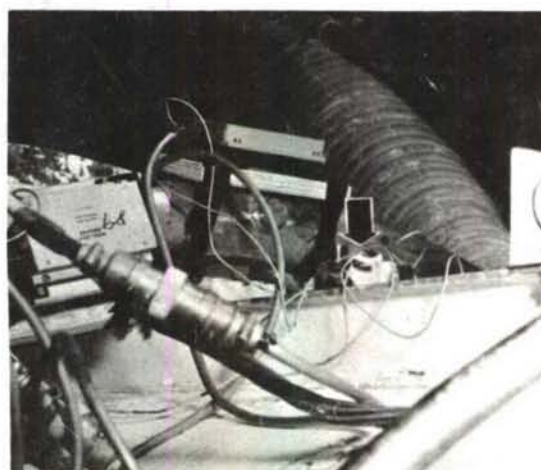


Figure 6. Accelerometer Installation  
TLM 18 Antenna Pod.



Figure 7. Accelerometer Installation  
NASA Steerable Helix Array.

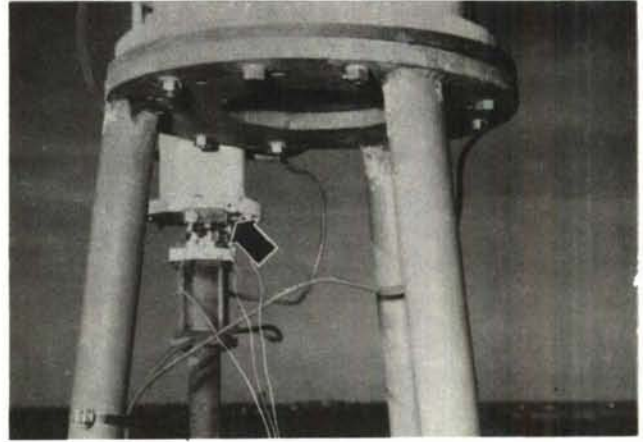


Figure 8. Accelerometer Installation  
Gabriel Antenna.



Figure 9.

Command Destruct  
Area showing gene-  
ral view of  
(1) NASA Steerable  
Helix Array,  
(2) Gabriel Antenna,  
and (3) RCA Tx  
Steerable Antenna



Figure 10. Accelerometer Installation  
RCA Tx Steerable Antenna Dish.

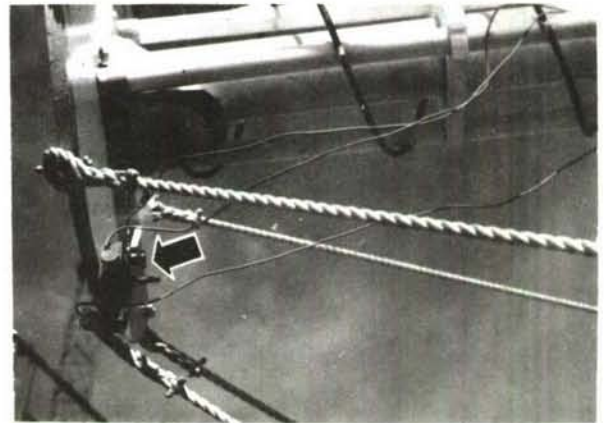


Figure 11. Accelerometer Installation  
RCA Tx Steerable Antenna Pod.



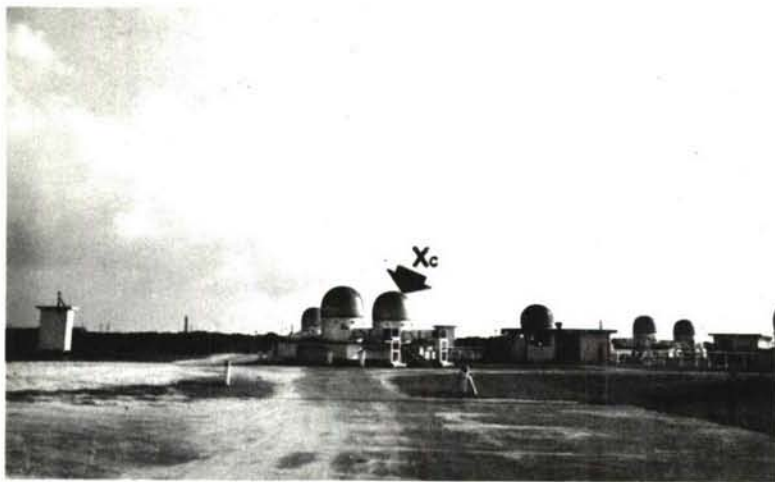


Figure 12.

Azusa MK I Area showing

$X_c$  Receiving Antenna

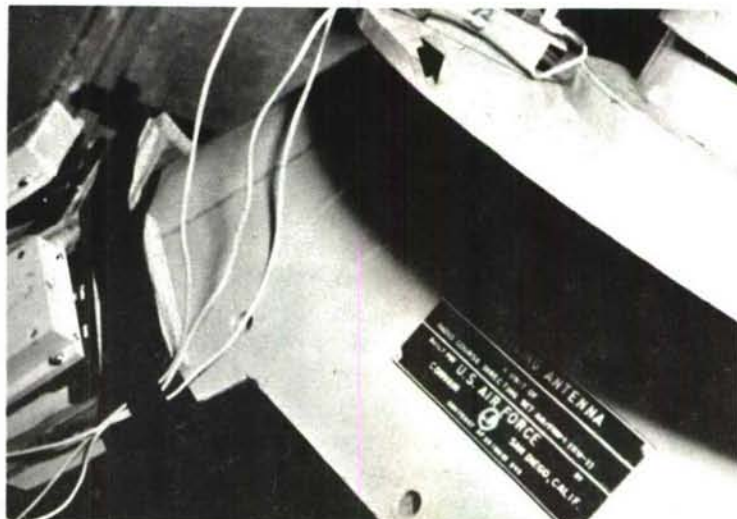
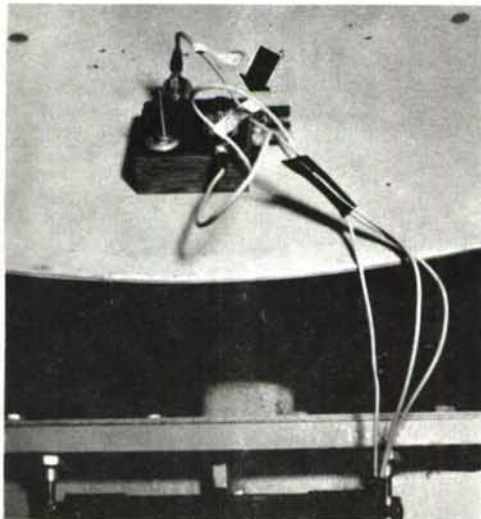


Figure 13. Accelerometer Installation  
 $X_c$  Receiving Antenna Dish.

Figure 14. Accelerometer Installation  
 $X_c$  Receiving Antenna Pedestal.

structures and the location of the accelerometers on each.

In the Azusa MK I area, the  $X_c$  Receiving Antenna was selected for vibration testing. The antenna and location of the acceleration sensors installed on this structure are shown in Figures 12 to 14.

Sound pressure level measurements at each vibration test area were made by the instrumentation described in Volume I of this report. Time correlation between sound pressure and vibration levels was achieved through the simultaneous recording of the range time signal.

#### B. Instrumentation

The complete instrumentation system used in sensing, recording and analyzing vibration produced by missile noise at various points on structures



at Cape Canaveral may be divided into two groups: (1) Vibration Sensing and Recording, and (2) Vibration Playback and Analyzing. Group 1 was operated from a mobile trailer setup at various test sites on the Cape while Group 2 was permanently located at Wright-Patterson Air Force Base, Ohio.

1. Description Vibration Sensing and Recording Instrumentation (Group 1):  
(Items described are number-keyed to blocks in Figure 15)

The vibration sensing elements Endevco Model 2217 (Block 1, Fig. 15) have a nominal sensitivity of 65 millivolts per "G". The output of the accelerometers were amplified by Endevco Model 2607 amplifiers (Block 2) which have variable gains up to 100, thus producing an overall maximum sensitivity of 6.5 volts per "G". The signals from the accelerometers and associated amplifiers up to a maximum of 12 each were recorded by an FM magnetic tape recorder Davies Model 501 (Block 4).

The frequency range of the complete recording instrumentation system was from 3 to 2000 cycles per second, the lower limit being determined by the accelerometer-amplifier combination while the upper limit was established by the magnetic tape recorder.

The wide-band dynamic range of the tape recorder was 0.01 to 1.0 volts (RMS) input. Therefore, with the recording system operating at full gain it was possible to detect vibrations as low as 56 db below one "G" in conditions of low noise and ambient vibration. Under narrow band analysis conditions this lower limit could be extended 6 to 10 db.

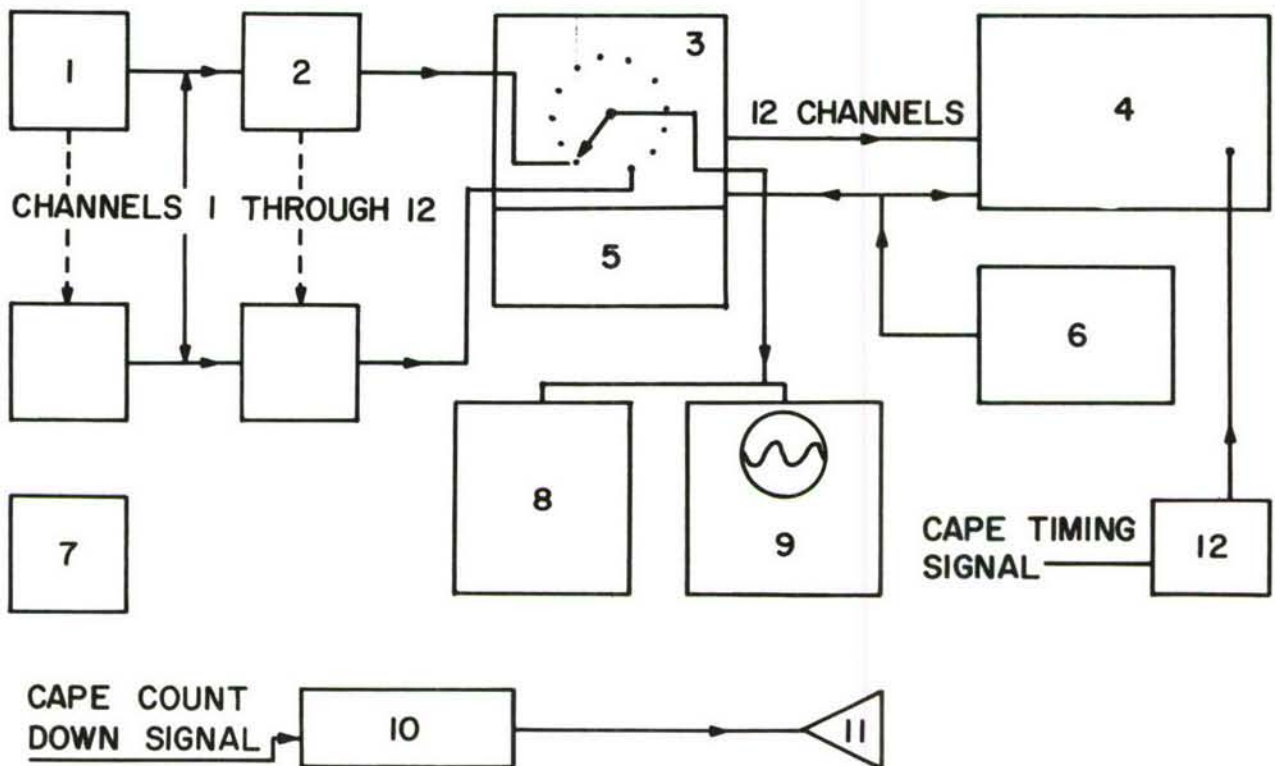
The calibrator (Block 7), voltmeter (Block 8), and oscilloscope (Block 9) were utilized to calibrate the accelerometer and amplifier combination in volts per "G" of vibration excitation. Calibration of the tape recorder was accomplished by use of its internal system.

The Cape Canaveral timing signal was wired into the instrumentation trailer through an isolation transformer, into an adjustable gain amplifier (Block 12), with its output being recorded on the tape recorder. This provided a means of correlation of time with missile count-down time, noise, and vibration produced.

Blocks 5 and 6 represent D.C. high- and low-voltage power packs required to furnish power to the accelerometer amplifiers and tape recorders.

Blocks 10 and 11 represent an audio amplifier and speaker system, supplied by the Cape, to furnish audible project count down to the instrumentation trailer.

During each project or missile shot upon which vibration tests were conducted, a recording, covering the time period from approximately four seconds before (T-4) to one hundred seconds after (T + 100) launch time, was taken to provide a means of determining the indicated ambient vibration level due to wind, electronic noise, time of arrival of noise and vibration produced by the missile, and variation in vibration level as time progressed.



1. ACCELEROMETER (12 EACH), ENDEVCO, MODEL 2217
2. AMPLIFIER (12 EACH), ENDEVCO, MODEL 2607
3. PATCH PANEL AND MONITORING CONTROL
4. RECORDER, MAGNETIC TAPE, DAVIES, MODEL 501
5. POWER SUPPLY, REGULATED (200VDC)
6. POWER PACK (28VDC)
7. CALIBRATOR, VIBRATION, B AND K TYPE 1606
8. VOLTMETER, ELECTRONIC, H-P MODEL 400 D
9. OSCILLOSCOPE, DuMont, 5"
10. POWER AMPLIFIER, AUDIO
11. SPEAKER
12. AMPLIFIER, H-P MODEL 450

Figure 15. Schematic Diagram of Vibration Sensing and Recording Instrumentation.

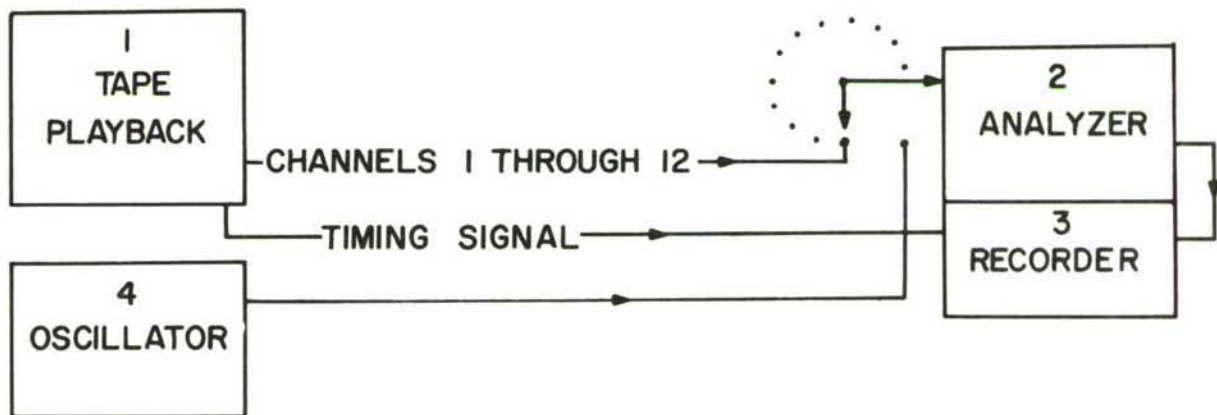


## 2. Description of Vibration Playback and Analyzing Instrumentation (Group 2)

After the completion of each vibration recording taken on a missile launch the recorded tape was transported to WPAFB for playback and analysis on Group 2 Instrumentation System, block diagrammed in Figure 16 (Items described are number-keyed to blocks in Figure 16).

The Magnetic Tape Recording and Reproducing System Honeywell Series 3170 (Block 1) reproduced the vibration signal that was recorded at the test site at a ratio of 1 to 1. Therefore, the signal applied to the 1/3 Octave Analyzer (Block 2) had the same magnitude and frequency components as the recorded signal.

Each recording was given a continuous 1/3 octave analysis with center frequencies at 10, 12.5, 16, 20, 25, 31.5, 40, 50, 63, 80, 100, 125, 160, 200, 250, 315, 400, 500, 630, 800, 1000, 1250, 1600, and 2000 cycles per second. The time period covered was from approximately 4 seconds before launch time to 100 seconds after. The analyzed signal output from the analyzer was recorded on the B and K Type 2305 Recorder (Block 3), along with the timing signal which was recorded on the event marker channel. The Calibrating Oscillator B and K Type 1014 (Block 4) was utilized to set a calibration reference "G" level on the analyzed recording from data obtained during the in-field calibration of the sensing elements and associated amplifiers. The final analyzed recording shows ambient vibration and time history of the vibration level in db reference to one "G" throughout the recorded launch period.



1. MAGNETIC TAPE RECORDING AND REPRODUCING SYSTEM, HONEYWELL  
SERIES 3170

2.\*ANALYZER, 1/3 OCTAVE, B AND K TYPE 2111

3.\*RECORDER, B AND K TYPE 2305

4.OSCILLATOR, (CALIBRATING) B AND K TYPE 1014

\*INSTRUMENTS 2 AND 3 ABOVE ASSEMBLED TOGETHER MAKE A  
COMPLETE UNIT, B AND K TYPE 3312

Figure 16. Schematic Diagram of Vibration Playback and  
Analyzing Instrumentation.



### C. Presentation of Data

Vibration data presented in this report is in graphical form showing one-third octave analysis over a frequency range of 10 to 2000 cycles per second. The plots show the maximum vibration level acoustically induced, in db reference to one "G", measured at each test point in three directions (vertical, lateral and fore/aft) during a missile launch. Also displayed for each frequency band are two plots showing (1) maximum acoustic noise level at the vibration test site and (2) ambient indicated background vibration produced by the combination of ambient wind velocity, operation of machinery on test structure, and electronic-noise level of the recording and analysis instrumentation.

The graphical presentations are shown in the Appendix in the sequence outlined in Table I which also contains other pertinent factual data, such as test number, date of test, type missile, launch-pad number, vibration-test site, and distance from launch pad to vibration-test site.

TABLE I  
DATA PRESENTATION SEQUENCE

Test No.	Date	Missile	Pad (a)	Test Site (b)	Distance a to b (ft.)	Test Data	
						Figure No.	Page
1251	6 July 61	Atlas	13	Tel-2	14,800	17-28	16-19
3211	25 July 61	Titan	19	Tel-2	7,500	29-40	20-23
5454	24 Oct. 61	Titan	20	Tel-2	6,300	41-49	24-26
4508	27 Oct. 61	Saturn	34	Tel-2	5,500	50-58	27-29
1805	8 Aug. 61	Atlas	13	Com-Dst.	24,300	59-67	30-32
1811	12 Aug. 61	Thor	17A	Com-Dst..	11,250	68-79	33-36
5050	23 Aug. 61	Ranger I (Atlas Agena)	14	Com-Dst.	25,000	80-91	37-40
1262	6 Sept. 61	Titan	20	Com-Dst.	29,700	92-103	41-44
3212	8 Sept. 61	Titan	19	Com-Dst.	28,275	104-115	45-48
1803	9 Sept. 61	Atlas	13	Com-Dst.	24,300	116-127	49-52
3765	29 Sept. 61	Titan	20	Az. MK-I	7,500	128-133	53-54
1252	2 Oct. 61	Atlas	11	Az. MK-I	8,500	134-139	55-56
1804	5 Oct. 61	Atlas	13	Az. MK-I	5,000	140-145	57-58
3764	7 Oct. 61	Titan	19	Az. Mk-I	5,700	146-151	59-60

#### D. Analysis of Data

The one-third octave band analysis of maximum sound pressure and vibration levels recorded at each test point (Figures 17 through 151) were visually examined to determine the following:

1. Maximum vibration level recorded at each test point during the survey.
2. Frequency band and direction of the maximum vibration.
3. Frequency bands of predominant vibration peaks at a test point for various missile launches.
4. Effect of positioning the TLM-18 antenna at Tel-2 in the vertical direction during test 4508 instead of being pointed horizontally at the launch pad during the first stage of the launch as in previous tests.
5. Methods of predicting future vibration levels with the advent of larger missiles producing greater sound pressure levels. Two methods of approach were used as follows:
  - (a) Comparison of maximum sound-pressure level with maximum vibration level for each missile launch at a test point for each one-third octave frequency band. Two samples of this procedure are portrayed in Figures 152 and 153.
  - (b) Determination of the ratio of the rate of decrease in vibration level to sound-pressure level by frequency bands during various missile launches. This study was conducted on the original frequency band analysis of sound pressure and vibration versus time during launch. Two samples are shown in Figures 155-158.

In both of these methods a large number of empiric cases were statistically used because many factors affect the accuracy of using only a few samples. Factors considered to be contributing to the accuracy of the results are: (a) Small differences in sound pressure level at vibration test sites for various missiles; (b) Proximity of the test vibration levels to vibrations caused by ambient noise; (c) Variation in the direction of sound propagation with respect to the test structure; (d) Change in orientation of the tracking antennas; (e) Doppler effect producing a shift in the sound frequency spectrum during launch; (f) Shift in spectrum frequency content within 1/3 octave bands for various type of missiles. Combinations of the various conditions affecting accuracy are apparent in the results and dictated statistical methods.



## SECTION III

### RESULTS

#### A. Tel-2, 80 Foot Communications Antenna

Vibration measurements on this structure were conducted during only two tests, 1251 and 3211. (See Figures 17-19, 29-31.)

A maximum vibration level of -42 db referenced to one "G" occurred during test 3211 in the vertical direction in the 1600 and 2000 cycle one-third octave center frequency bands.

Three apparent resonant peaks showed up in both tests in the fore and aft directions occurring in the 160, 500 and 1600-2000 cycle one-third octave center frequency bands with maximum vibration levels of -42db, -43 db and -44 db respectively.

#### B. Tel-2, Tri-Helix #4

Vibration measurements were conducted on this structure during four tests, 1251, 3211, 5454 and 4508. (See Figures 20-22, 32-34, 41-43, and 50-52.)

In general, vibration levels were distributed uniformly over the entire measured frequency spectrum without any predominant, regularly occurring peaks.

A maximum vibration level occurred during test 4508 in the fore and aft direction of -29 db in the 63 cycle one-third octave center frequency band.

#### C. Tel-2, TLM-18 Antenna Dish

Vibration measurements were conducted during four tests, 1251, 3211, 5454 and 4508 on the dish at the spar attachment point. (See Figures 23-25, 35-37, 44-46, and 53-55.)

A maximum vibration level of -17 db was recorded during test 4508 in the vertical direction in the 80 - 125 cycle one-third octave center frequency bands. Maximum vibration of -19 db occurred in the lateral direction in the 125 to 200 cycle one-third octave center frequency bands.

A maximum vibration level of -12 db occurred during test 5454 in the fore and aft direction in the 125 cycle one-third octave center frequency band.

During the first part of launch on test 4508 the TLM-18 antenna was pointed vertically instead of horizontally toward the launch pad. This affected the vibration produced at this point in three readily recognizable ways.

1. Lowered the frequency of maximum vibration level in the vertical direction from the 125 to 200 cycle to the 80 to 125 cycle one-third



octave center frequency bands. Comparison of figures 23, 35, 44, and 53 illustrates this point.

2. Reduced the expected vibration in the fore and aft direction (perpendicular to dish) by at least 20 db in all one-third octave frequency bands below 250 cycles. (Note figures 25, 37, 46, and 55.)
3. Increased the vibration level in the high end of the spectrum by approximately 8 db without appreciable increase in sound pressure level.

#### D. Tel-2, TLM-18 Antenna Pod

Vibration was measured at this structural point during four tests 1251, 3211, 5454 and 4508. (See Figures 26-28, 38-40, 47-49, and 56-58.)

A maximum vibration level of -12 db was measured at this point in the vertical direction during test 4508 in the region of the 250 cycle, one-third octave center frequency band.

In the vertical and lateral directions during all tests the vibration had repeatable peaks occurring in the respective 200 to 630 cycle and 315 to 630 cycle one-third octave center frequency bands.

In the fore and aft direction the vibration amplitude was uniformly distributed over the frequency spectrum without any pronounced peaks.

#### E. Command Destruct, Steerable Helix Array

Vibration recordings were made on this structure during five tests: 1811, 5050, 1262, 3212 and 1803. (See Figures 68-70, 80-82, 92-94, 104-106, and 116-118.)

A maximum vibration level of -29 db occurred at this test point during test 1811 in the fore and aft direction in the 40 cycle one-third octave center frequency band.

In general, peak vibrations occurred during all tests in the vertical and lateral directions in the 160 to 315 cycle one-third octave center frequency bands. In the fore and aft direction, peak vibrations occurred in the frequency region from 31.5 to 100 cycle one-third octave center frequency bands.

#### F. Command Destruct, Base of Gabriel Antenna

Vibration measurements at this test point were conducted during six tests: 1805, 1811, 5050, 1262, 3212 and 1803. (See Figures 59-61, 71-73, 83-85, 95-97, 107-109, and 119-121.)

A maximum vibration level of -46 db occurred in the fore and aft direction during test 1811 in the 100 cycle one-third octave center frequency band. Vibrations predominantly peaked in this direction in the 80 to 100 cycle one-third octave center frequency bands.

G. Command Destruct, RCA Steerable TX Antenna Dish

Vibration levels were recorded at this point during six tests: 1805, 1811, 5050, 1262, 3212, and 1803. (See Figures 62-64, 74-76, 86-88, 98-100, 110-112, and 122-124.)

During test 1811 a maximum vibration of -35 db was recorded in the fore and aft direction in the 160 cycle one-third octave center frequency band.

Vibration levels predominantly peaked in the vertical and fore and aft directions in the range of 160 to 250 cycle one-third octave center frequency bands. No regularly occurring peaks were observed in the lateral direction.

H. Command Destruct, RCA Steerable TX Antenna Pod

Vibration measurements at this point were recorded during six tests: 1805, 1811, 5050, 1262, 3212 and 1803. (See Figures 65-67, 77-79, 89-91, 101-103, 113-115, and 125-127.)

A maximum vibration level of -41 db was recorded during test 1811 in the fore and aft direction in the 80 cycle one-third octave center frequency band.

Vibrations predominantly peaked in the 80 cycle one-third octave center frequency band in the fore and aft direction while no regular peaks were noted in the vertical and lateral direction.

I. Azusa, MK-1, Pedestal of X<sub>C</sub> Receiving Antenna

Vibration measurements were conducted at this point during four tests: 3765, 1252, 1804 and 3764. (See Figures 128-130, 134-136, 140-142, 146-148.)

A maximum vibration level of -29 db occurred at this point during test 1804 in the vertical direction in the 800 cycle one-third octave center frequency band.

Vibrations predominantly peaked in the vertical and lateral directions in the 800 cycle one-third octave center frequency band during all vibration tests performed at this point.

J. Azusa MK-1 Dish of X<sub>C</sub> Receiving Antenna

Vibration level measurements were conducted at this point during four tests: 3765, 1252, 1804 and 3764. (See Figures 131-133, 137-139, 143-145, and 149-151.)

A maximum vibration level of -2 db was recorded at this point during test 1804 in the fore and aft direction in the 160 cycle one-third octave center frequency band. This was the maximum vibration level recorded during the entire vibration survey.



During all tests at this point vibrations predominantly peaked in the fore and aft direction in the 80 to 160 cycle one-third octave center frequency bands.

#### K. Special Studies

The study of 136 cases to determine expected vibration versus sound pressure level at a structural test point by comparing maximum noise and vibration levels for each one-third octave frequency band during launch of various missiles is displayed graphically in Figure 154.

Results of the analysis of 198 recordings of noise and vibration rate of decay by frequency bands during various missile launches is illustrated in Figure 159.

Combining the results of the two above methods Figure 160, it is found that 60% of the studied cases indicate that a change in sound pressure level of one (1) db is followed by 0.75 to 1.25 db change in vibration level.

### SECTION IV

#### CONCLUSIONS

1. Vibration levels were relatively low at all test points during this survey.

2. Vibration levels are expected to increase one db per db sound pressure level increase up to the point of nonlinear structural response.

3. Experience with numerous aircraft vibration studies, and structural and instrumentation failures, makes it appear unlikely that future missile launch sound-pressure levels which can be predicted by the procedures outlined in Volume 1 of this report will reach the nonlinearity point or be destructive to the far-field representative antenna structures included in this report.



APPENDIX  
GRAPHIC PRESENTATION OF DATA

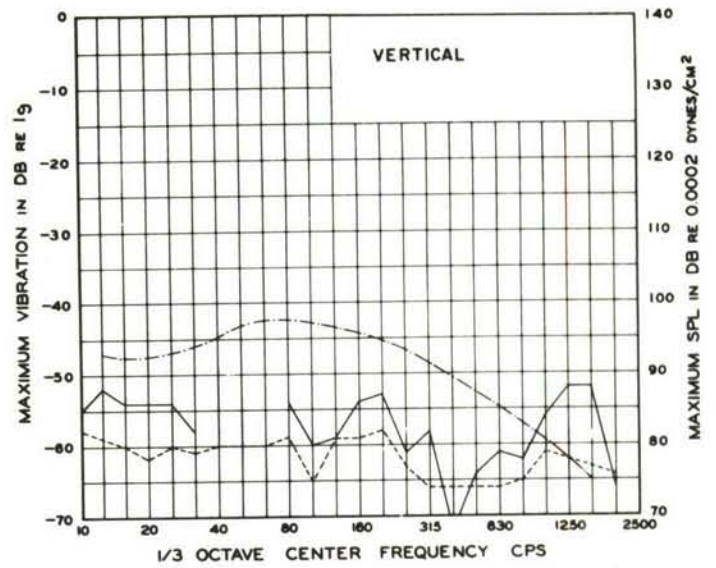


Figure 17.

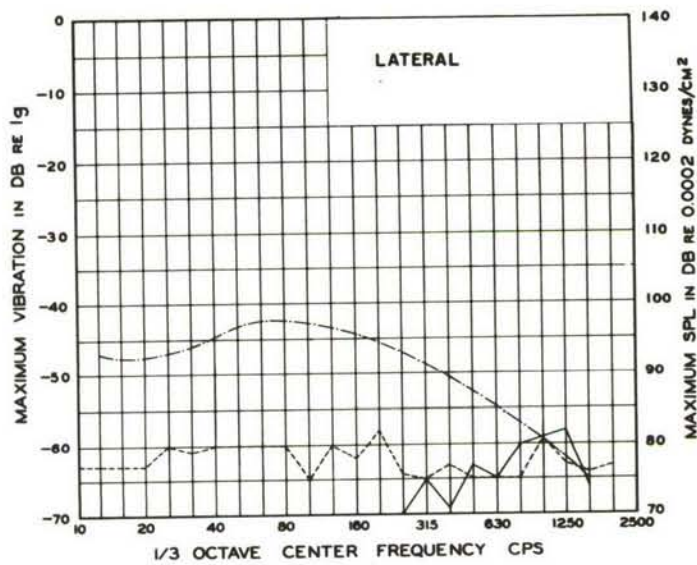


Figure 18.

Test No: 1251

Location: Tel-2, -On 80 ft.  
Communication Antenna

--- Ambient Vibration  
— Noise Induced Vibration  
-.-.- Noise Level

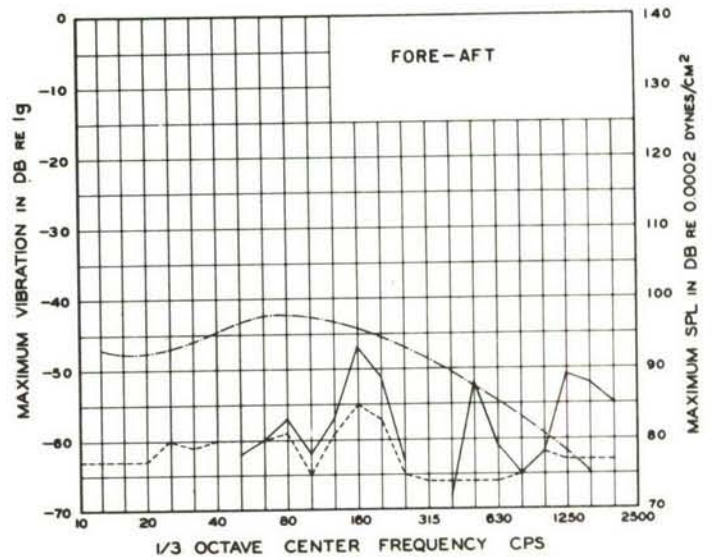


Figure 19.

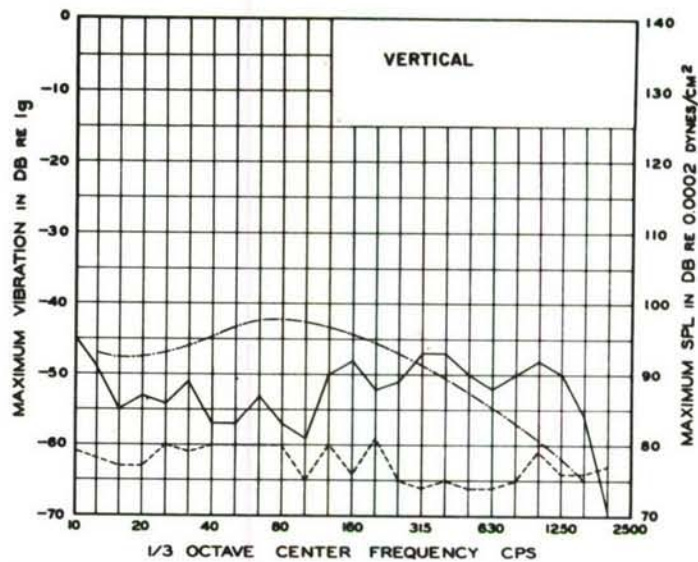


Figure 20.

Test No: 1251

Location: Tel-2, -On Tri-Helix #4

- - - Ambient Vibration
- Noise Induced Vibration
- . - Noise Level

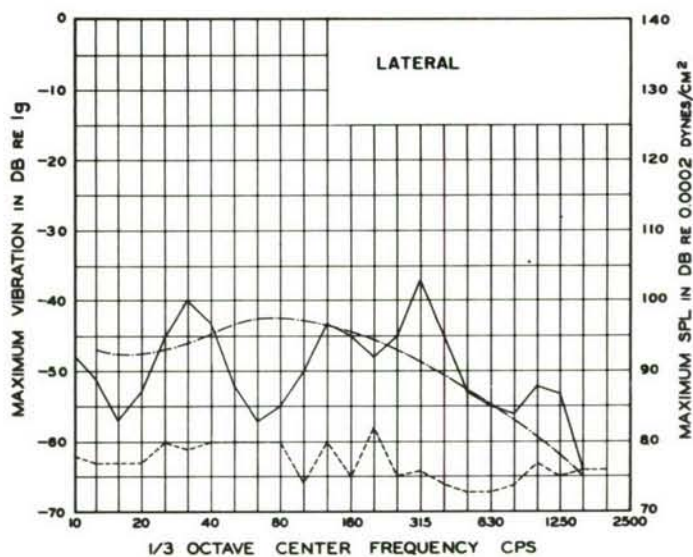


Figure 21.

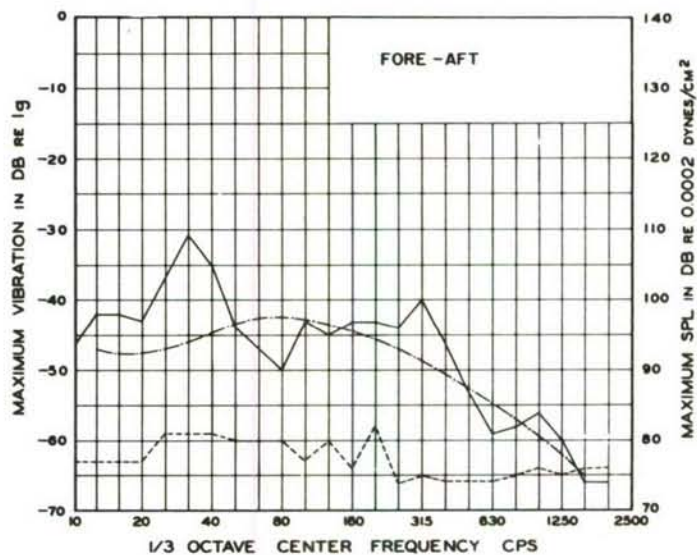


Figure 22.



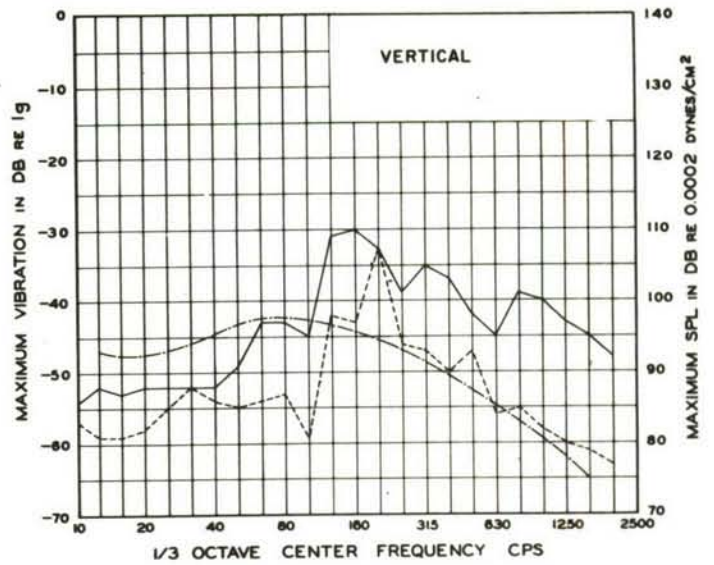


Figure 23.

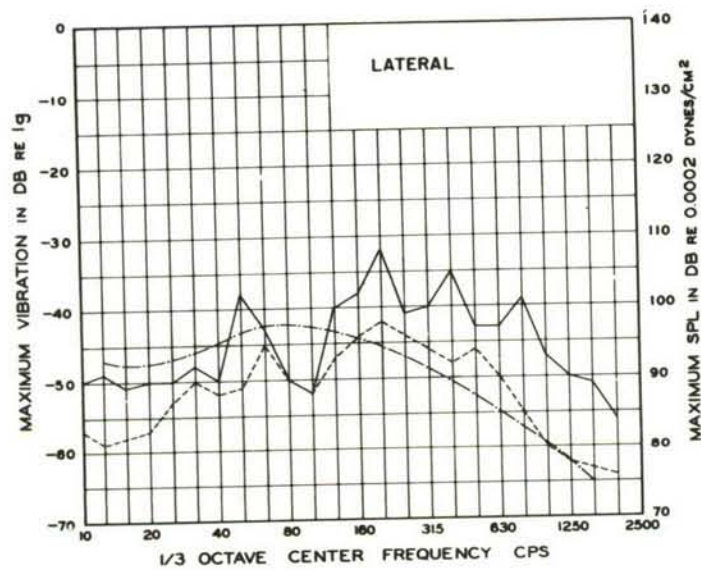


Figure 24.

Test No: 1251

Location: Tel-2, -On TLM-18  
Antenna Dish

--- Ambient Vibration  
— Noise Induced Vibration  
-.- Noise Level

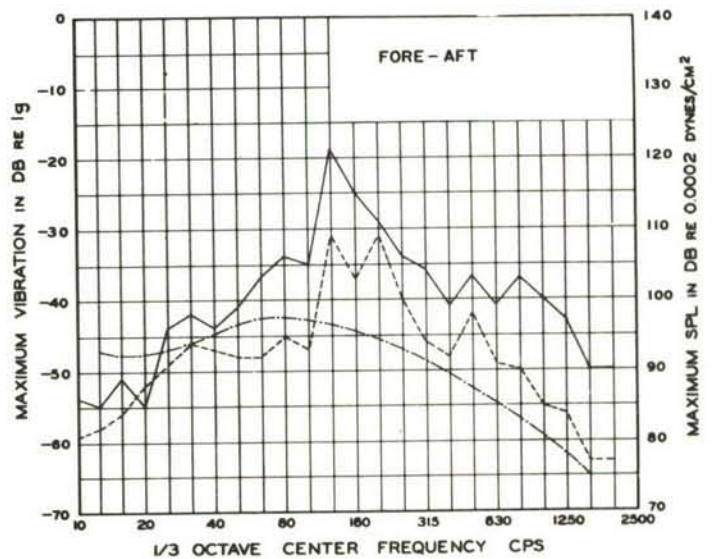


Figure 25.

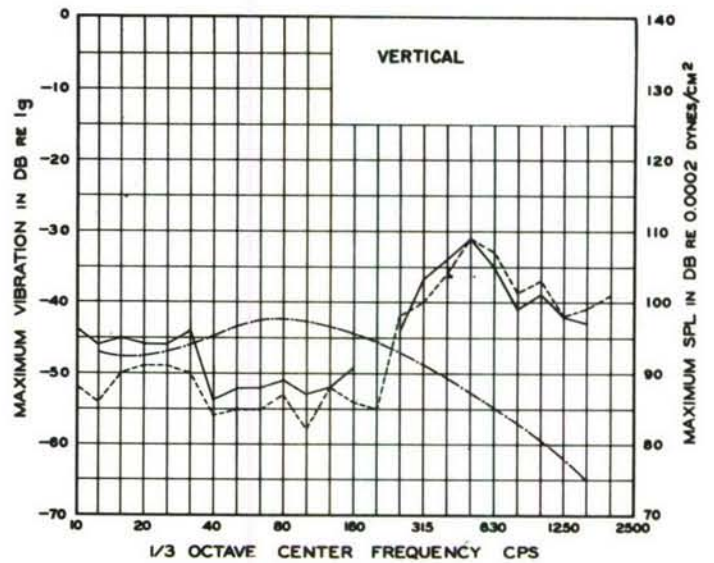


Figure 26.

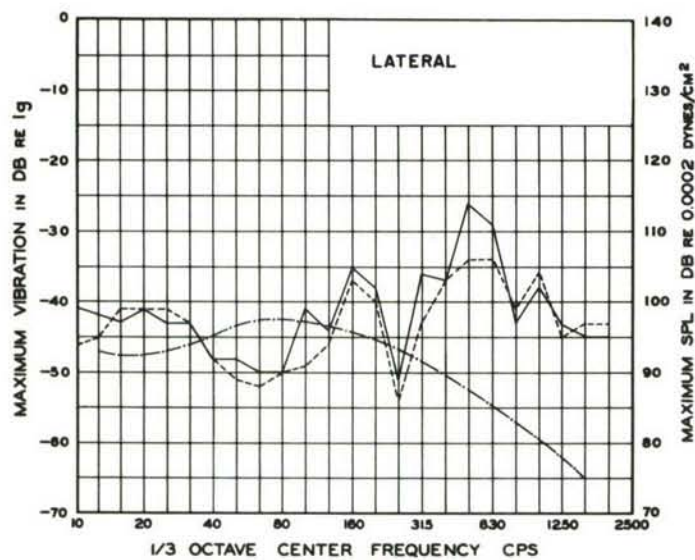


Figure 27

Test No: 1251

Location: Tel-2, -On TLM-18  
Antenna Pod

--- Ambient Vibration  
— Noise Induced Vibration  
-.- Noise Level

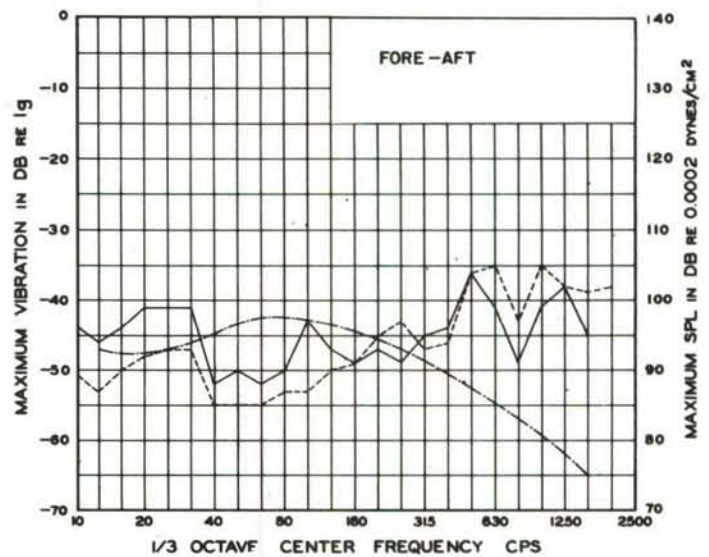


Figure 28.

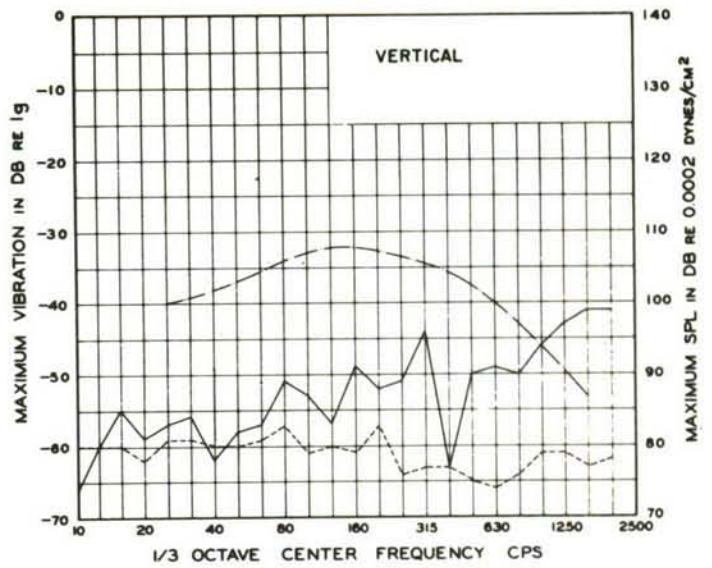


Figure 29.

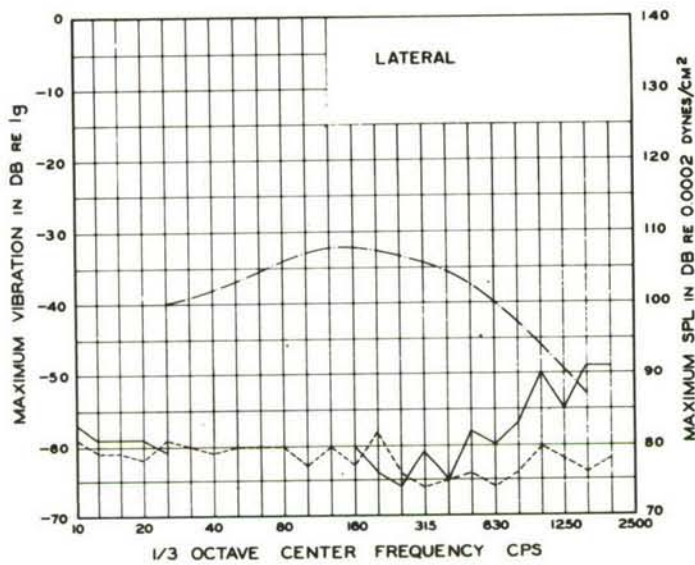


Figure 30.

Test No: 3211

Location: Tel-2, -On 80 ft.  
Communication Antenna

--- Ambient Vibration  
— Noise Induced Vibration  
-.- Noise Level

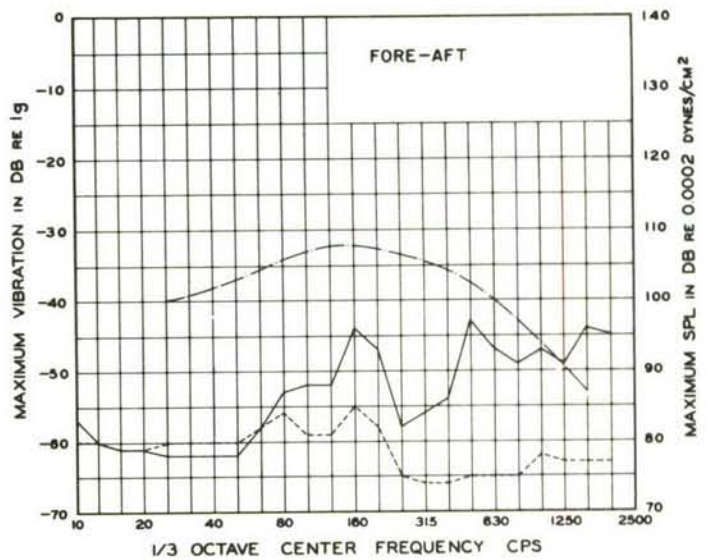


Figure 31.



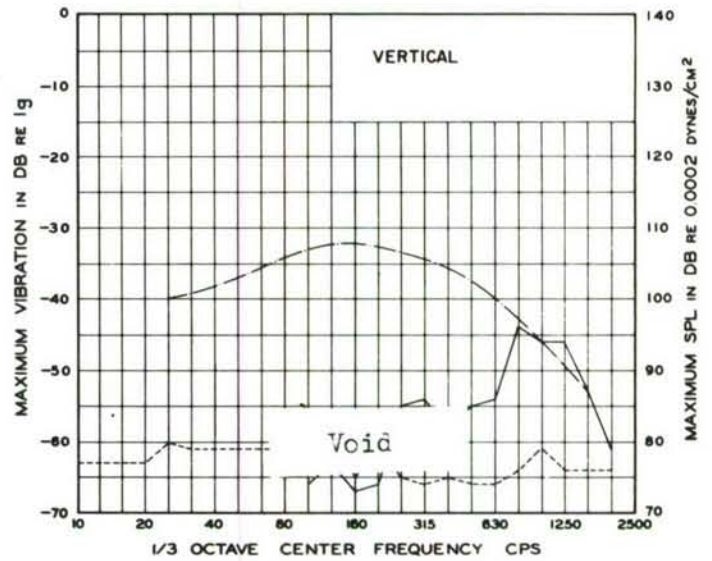


Figure 32.

Test No: 3211

Location: Tel-2, -On Tri-Helix #4

-- Ambient Vibration  
 — Noise Induced Vibration  
 -.- Noise Level

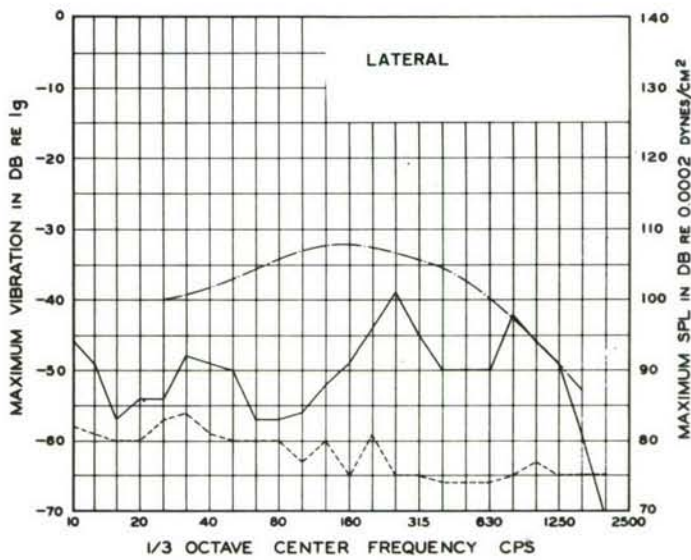


Figure 33.

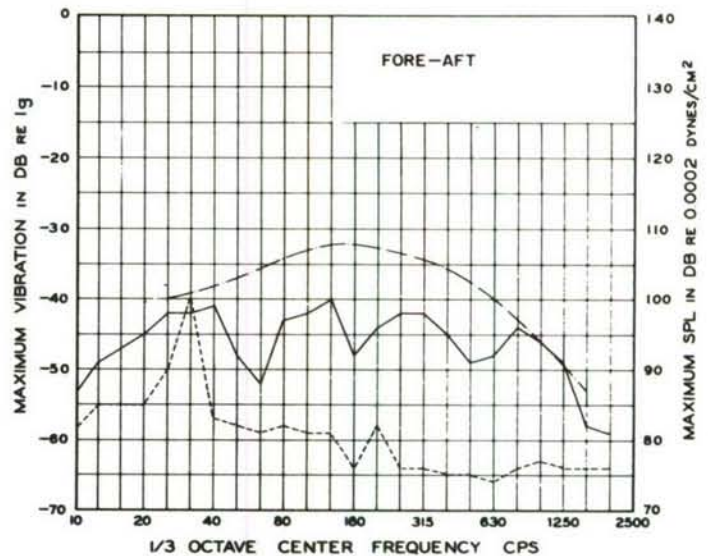


Figure 34.

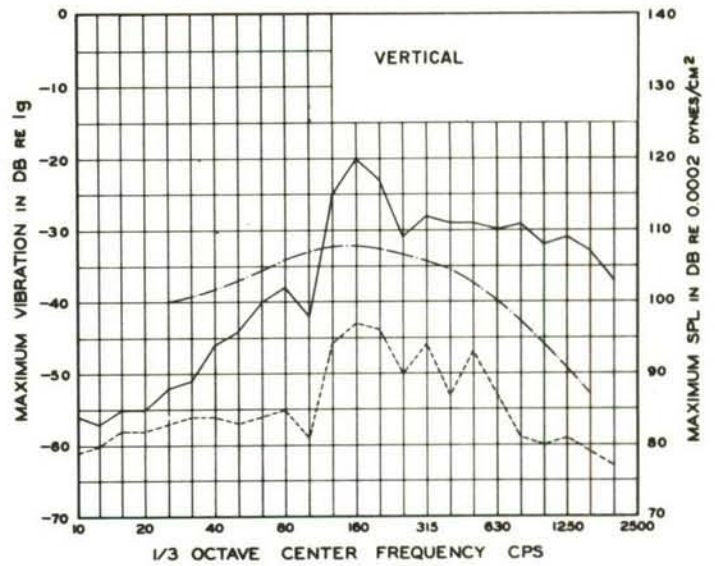


Figure 35.

Test No: 3211

Location: Tel-2, -On TLM-18  
Antenna Dish

--- Ambient Vibration  
— Noise Induced Vibration  
... Noise Level

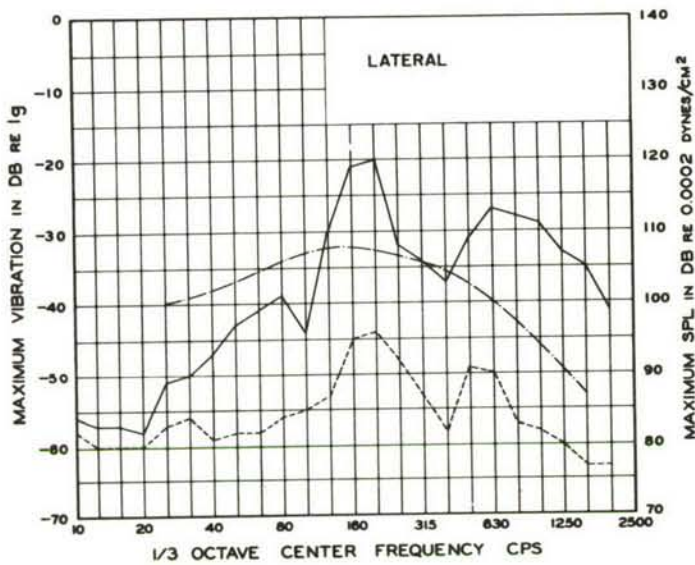


Figure 36.

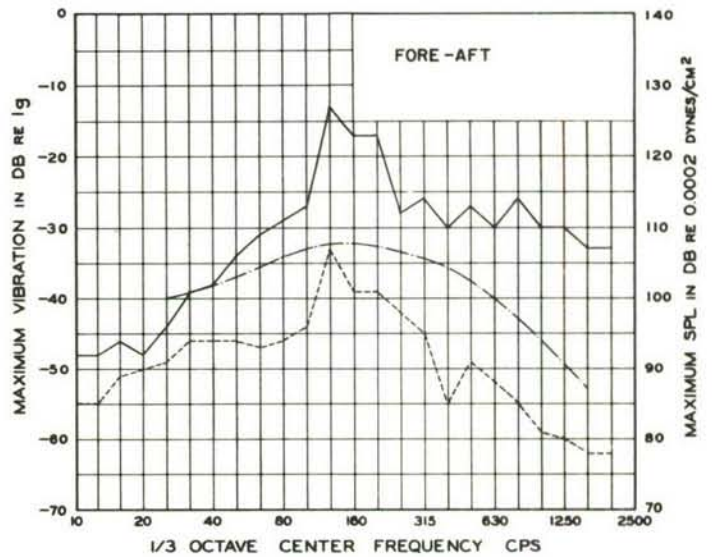


Figure 37.

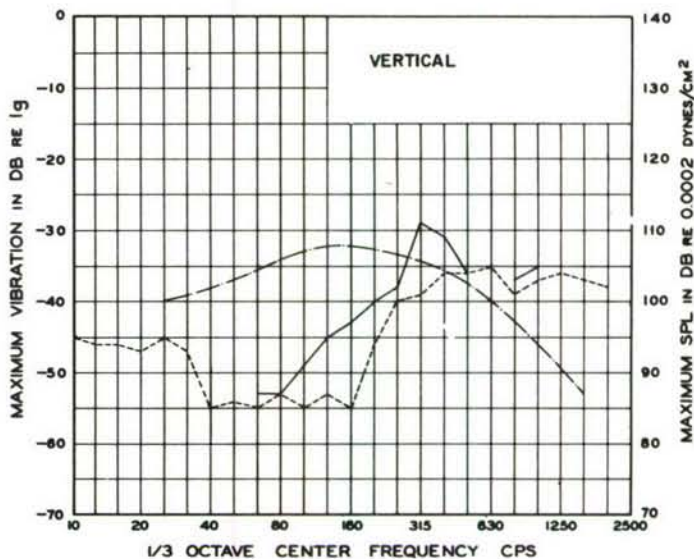


Figure 38.

Test No: 3211

Location: Tel-2, -On TLM-18  
Antenna Pod

--- Ambient Vibration  
— Noise Induced Vibration  
-.- Noise Level

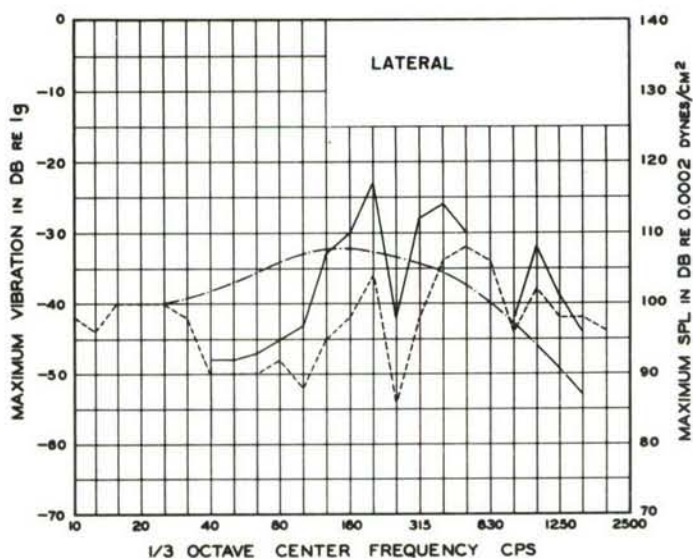


Figure 39.

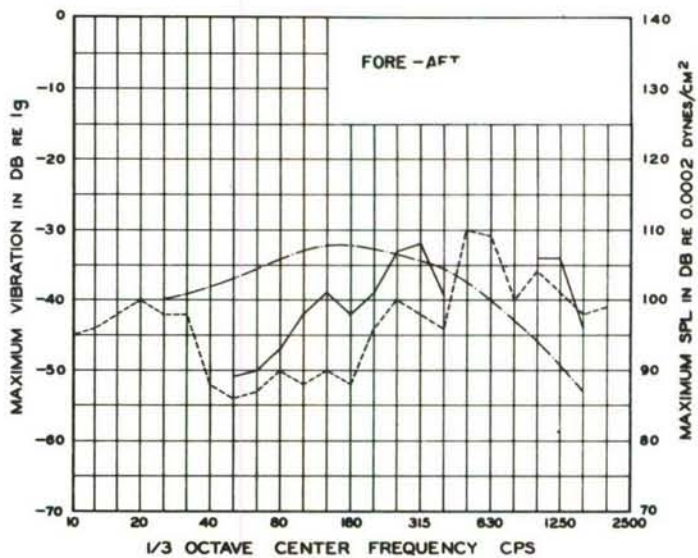


Figure 40.



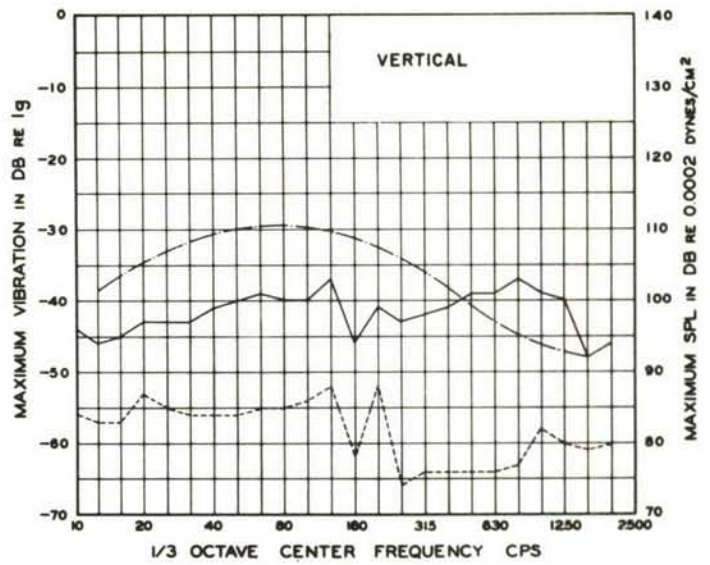


Figure 41.

Test No: 5454

Location: Tel-2, -On Tri-Helix #4

- Ambient Vibration
- Noise Induced Vibration
- .-.- Noise Level

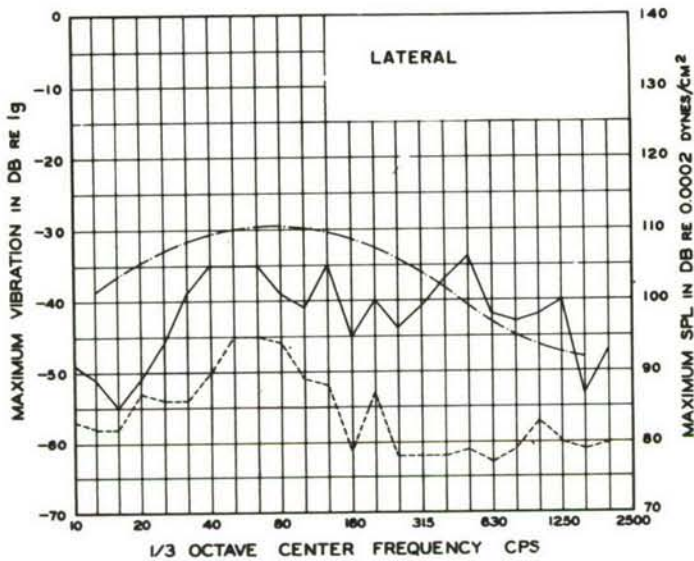


Figure 42.

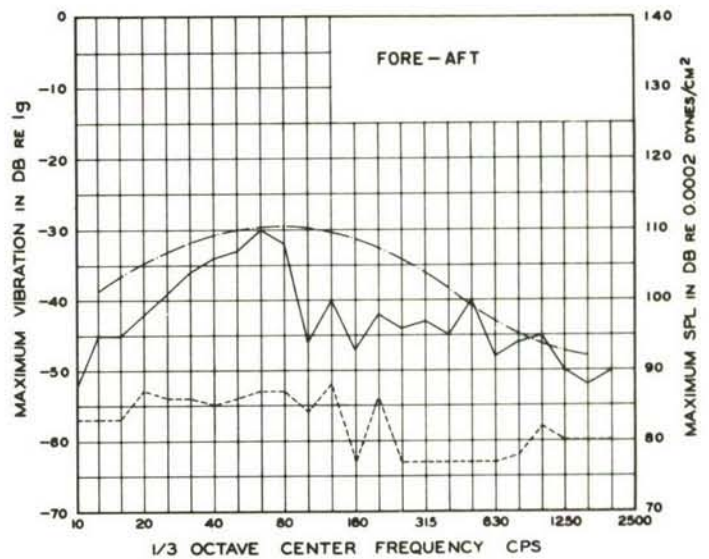


Figure 43.

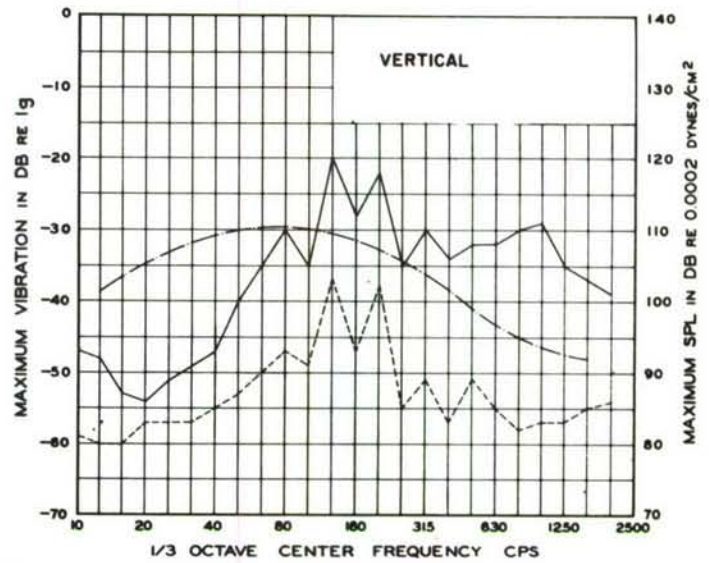


Figure 44.

Test No: 5454

Location: Tel-2, -On TLM-18  
Antenna Dish

--- Ambient Vibration  
— Noise Induced Vibration  
-.- Noise Level

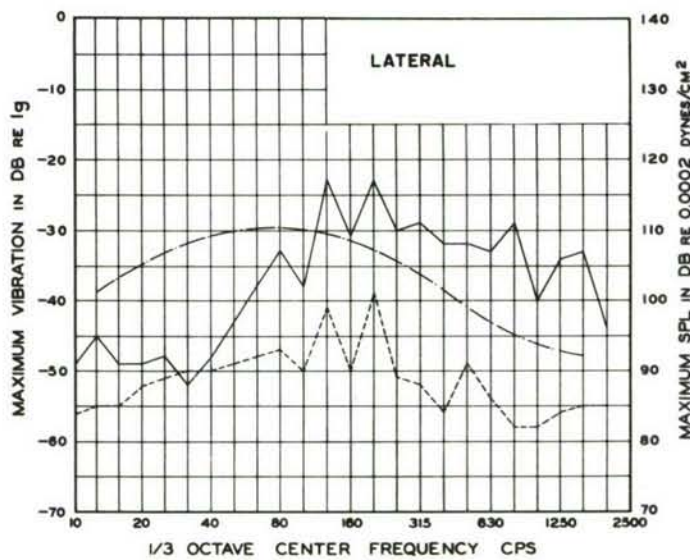


Figure 45.

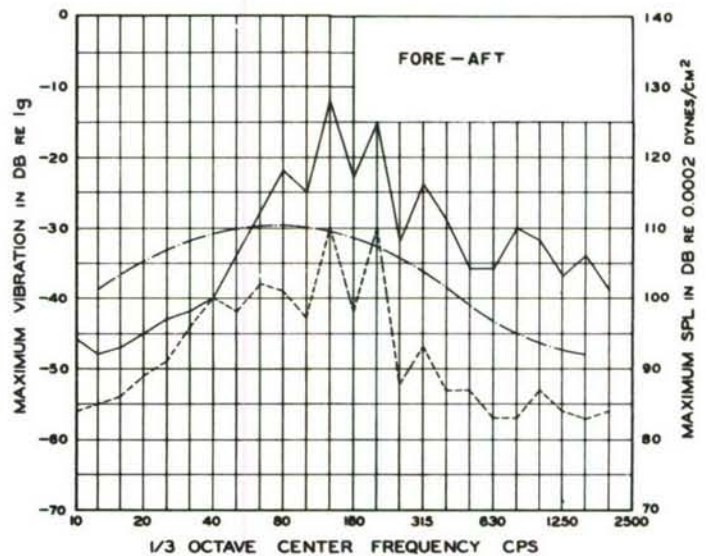


Figure 46.

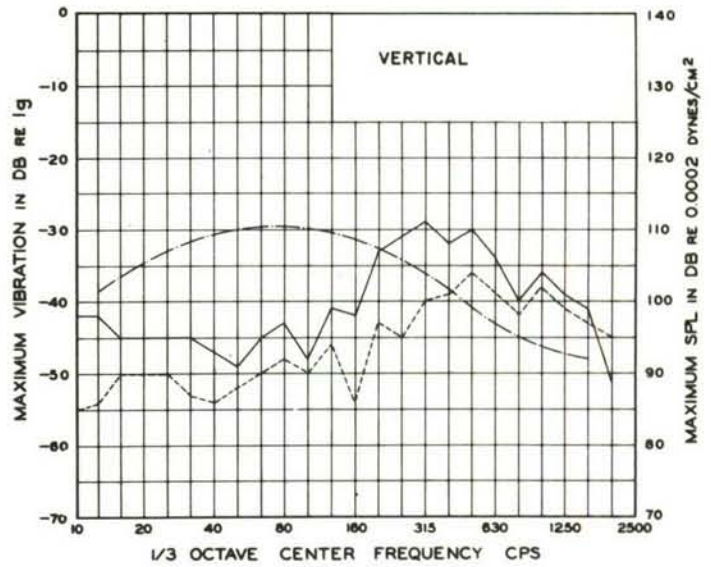


Figure 47.

Test No: 5454

Location: Tel-2, -On TLM-18  
Antenna Pod

--- Ambient Vibration  
— Noise Induced Vibration  
-.- Noise Level

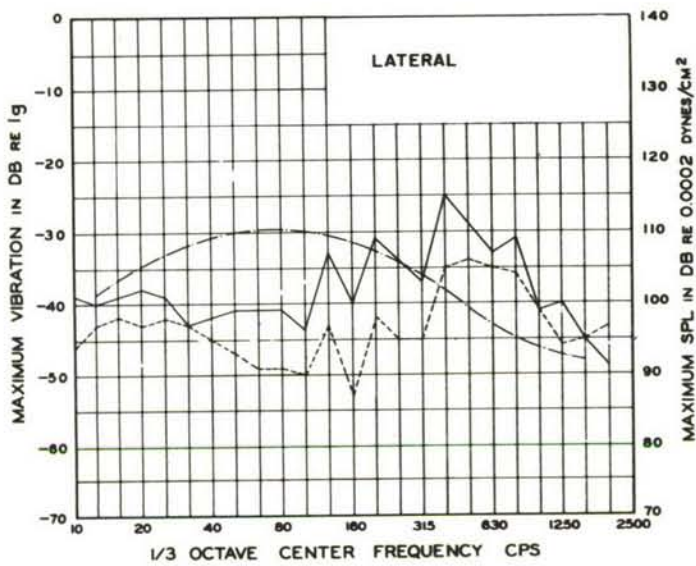


Figure 48.

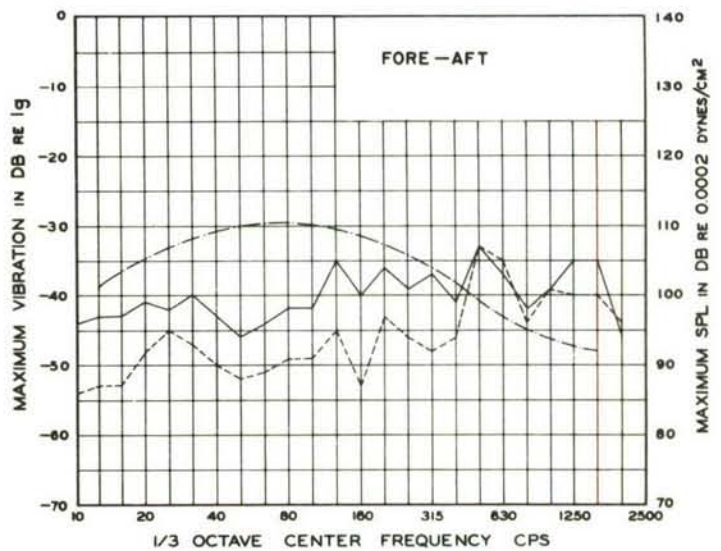


Figure 49.



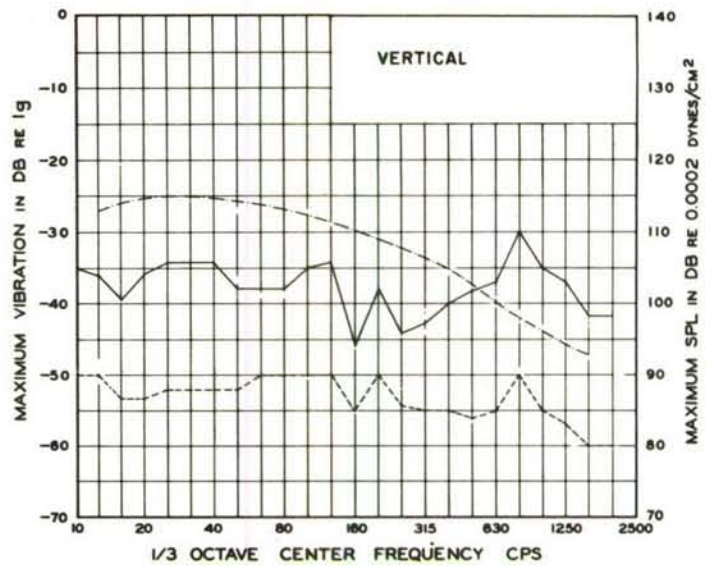


Figure 50.

Test No: 4508

Location: Tel-2, -On Tri-Helix #4

--- Ambient Vibration  
 — Noise Induced Vibration  
 -.- Noise Level

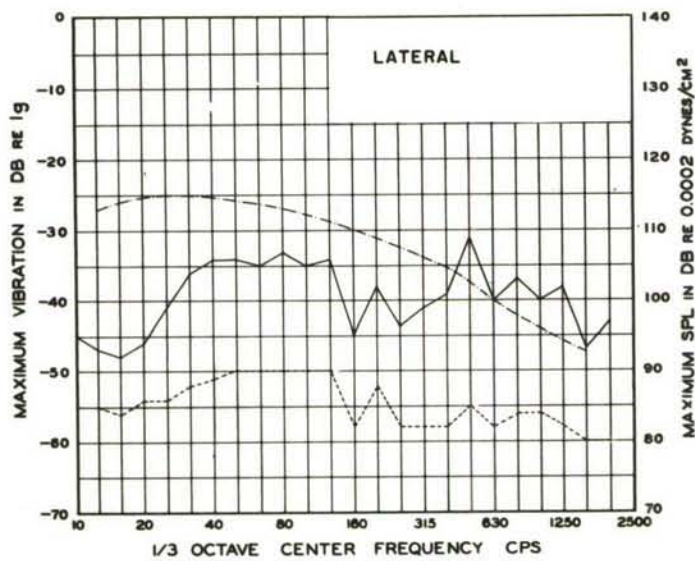


Figure 51.

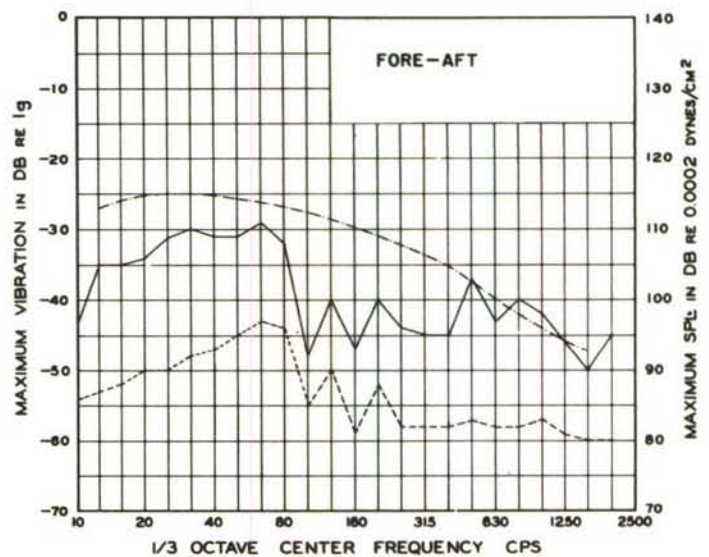


Figure 52.

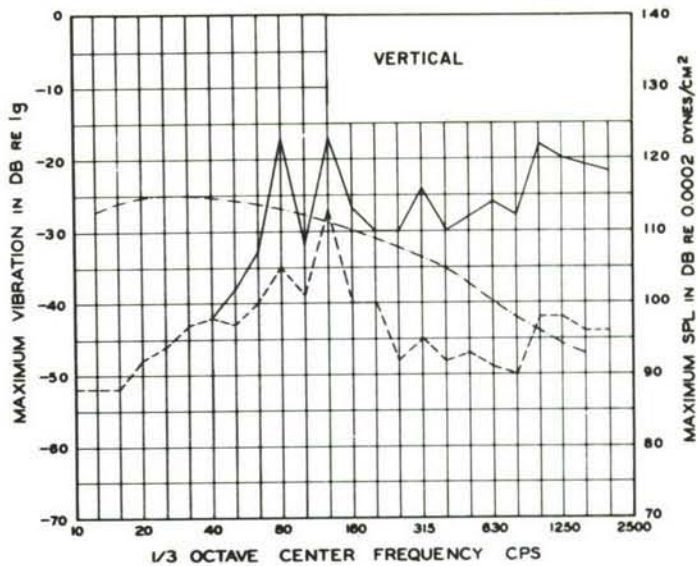


Figure 53.

Test No: 4508

Location: Tel-2, -On Spar Attachment Point of TLM-18

- Ambient Vibration
- Noise Induced Vibration
- .-.- Noise Level

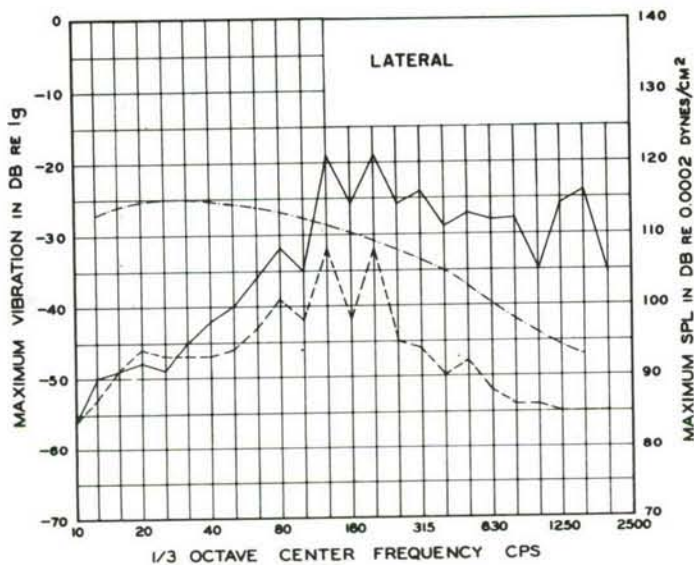


Figure 54.

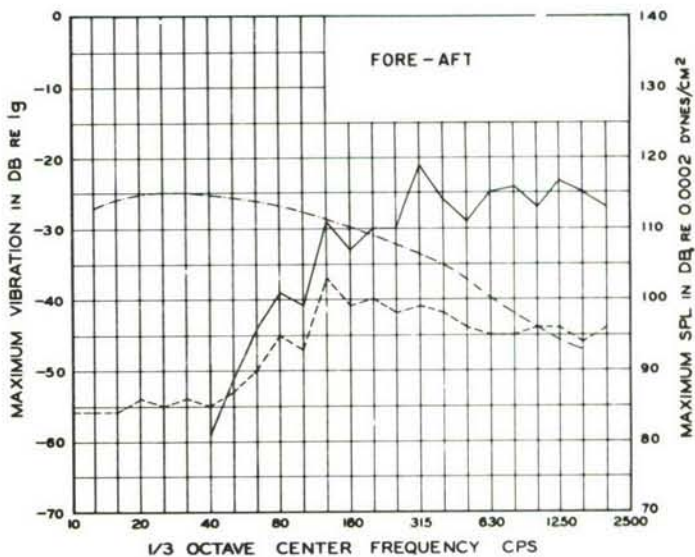


Figure 55.

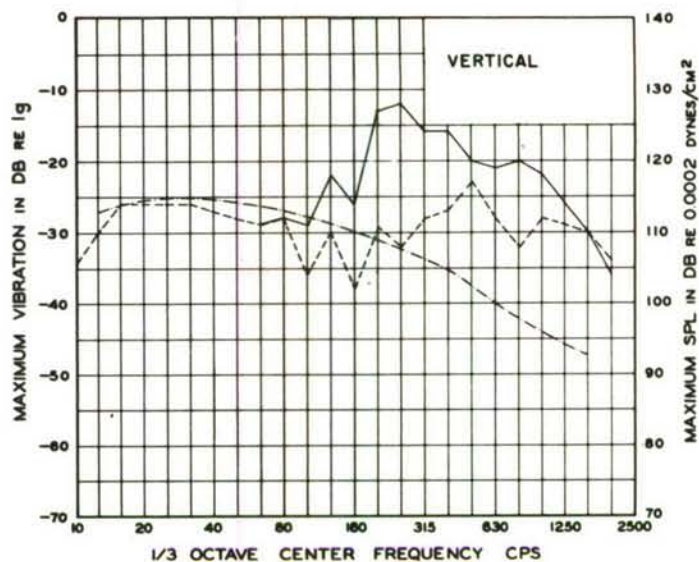


Figure 56.

Test No: 4508

Location: Tel-2, -On TLM-18  
Antenna Pod

-- Ambient Vibration  
— Noise Induced Vibration  
-.- Noise Level

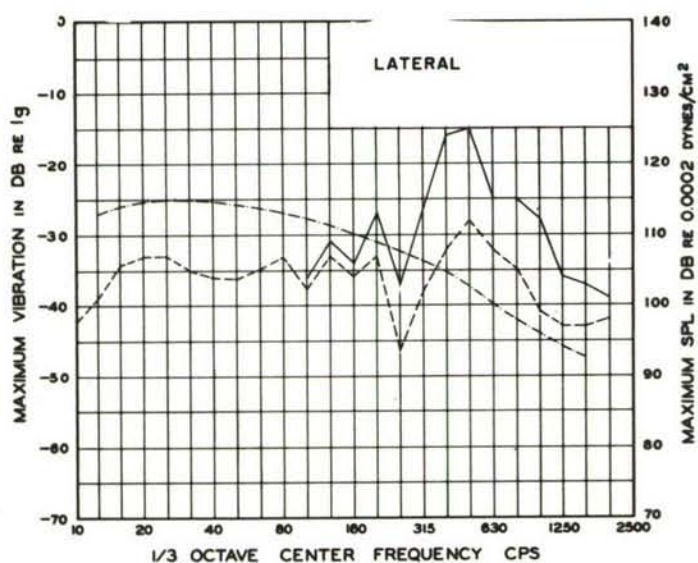


Figure 57.

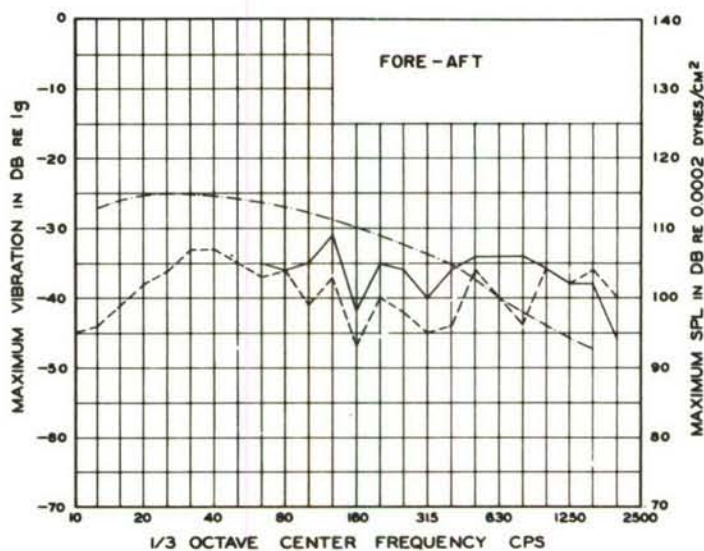


Figure 58.



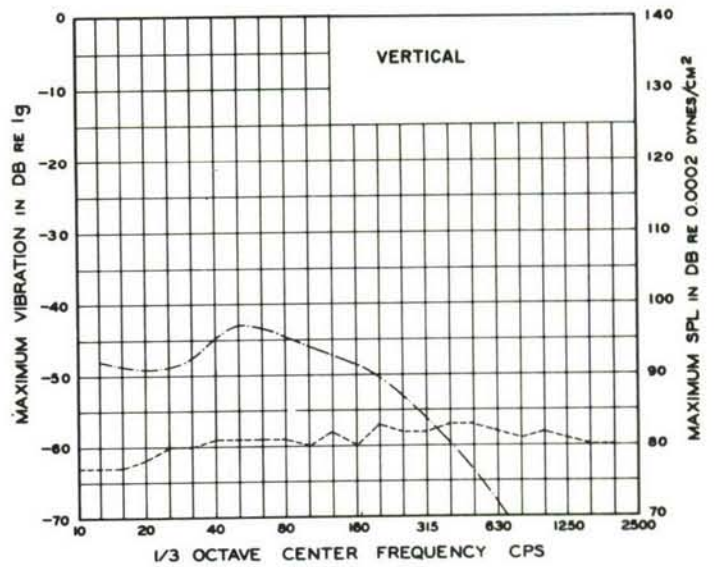


Figure 59.

Test No: 1805

Location: Command Destruct,  
-At Base of Gabriel Antenna

- - - Ambient Vibration
- Noise Induced Vibration
- · - Noise Level

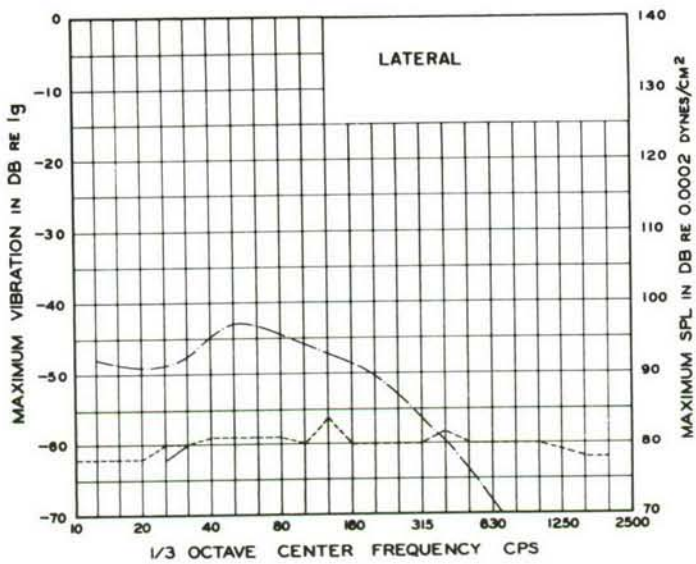


Figure 60.

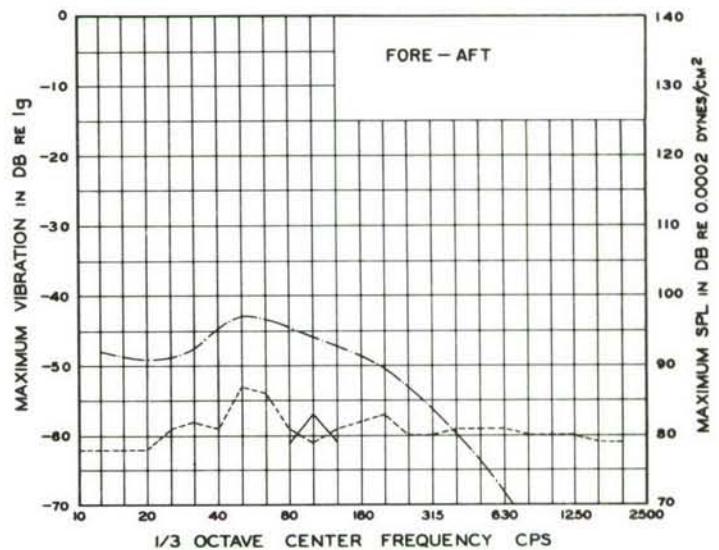


Figure 61.

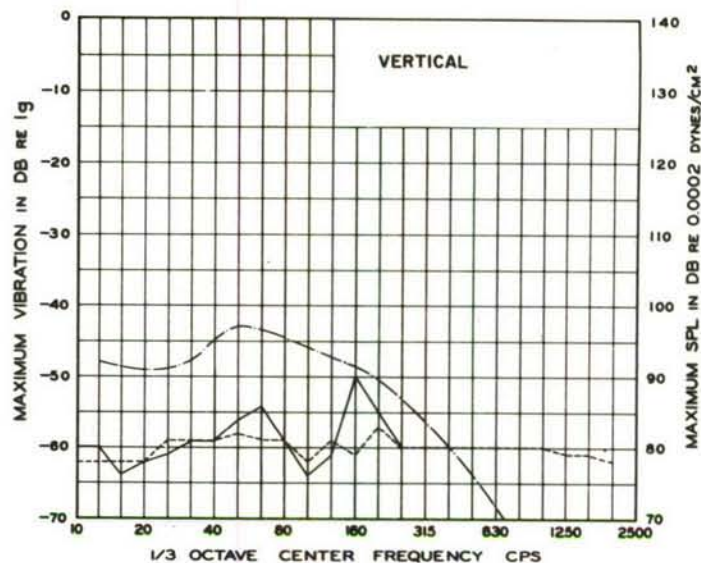


Figure 62.

Test No: 1805

Location: Command Destruct, -On Dish  
of RCA Tx. Steerable Antenna

--- Ambient Vibration  
— Noise Induced Vibration  
-.- Noise Level

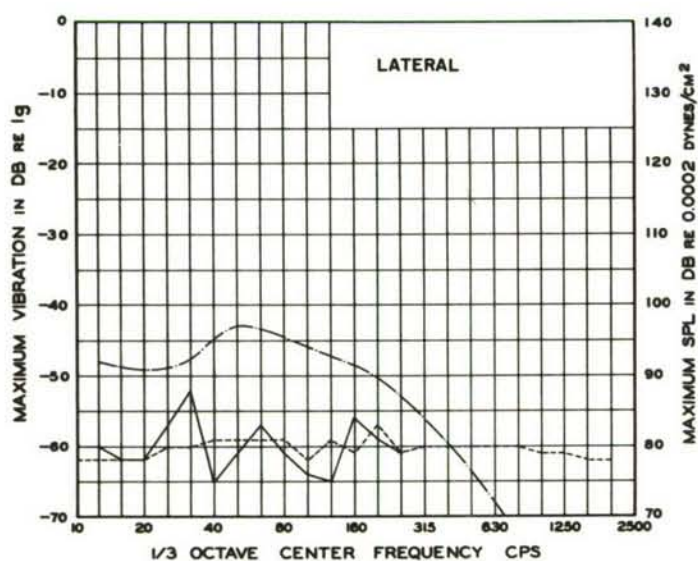


Figure 63.

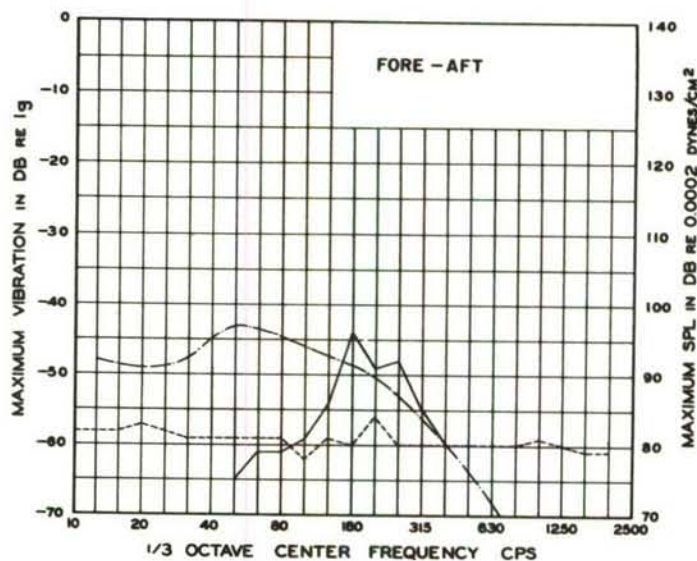


Figure 64.

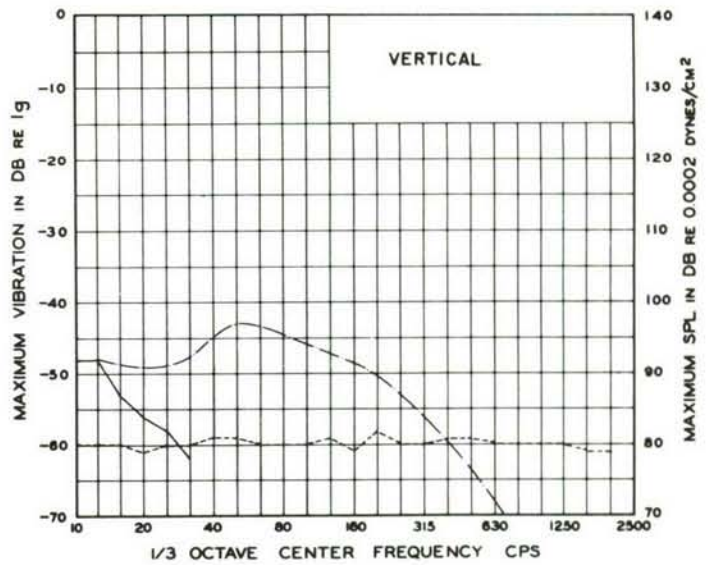


Figure 65.

Test No: 1805

Location: Command Destruct, -On Pod  
of RCA Tx. Steerable Antenna

--- Ambient Vibration  
— Noise Induced Vibration  
-.- Noise Level

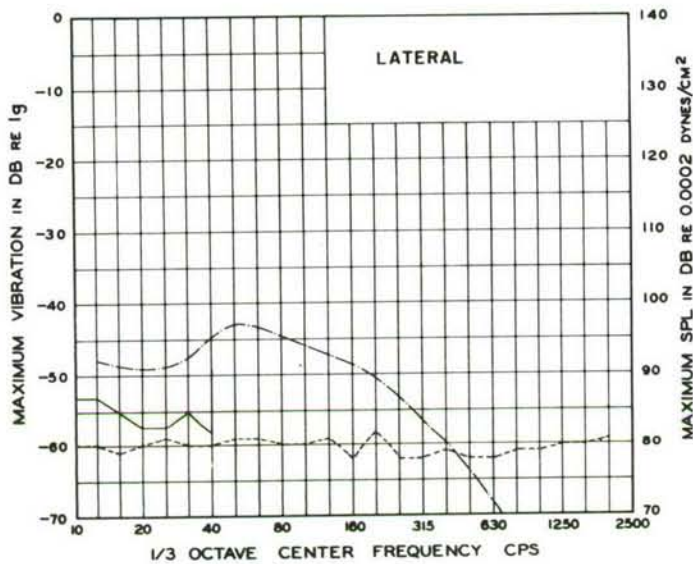


Figure 66.

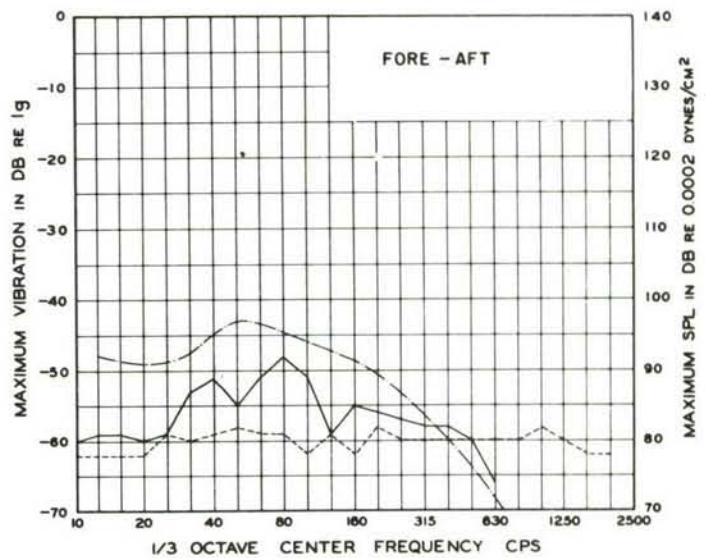


Figure 67.



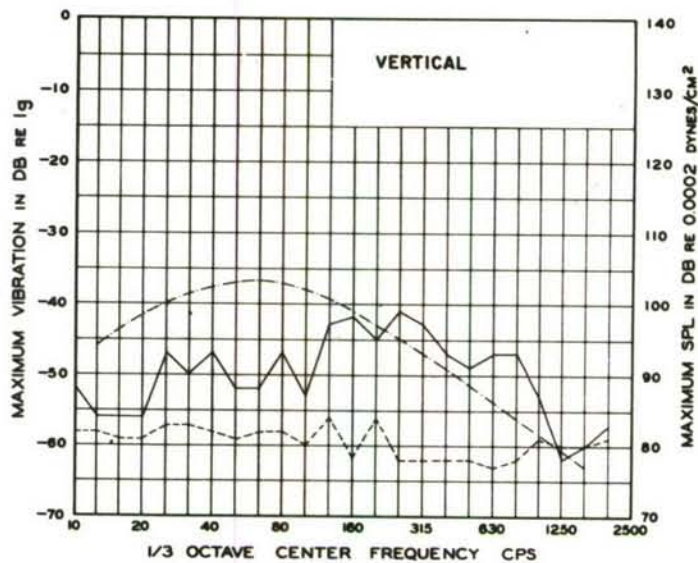


Figure 68.

Test No: 1811

Location: Command Destruct,  
-On Steerable Helix Array

--- Ambient Vibration  
— Noise Induced Vibration  
-.- Noise Level

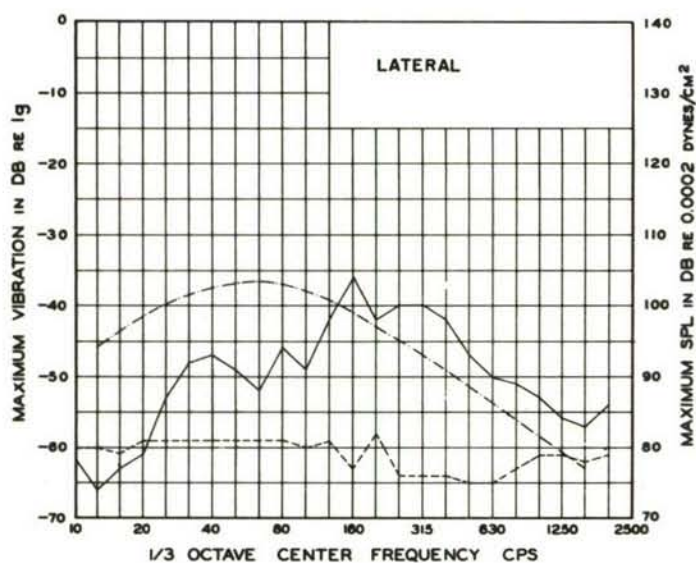


Figure 69.

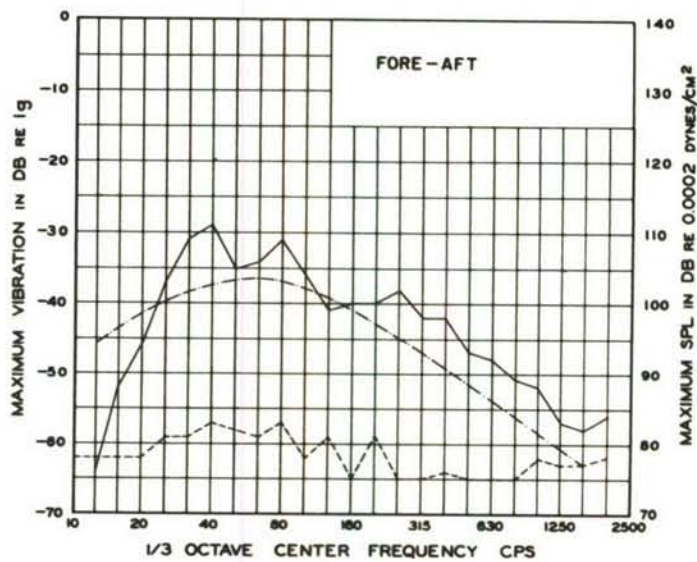


Figure 70.

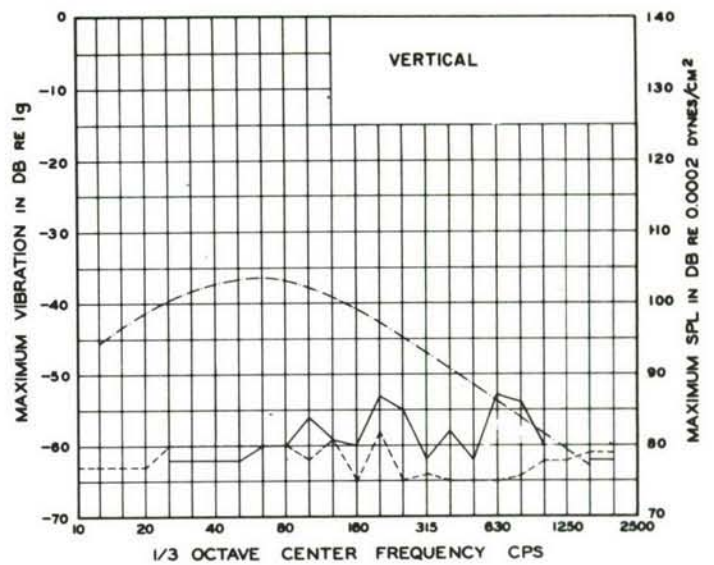


Figure 71.

Test No: 1811

Location: Command Destruct,  
-On Base of Gabriel Antenna

--- Ambient Vibration  
— Noise Induced Vibration  
-.- Noise Level

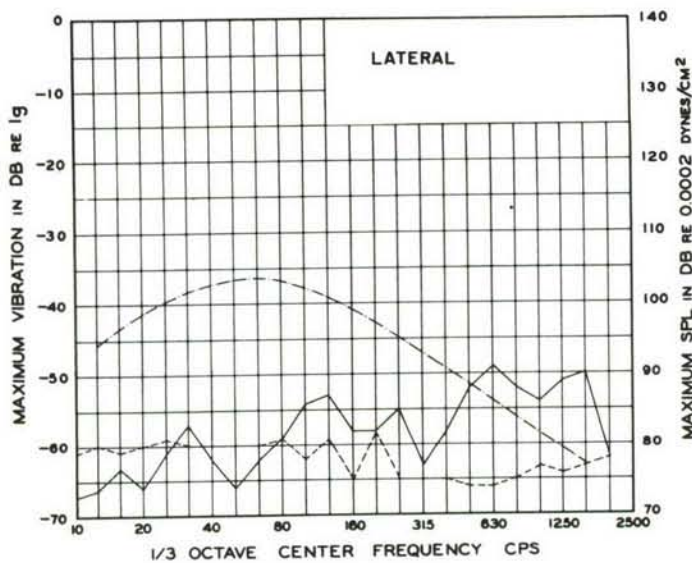


Figure 72.

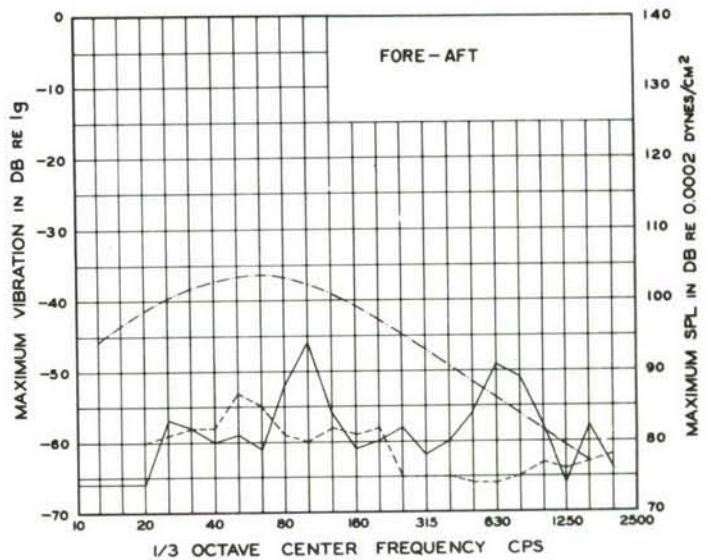


Figure 73.

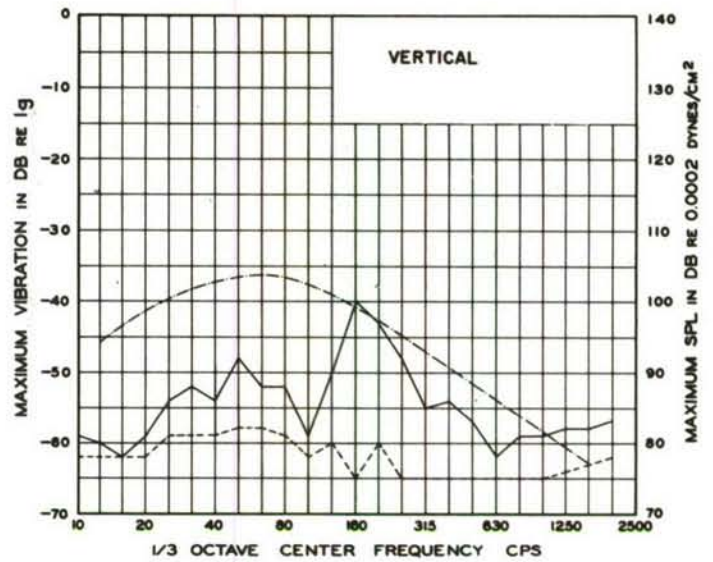


Figure 74.

Test No: 1811

Location: Command Destruct, -On Dish  
of RCA Tx. Steerable Antenna

- Ambient Vibration
- Noise Induced Vibration
- .- Noise Level

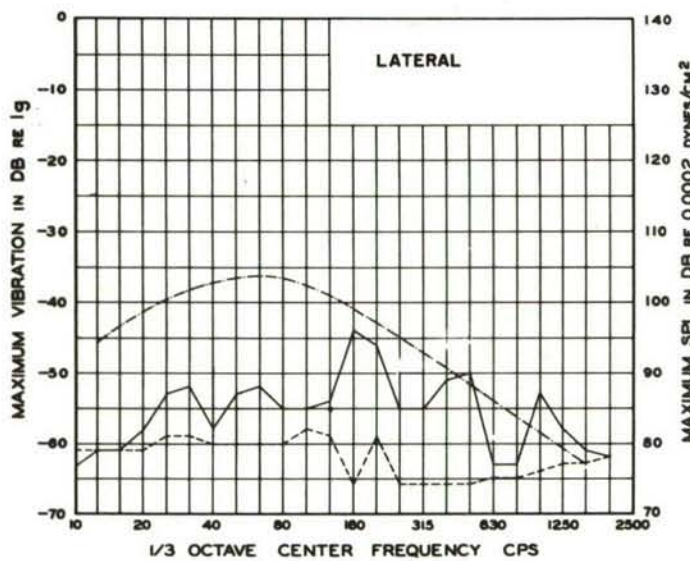


Figure 75.

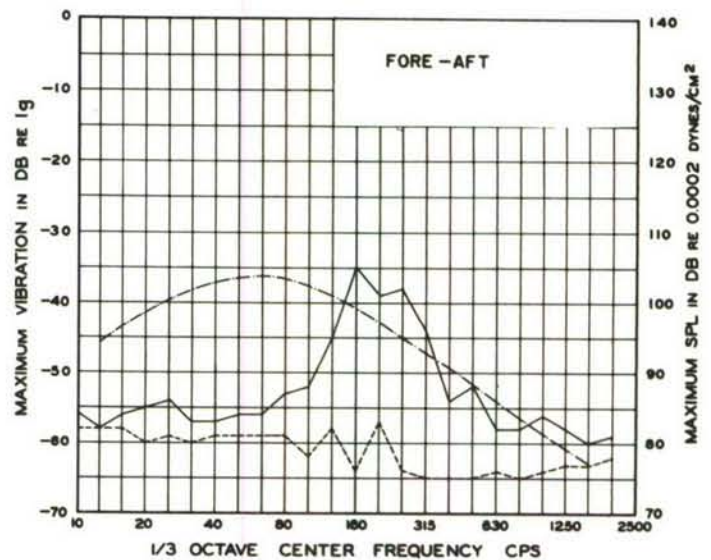


Figure 76.



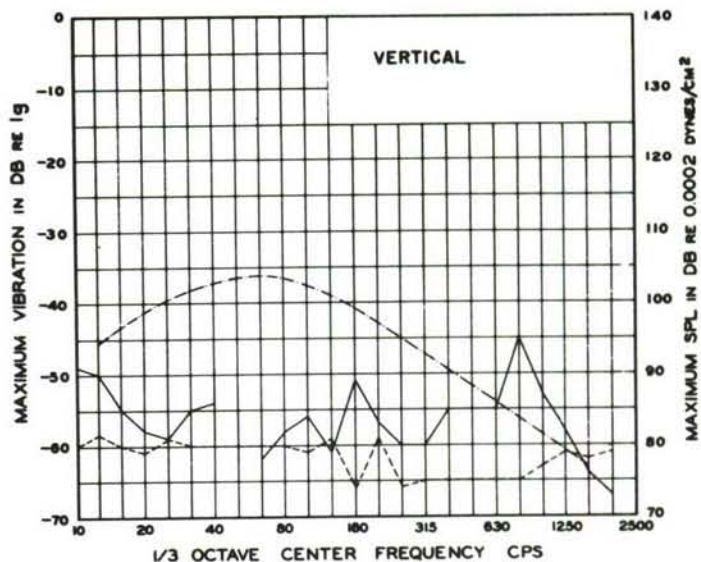


Figure 77.

Test No: 1811

Location: Command Destruct,-On Pod  
of RCA Tx. Steerable Antenna

--- Ambient Vibration  
— Noise Induced Vibration  
-.- Noise Level

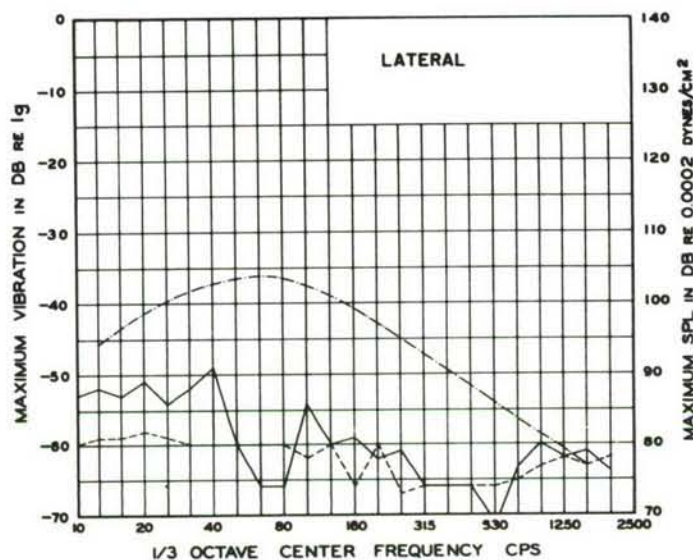


Figure 78.

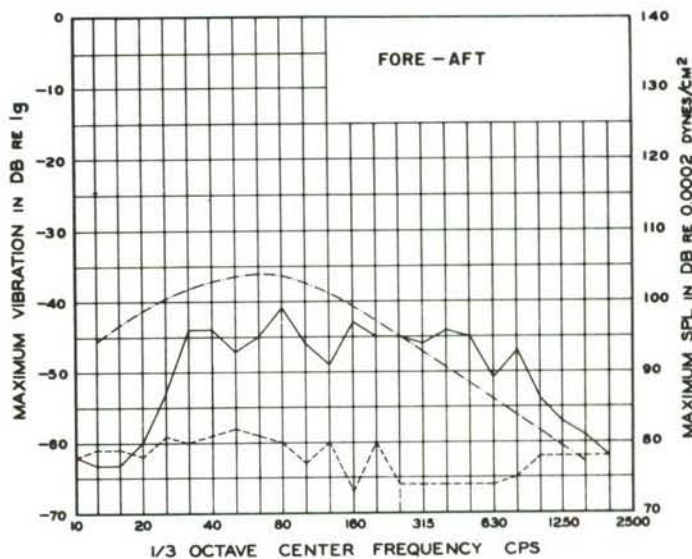


Figure 79.

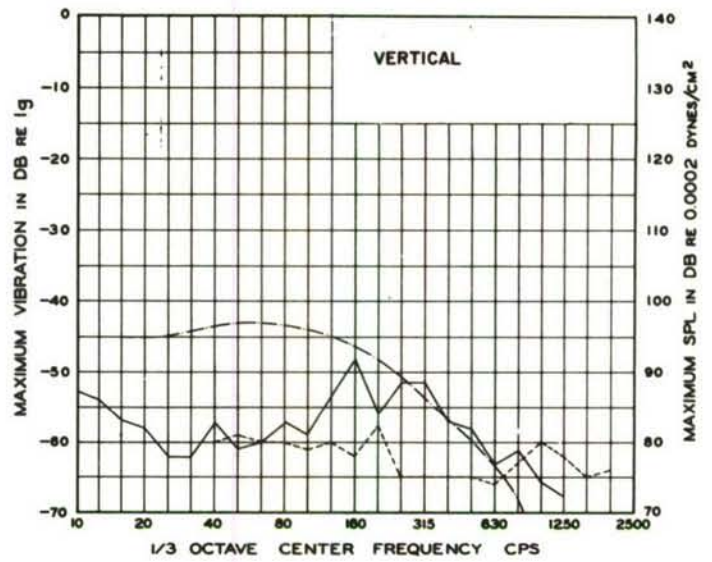


Figure 80.

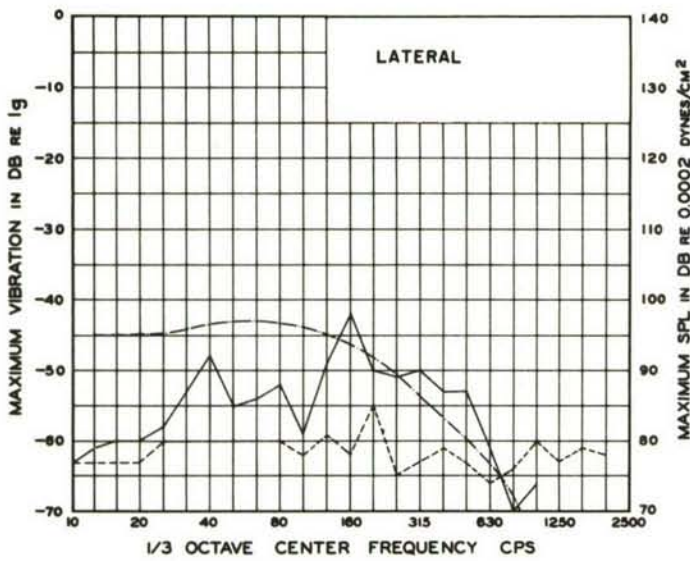


Figure 81.

Test No: 5050

Location: Command Destruct,  
-On Steerable Helix Array

--- Ambient Vibration  
— Noise Induced Vibration  
-.- Noise Level

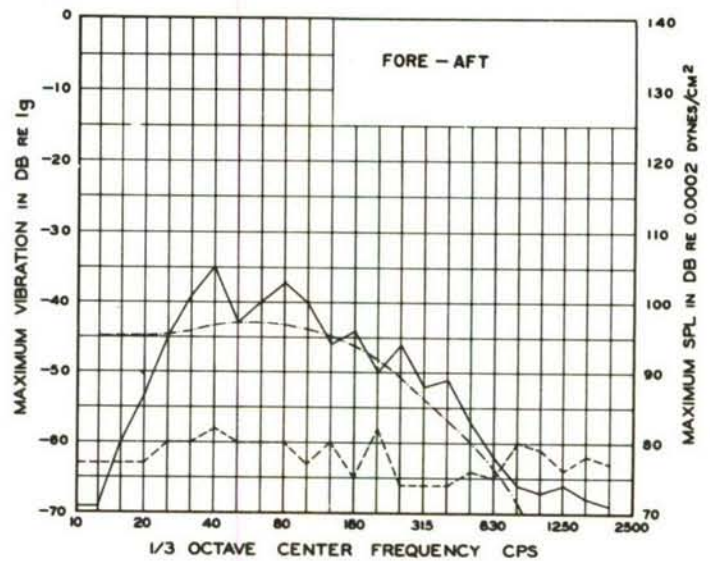


Figure 82.

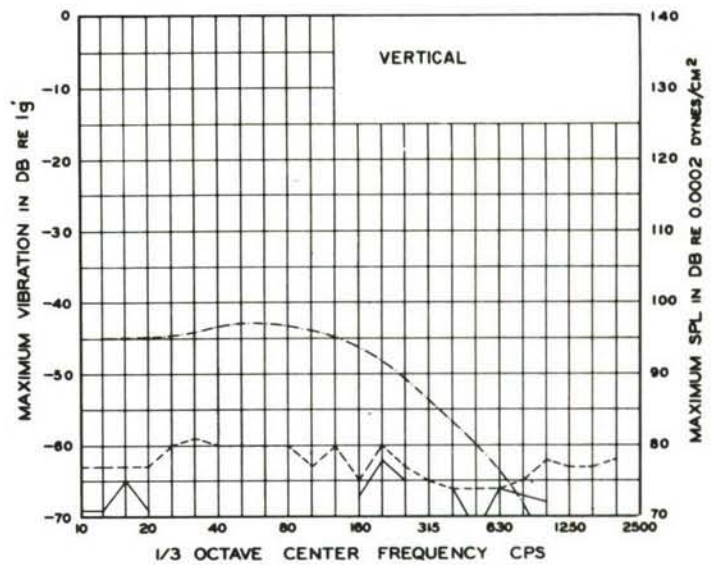


Figure 83.

Test No: 5050

Location: Command Destruct,  
-At Base of Gabriel Antenna

--- Ambient Vibration  
— Noise Induced Vibration  
-.- Noise Level

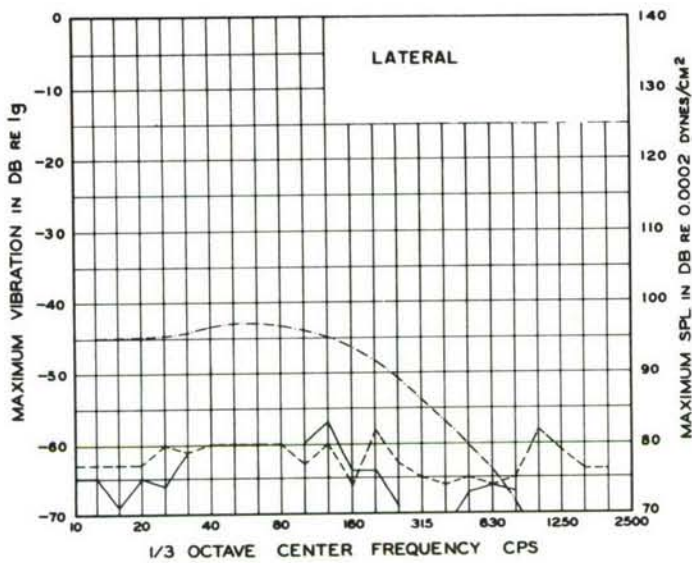


Figure 84.

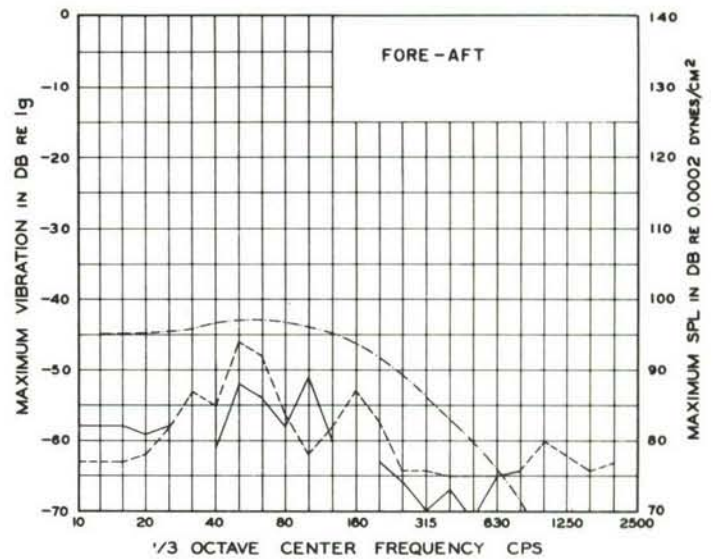


Figure 85.



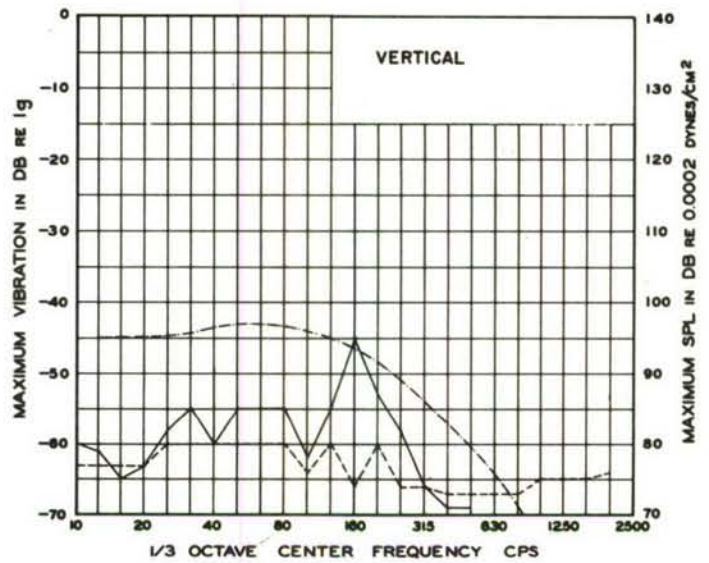


Figure 86.

Test No: 5050

Location: Command Destruct, -On  
Dish of RCA Tx. Steerable Antenna

--- Ambient Vibration  
— Noise Induced Vibration  
-.- Noise Level

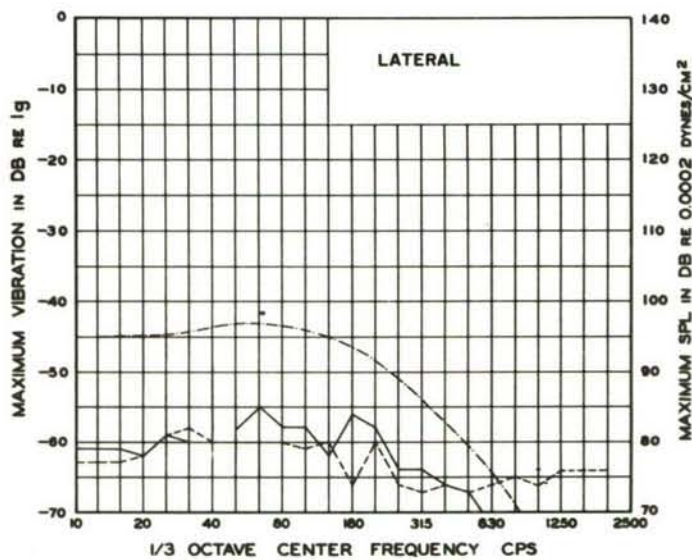


Figure 87.

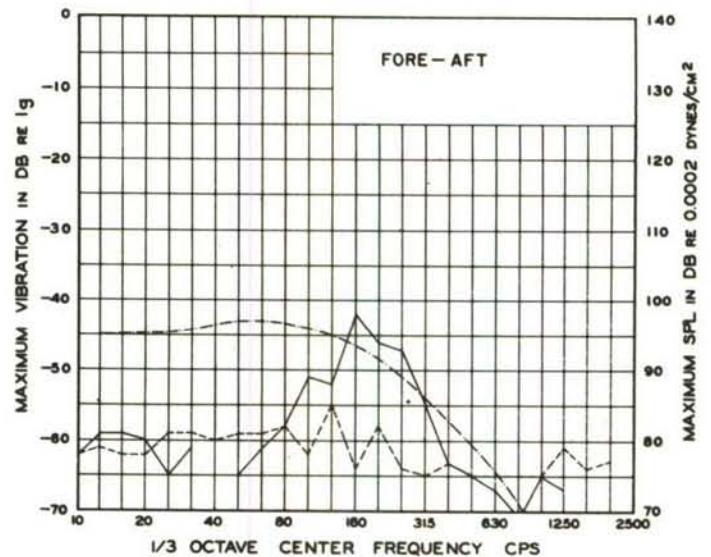


Figure 88.

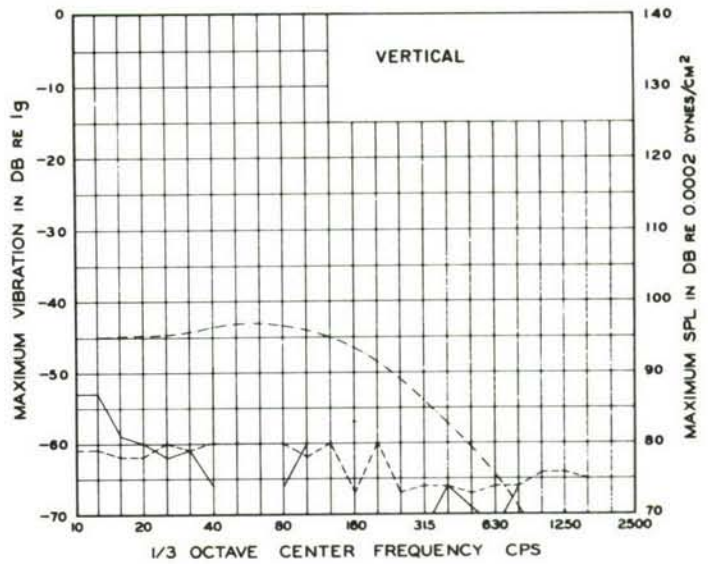


Figure 89.

Test No: 5050

Location: Command Destruct, -On  
Pod of RCA Tx. Steerable Antenna

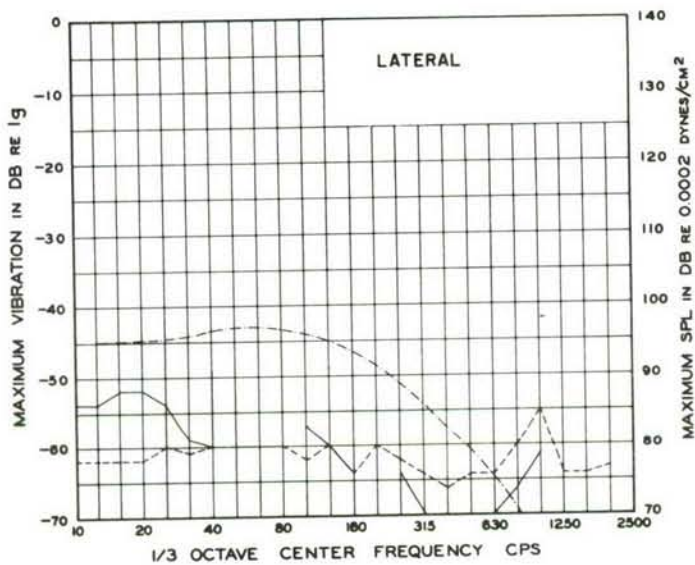


Figure 90.

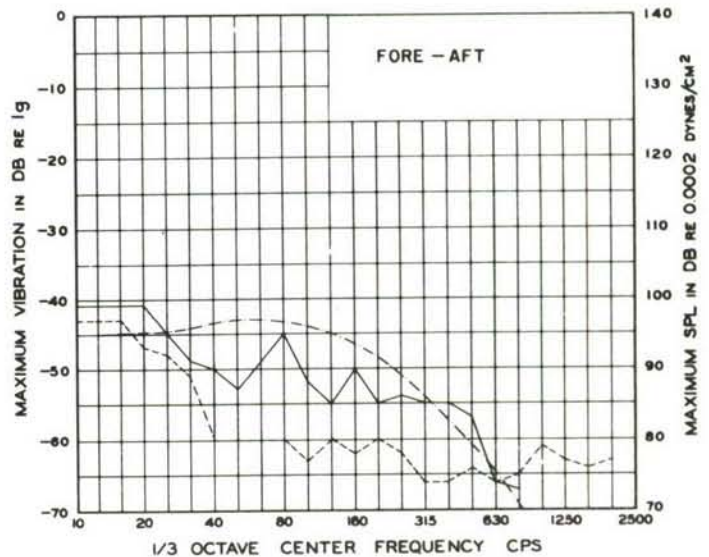


Figure 91.

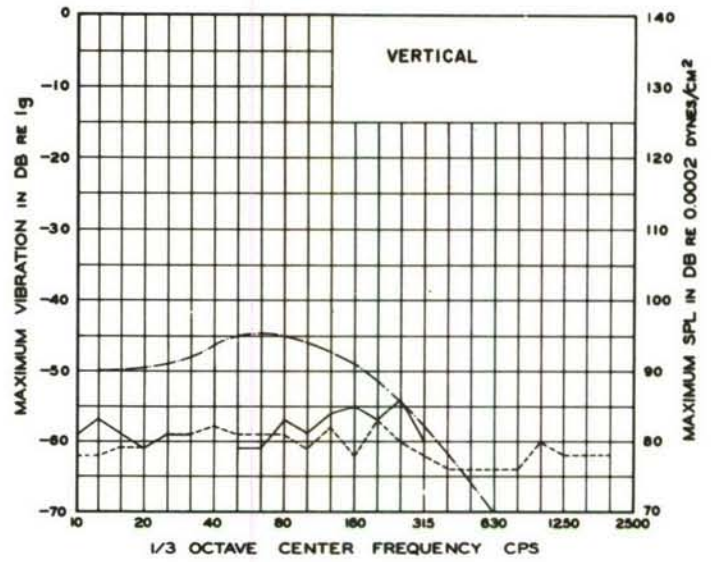


Figure 92.

Test No: 1262

Location: Command Destruct,  
-On Steerable Helix Array

--- Ambient Vibration  
— Noise Induced Vibration  
-.- Noise Level

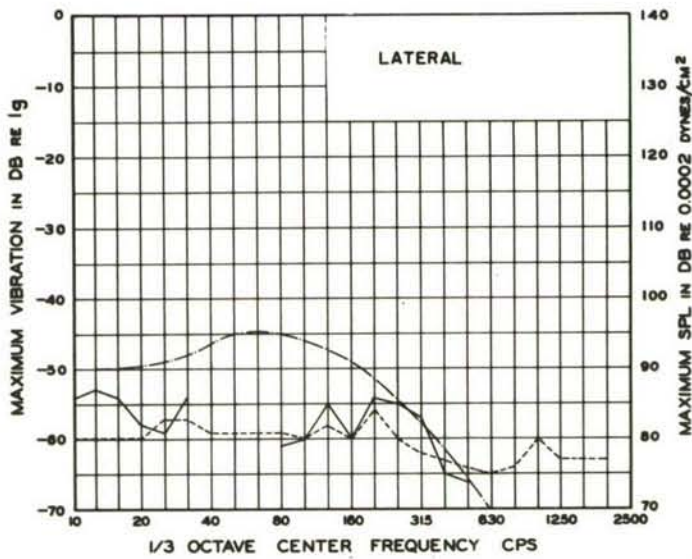


Figure 93.

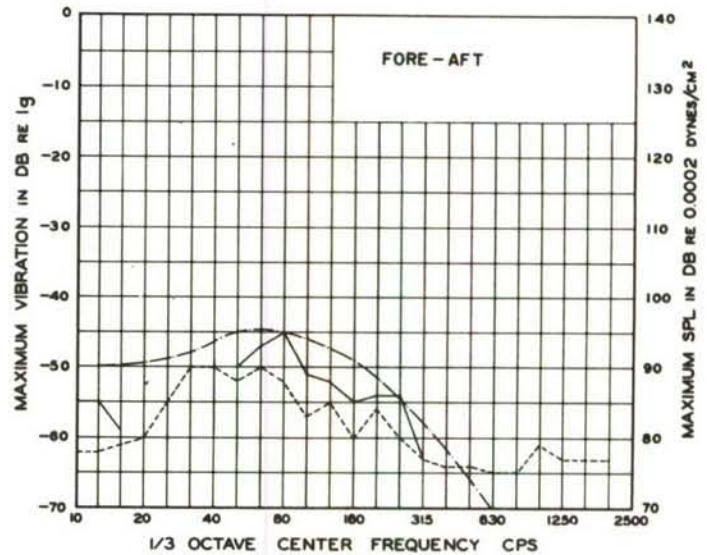


Figure 94.



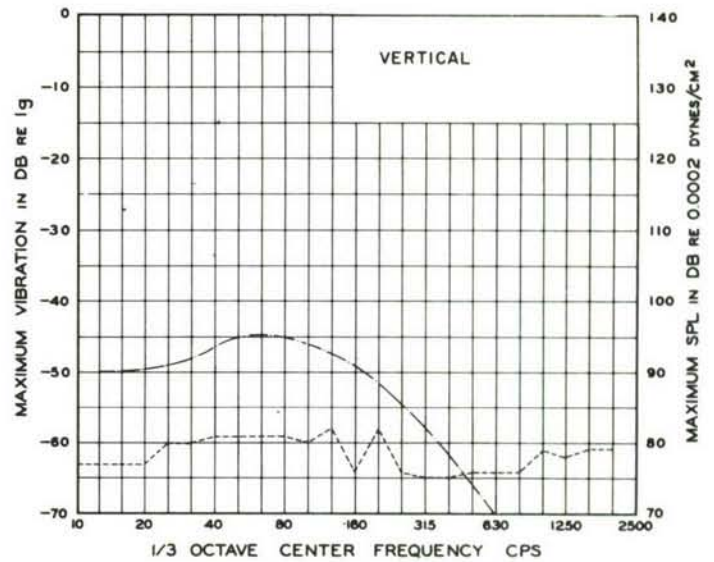


Figure 95.

Test No: 1262

Location: Command Destruct,  
-At Base of Gabriel Antenna

--- Ambient Vibration  
— Noise Induced Vibration  
... Noise Level

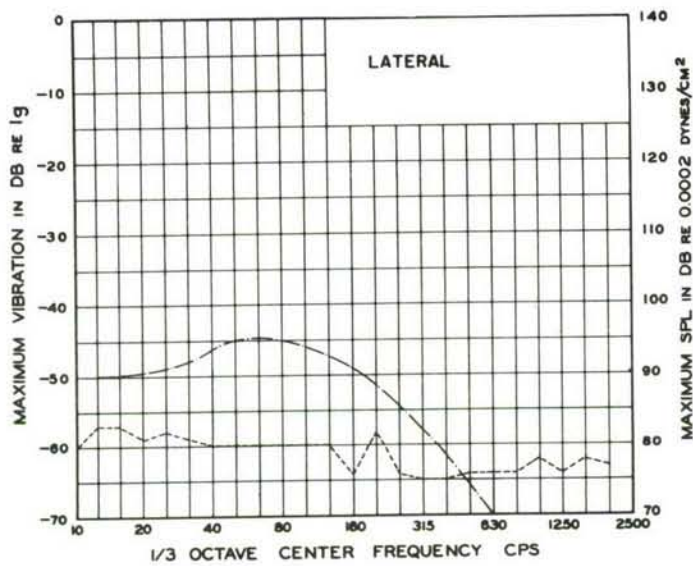


Figure 96.

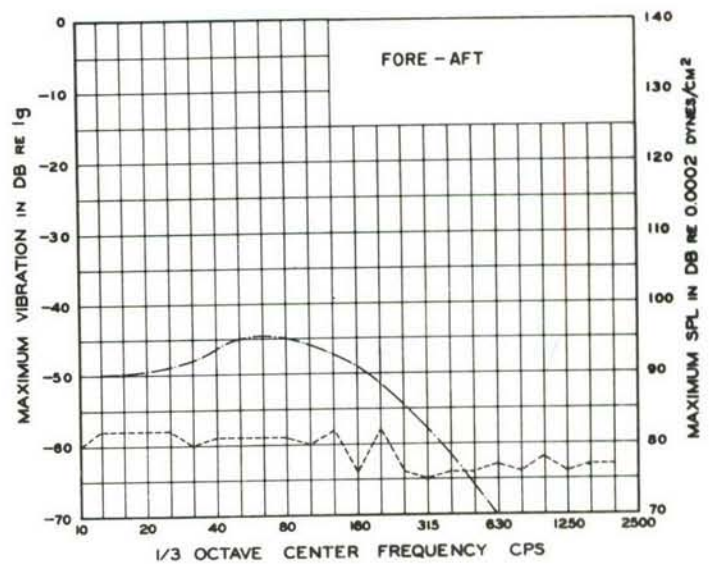


Figure 97.

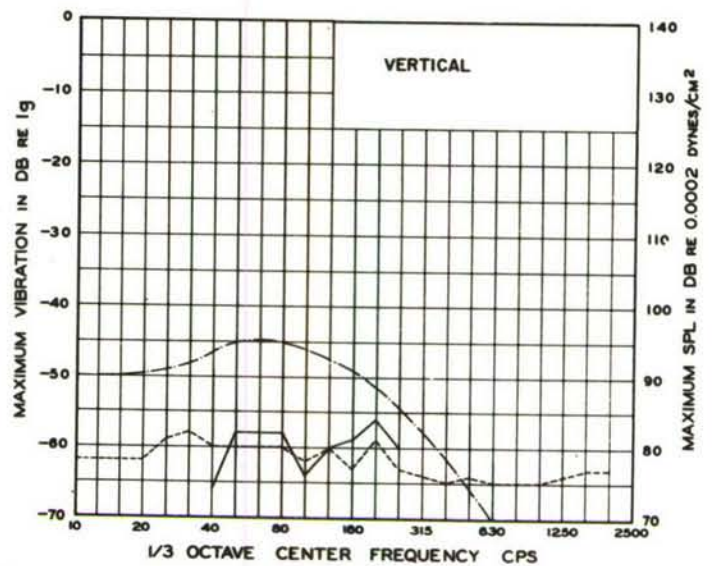


Figure 98.

Test No: 1262

Location: Command Destruct, -On Dish  
of RCA Steerable Tx. Antenna

- Ambient Vibration
- Noise Induced Vibration
- .- Noise Level

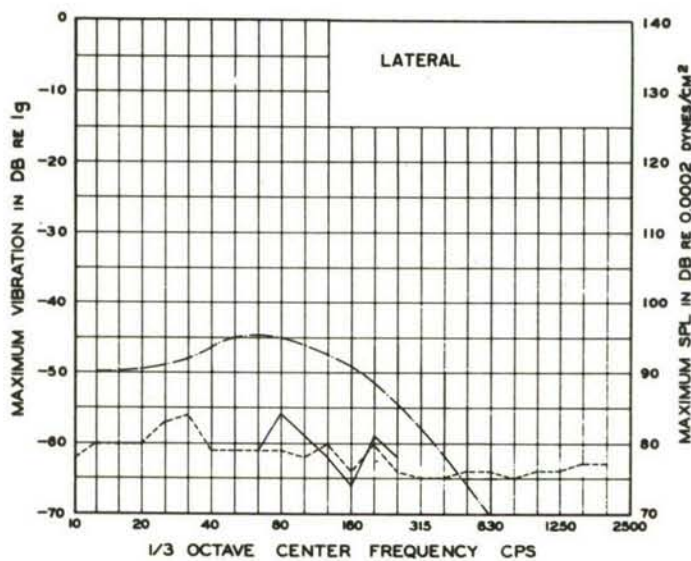


Figure 99.

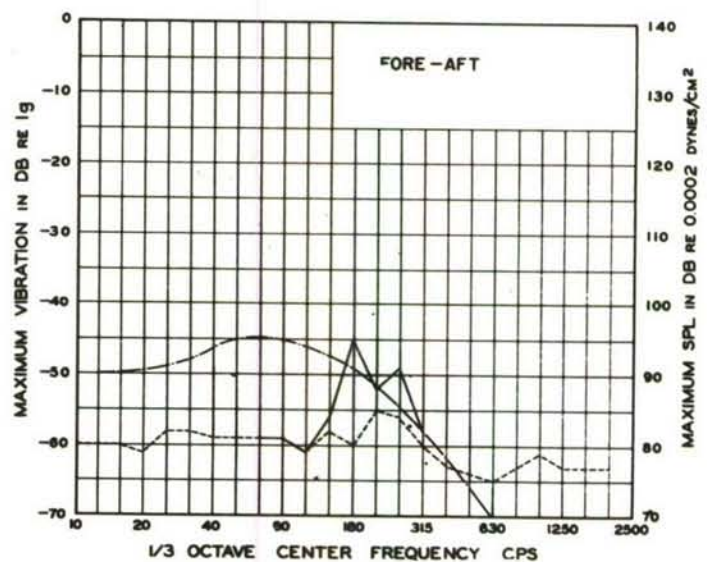


Figure 100.

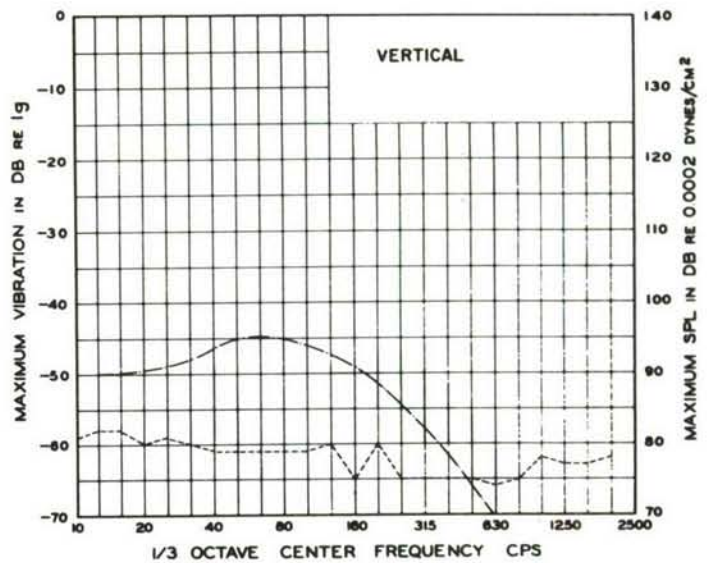


Figure 101.

Test No: 1262

Location: Command Destruct, -On Pod of  
RCA Steerable Tx. Antenna

--- Ambient Vibration  
— Noise Induced Vibration  
-.- Noise Level

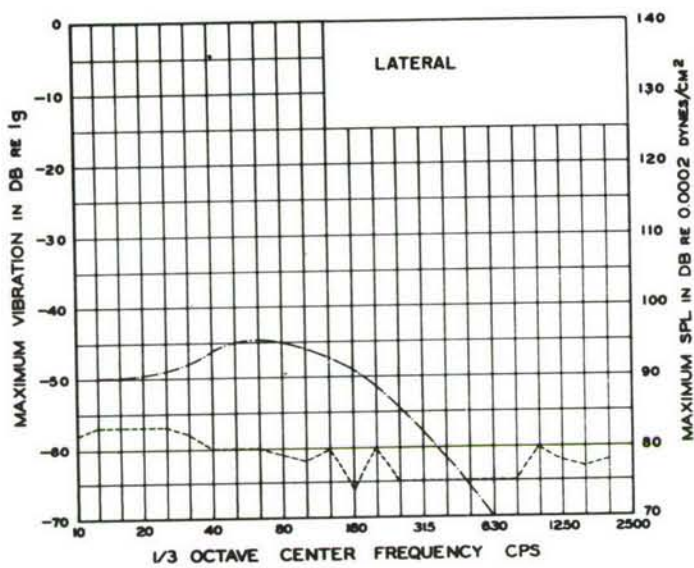


Figure 102.

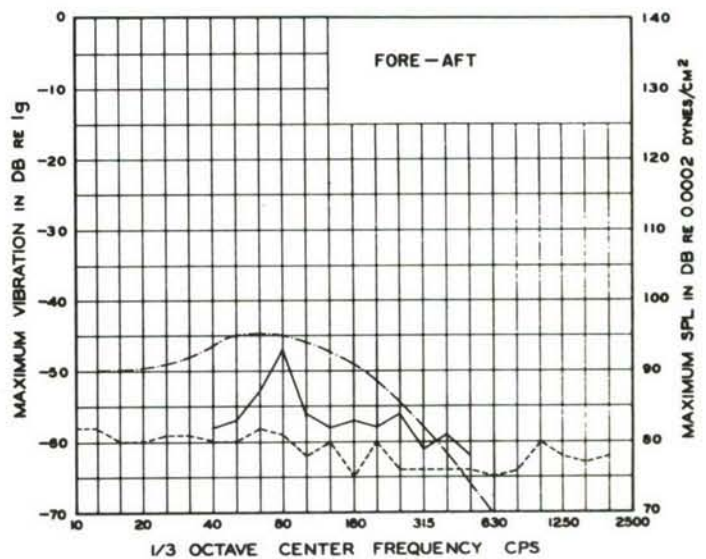


Figure 103.



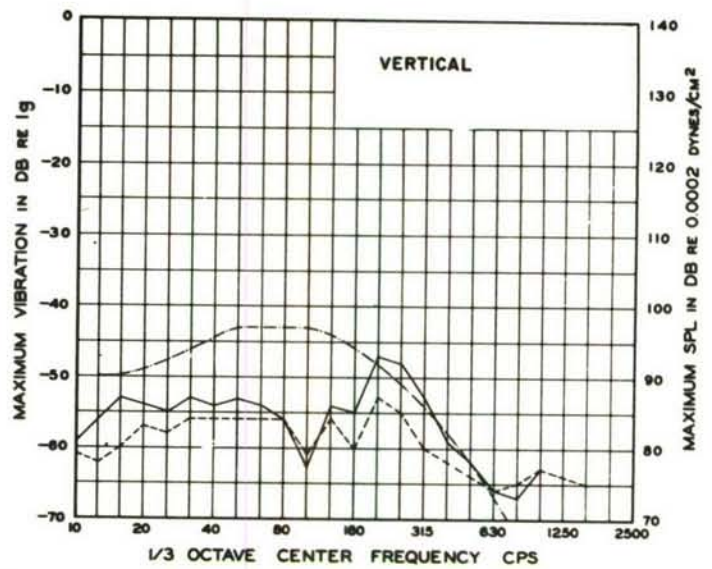


Figure 104.

Test No: 3212

Location: Command Destruct,  
-On Steerable Helix Array

--- Ambient Vibration  
— Noise Induced Vibration  
-.- Noise Level

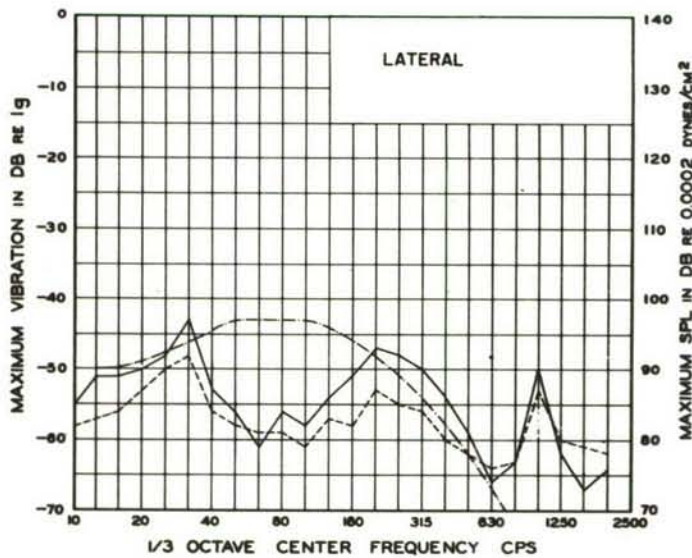


Figure 105.

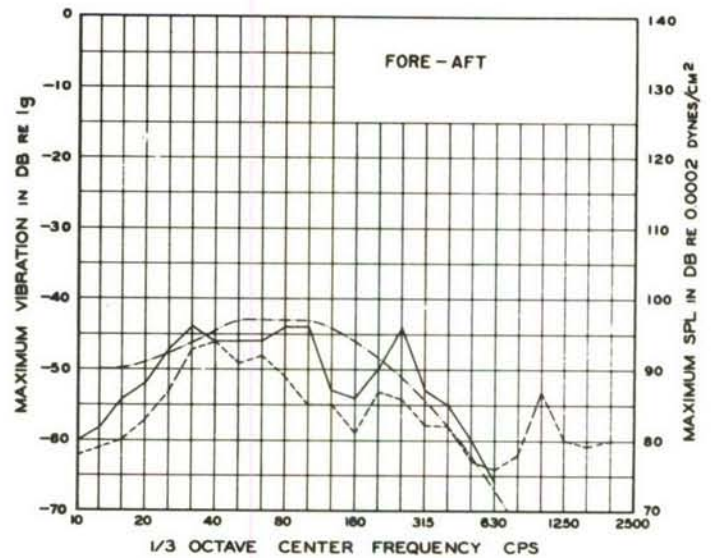


Figure 106.

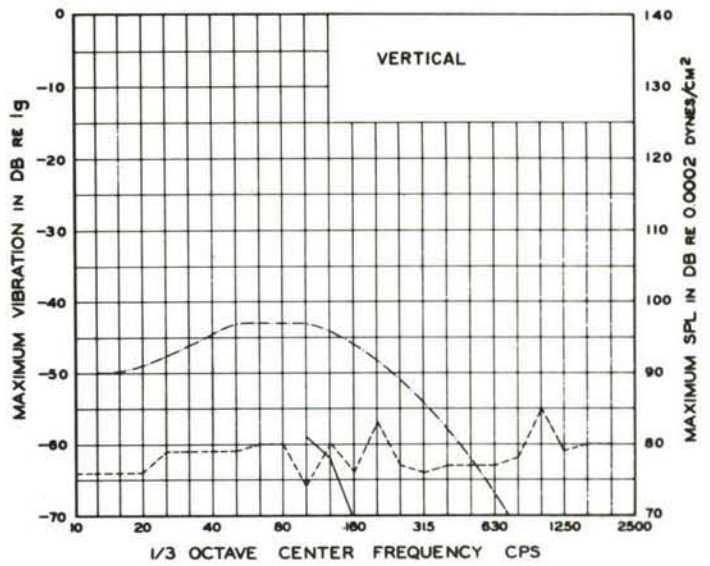


Figure 107.

Test No: 3212

Location: Command Destruct,  
-On Base of Gabriel Antenna

--- Ambient Vibration  
— Noise Induced Vibration  
-.- Noise Level

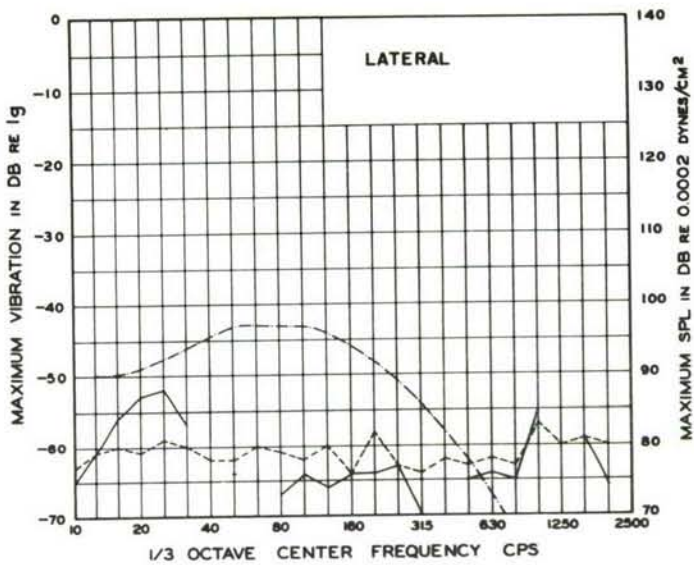


Figure 108.

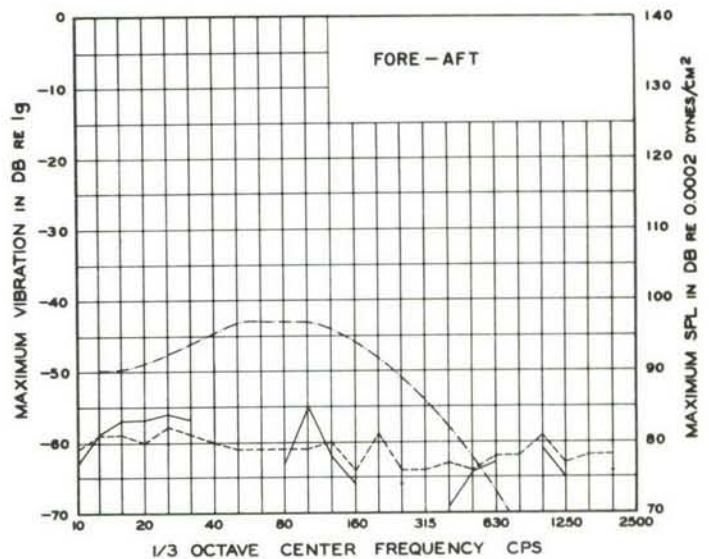


Figure 109.

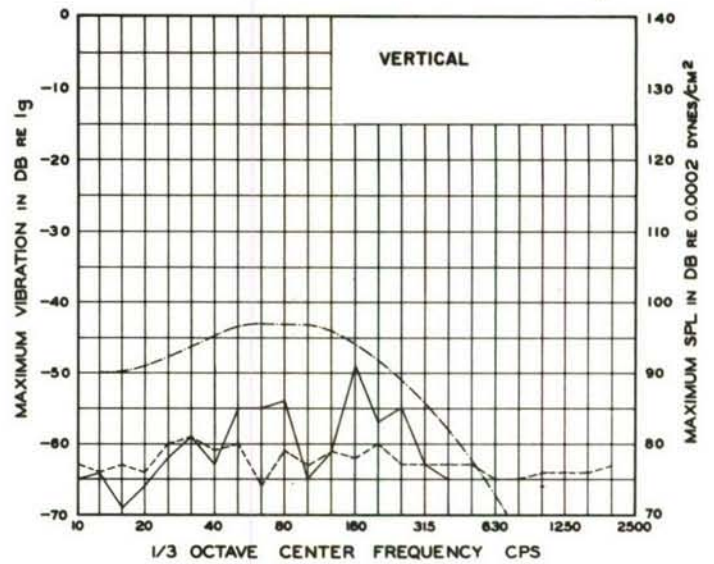


Figure 110.

Test No: 3212

Location: Command Destruct, -On Dish  
of RCA Steerable Tx. Antenna

- Ambient Vibration
- Noise Induced Vibration
- .-.- Noise Level

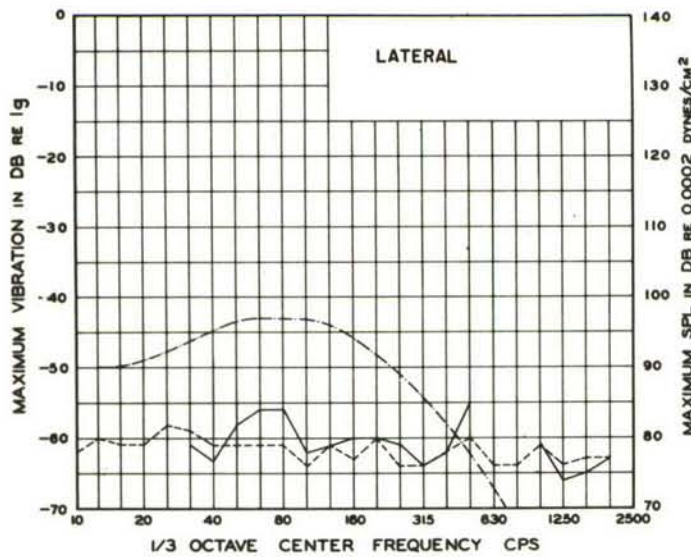


Figure 111.

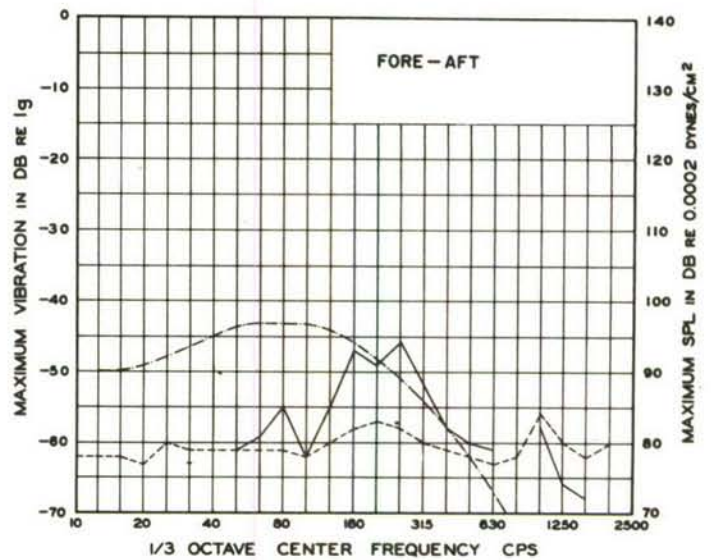


Figure 112.



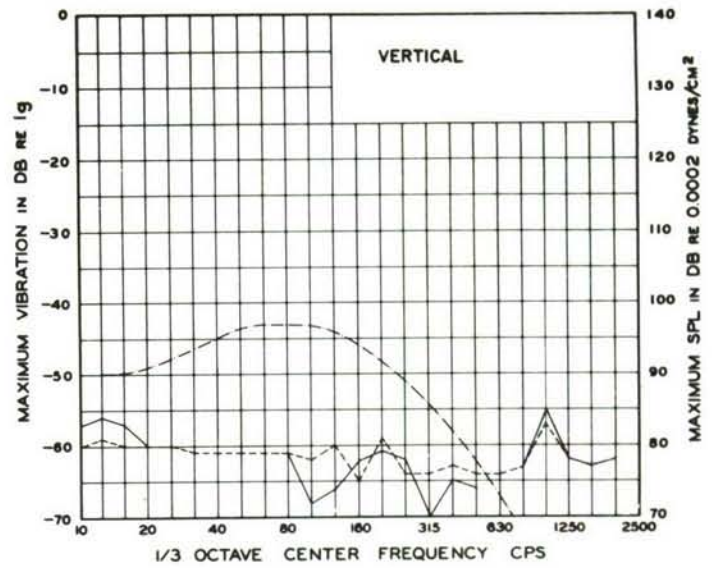


Figure 113.

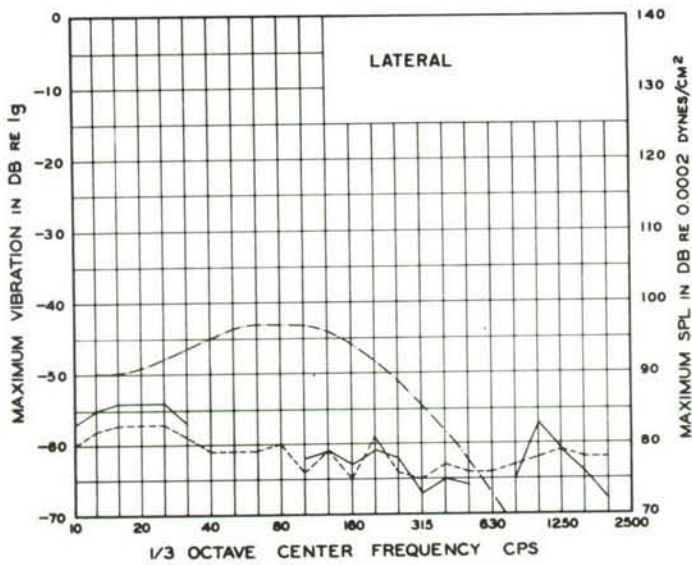


Figure 114.

Test No: 3212

Location: Command Destruct, -On Pod  
of RCA Steerable Tx. Antenna

--- Ambient Vibration  
— Noise Induced Vibration  
-.- Noise Level

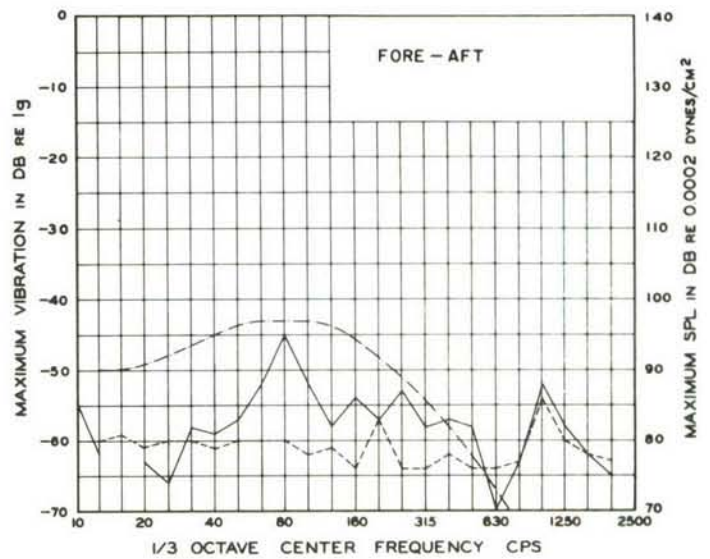


Figure 115.

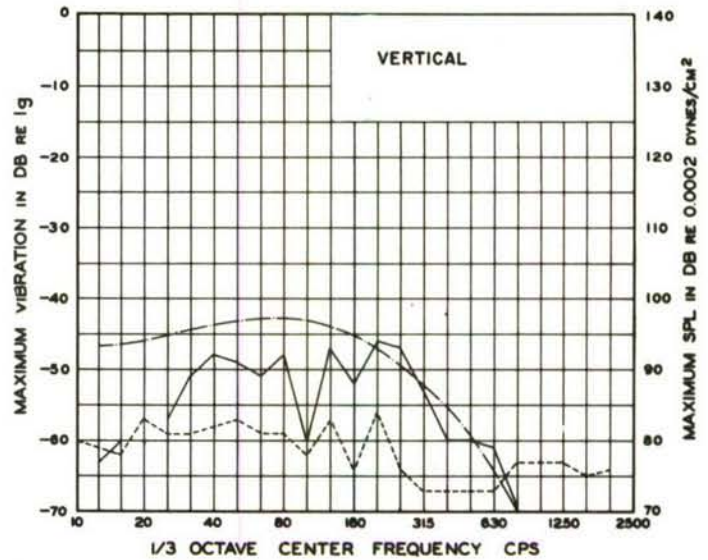


Figure 116.

Test No: 1803

Location: Command Destruct,  
-On Steerable Helix Array

--- Ambient Vibration  
— Noise Induced Vibration  
-.- Noise Level

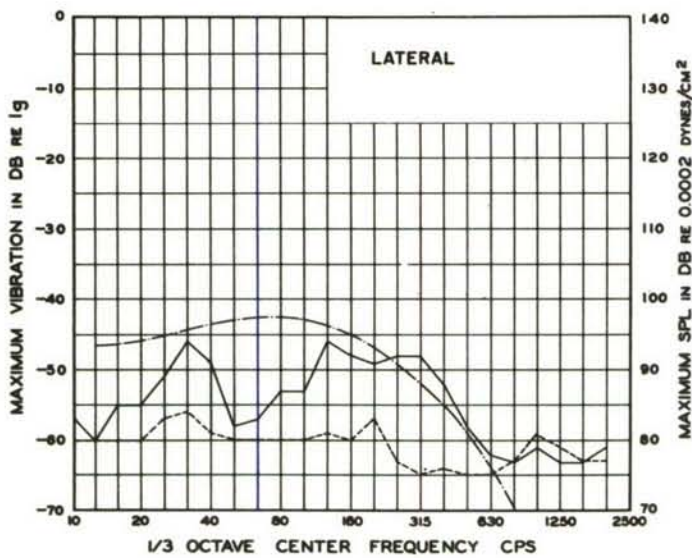


Figure 117.

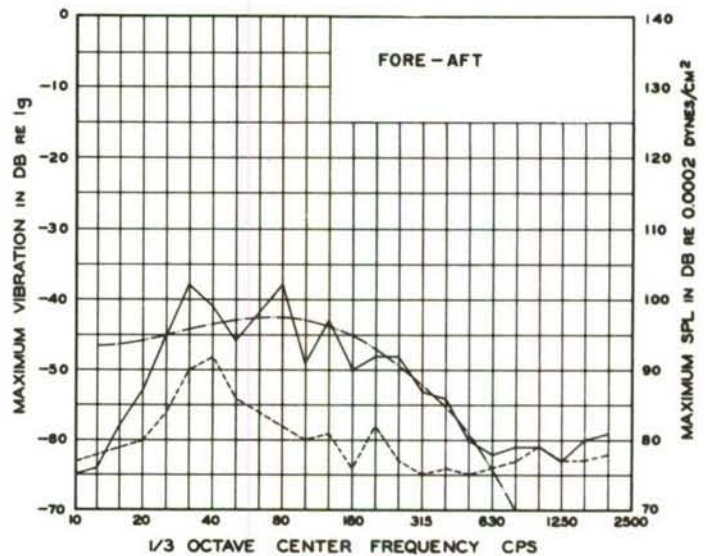


Figure 118.

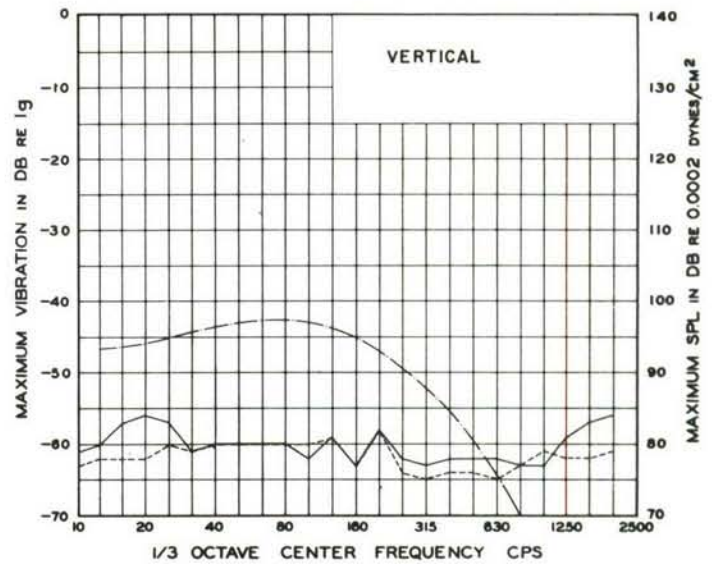


Figure 119.

Test No: 1803

Location: Command Destruct,  
-On Base of Gabriel Antenna

--- Ambient Vibration  
— Noise Induced Vibration  
-.- Noise Level

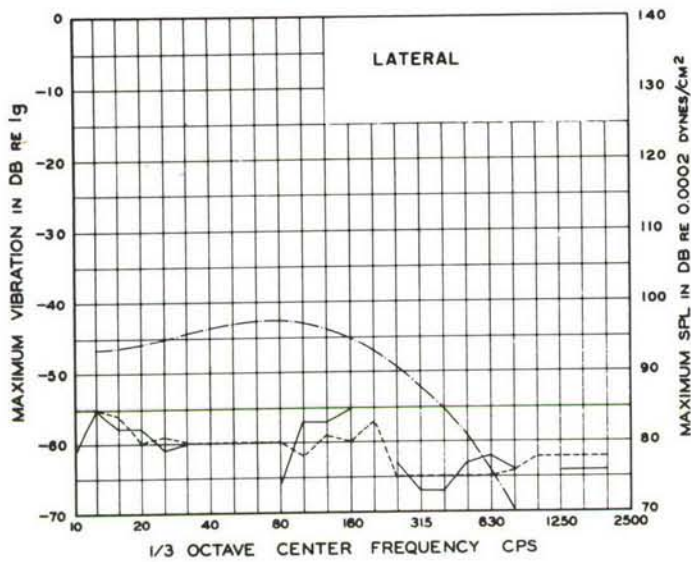


Figure 120.

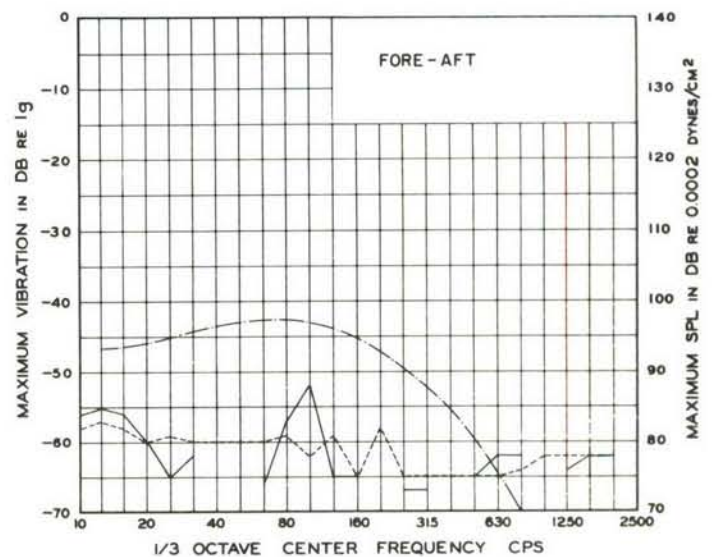


Figure 121



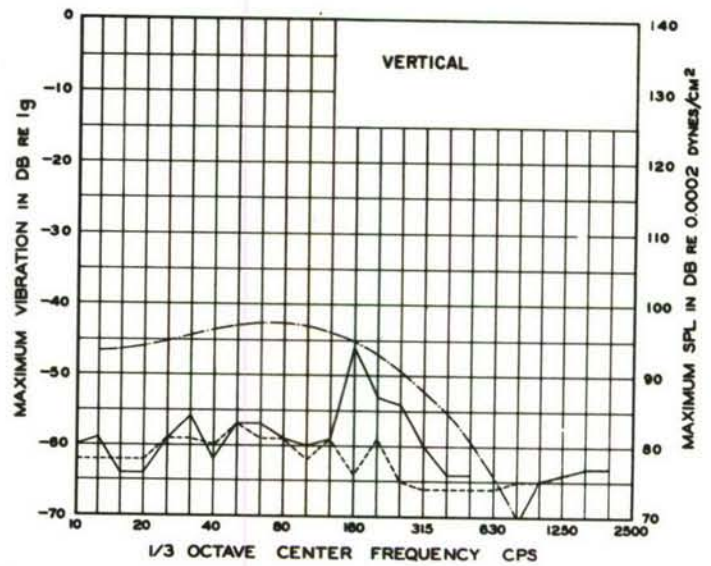


Figure 122.

Test No: 1803

Location: Command Destruct, -On Dish  
of RCA Steerable Tx. Antenna

--- Ambient Vibration  
— Noise Induced Vibration  
-.- Noise Level

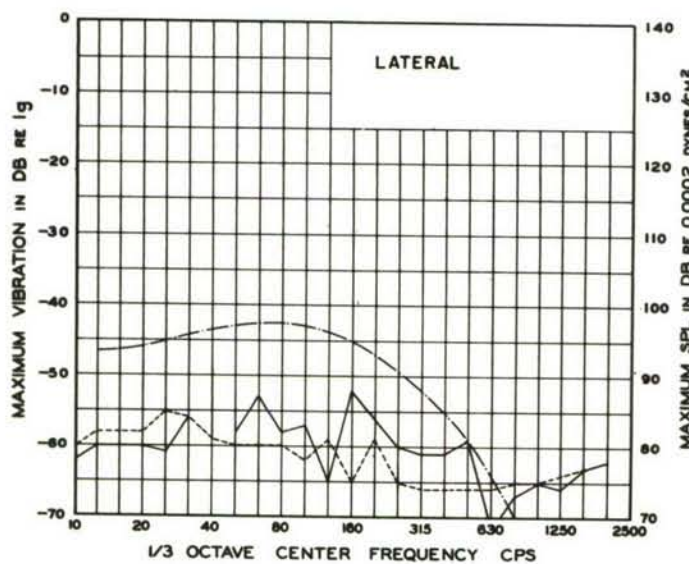


Figure 123.

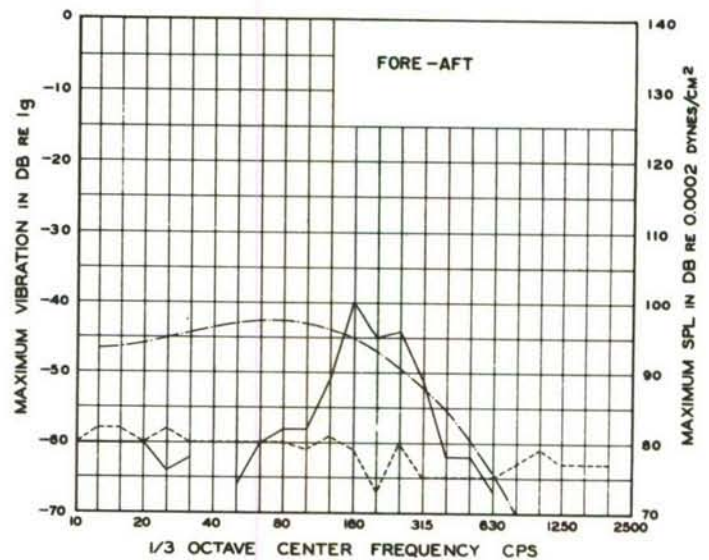


Figure 124.

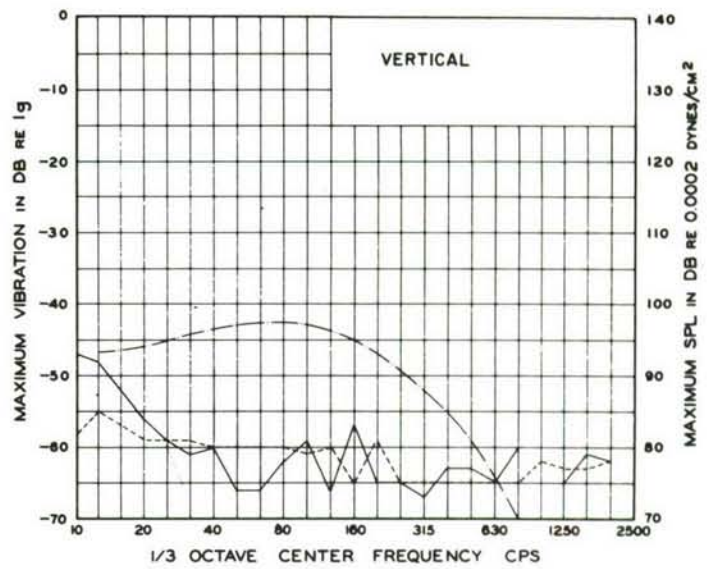


Figure 125.

Test No: 1803

Location: Command Destruct, -On Pod  
of RCA Steerable Tx. Antenna

--- Ambient Vibration  
— Noise Induced Vibration  
-.- Noise Level

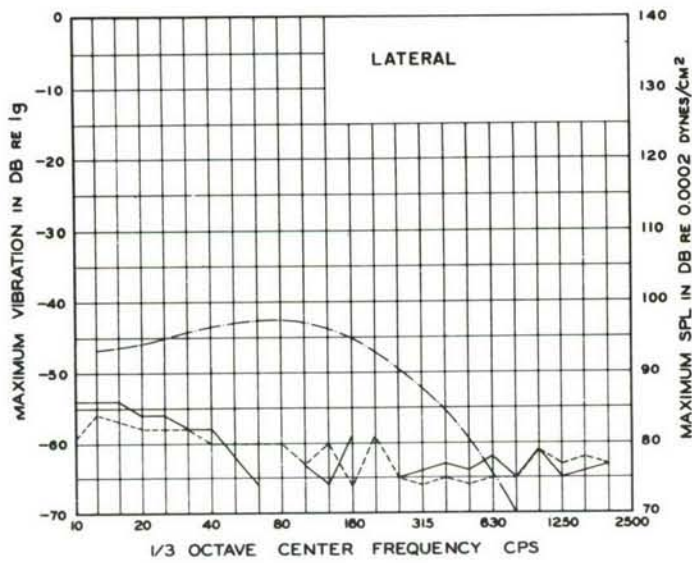


Figure 126.

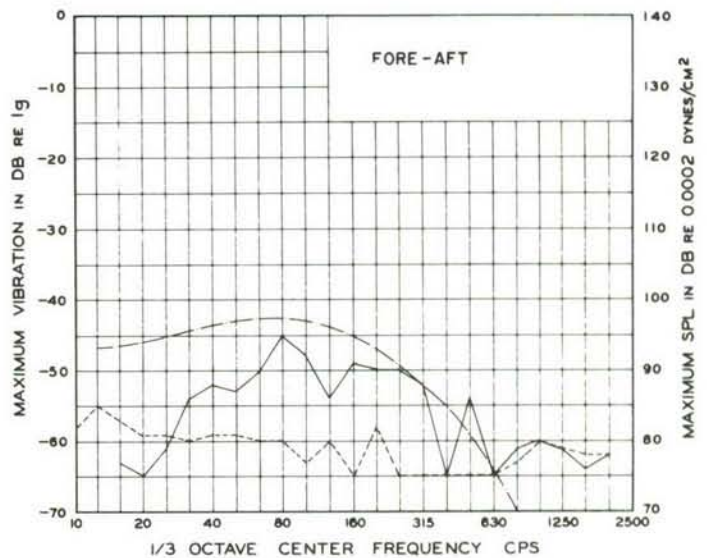


Figure 127.

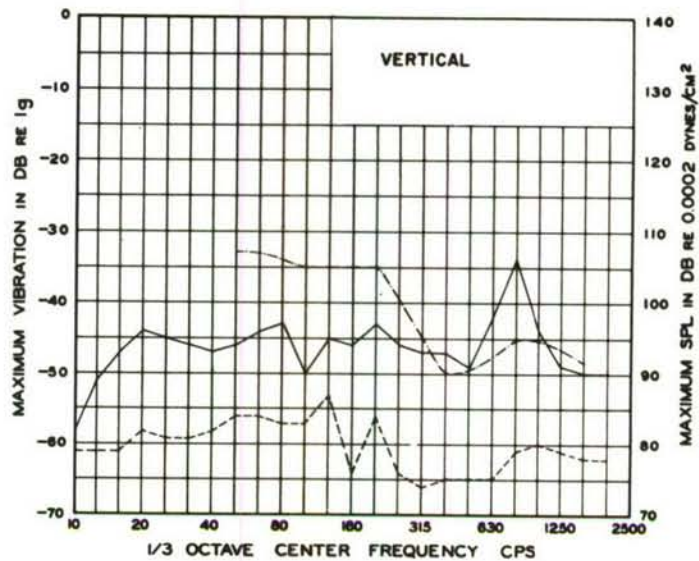


Figure 128.

Test No: 3765

Location: Azusa MKI, -On Pedestal  
of  $X_C$  Receiving Antenna

--- Ambient Vibration  
— Noise Induced Vibration  
-.- Noise Level

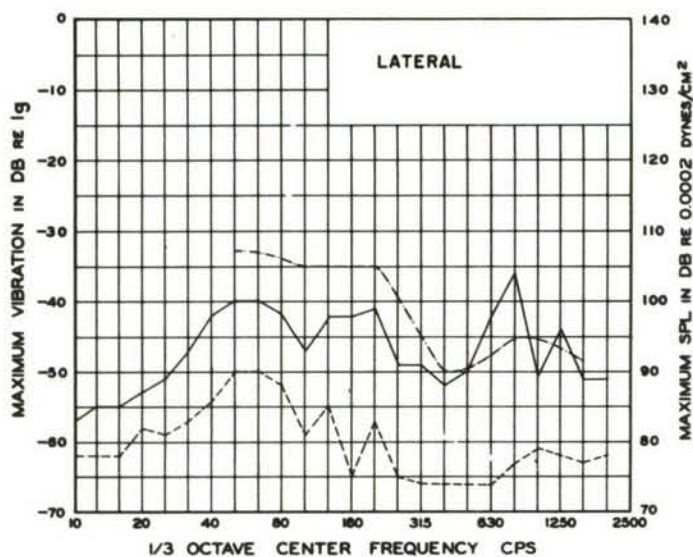


Figure 129.

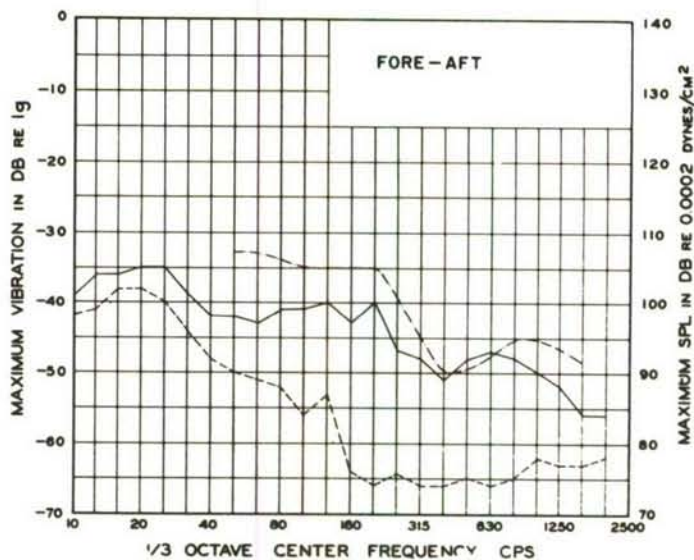


Figure 130.



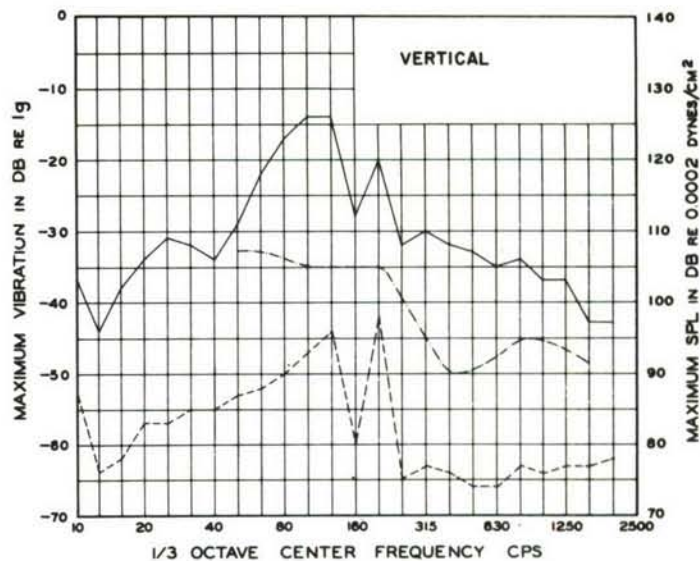


Figure 131.

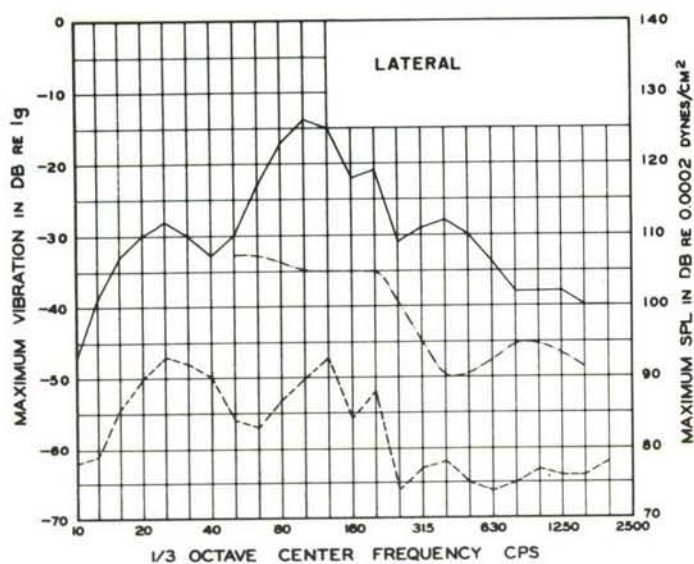


Figure 132.

Test No: 3765

Location: Azusa MKI, -On Dish  
of  $X_c$  Receiving Antenna

--- Ambient Vibration  
— Noise Induced Vibration  
-.- Noise Level

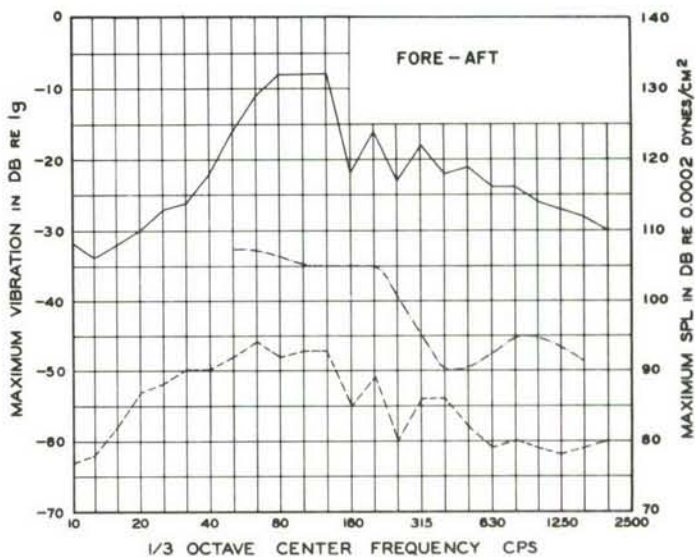


Figure 133.

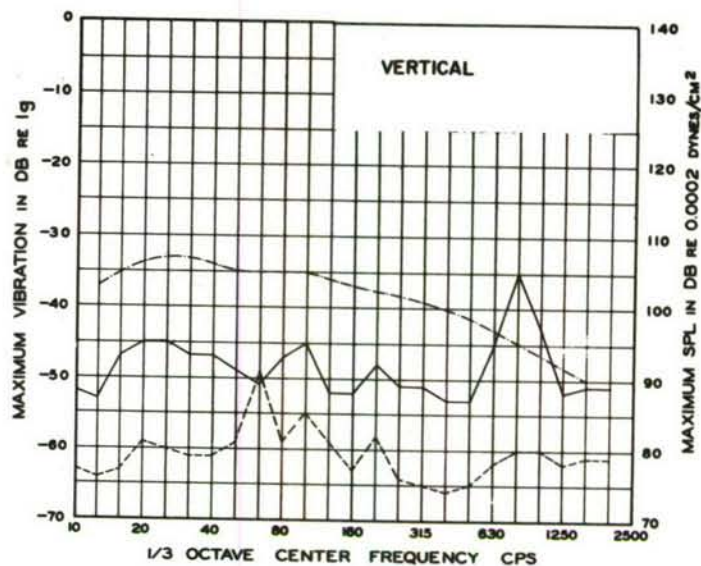


Figure 134.

Test No: 1252

Location: Azusa MKI, -On Pedestal of  
X<sub>C</sub> Receiving Antenna

--- Ambient Vibration  
— Noise Induced Vibration  
- · - Noise Level

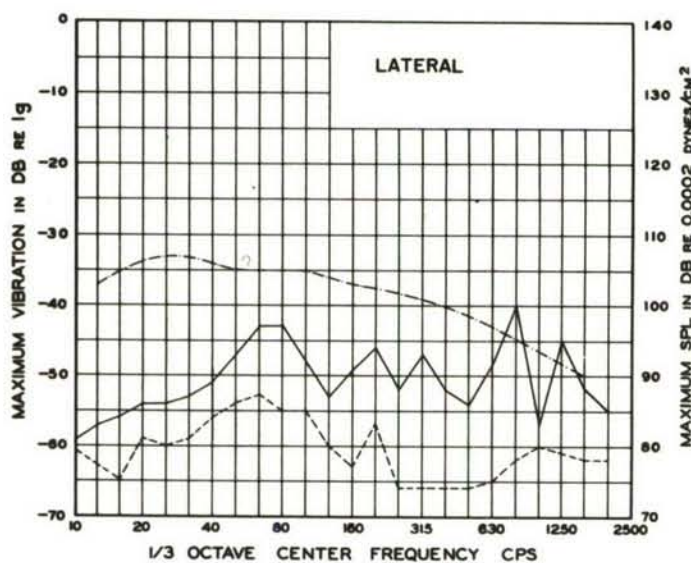


Figure 135.

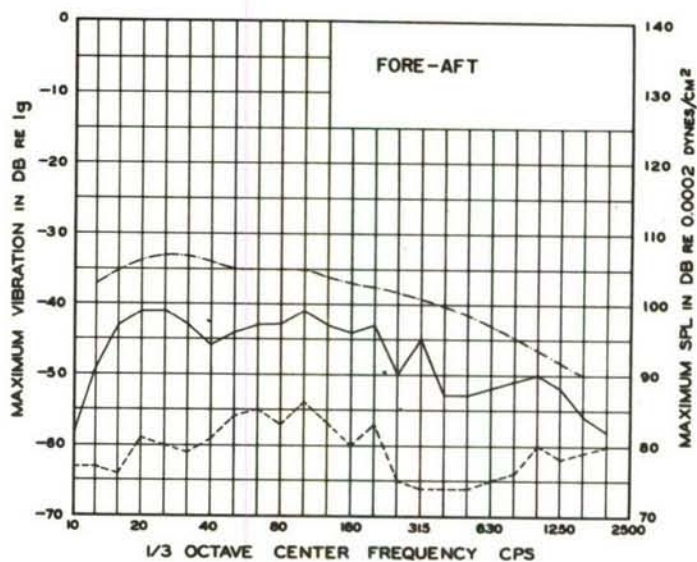


Figure 136.

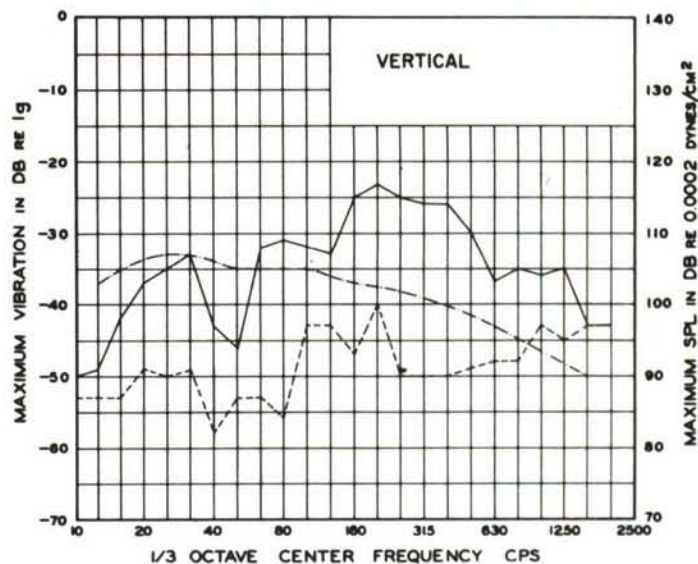


Figure 137.

Test No: 1252

Location: Azusa MKI, -On Dish of  
X<sub>c</sub> Receiving Antenna

--- Ambient Vibration  
— Noise Induced Vibration  
-.- Noise Level

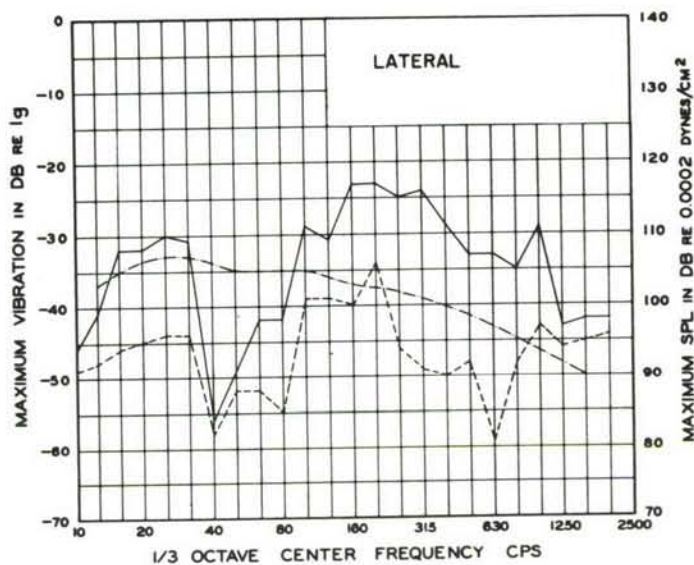


Figure 138.

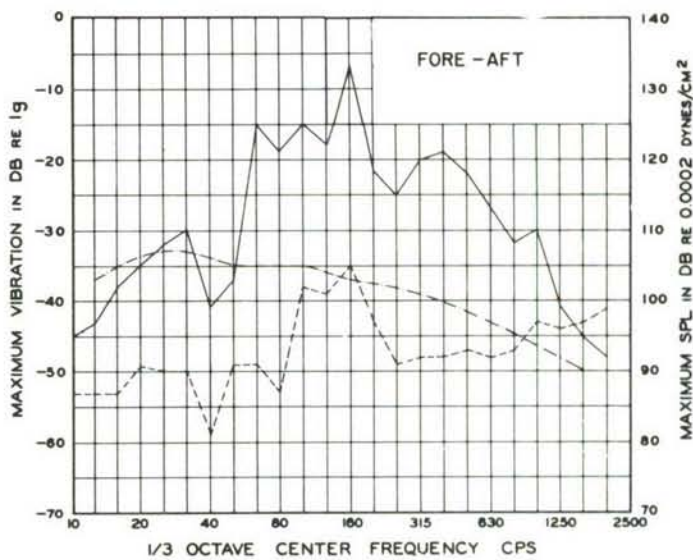


Figure 139.



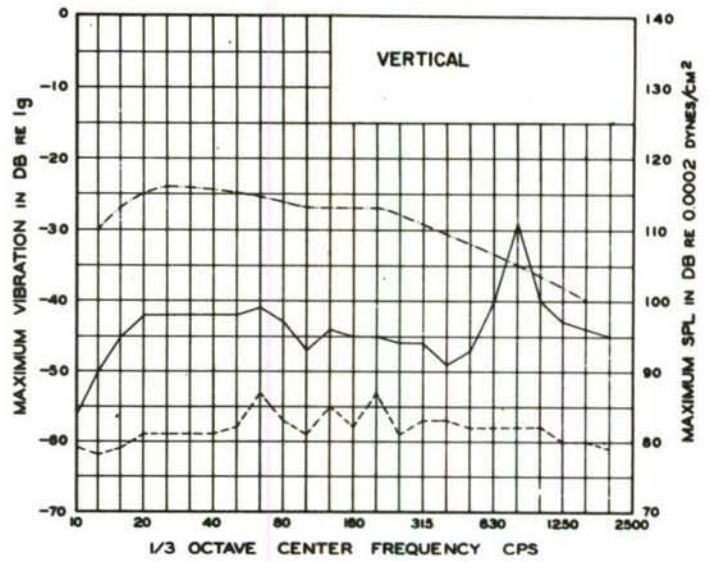


Figure 140.

Test No: 1804

Location: Azusa MKI, -On Pedestal of  
X<sub>C</sub> Receiving Antenna

--- Ambient Vibration  
— Noise Induced Vibration  
-.- Noise Level

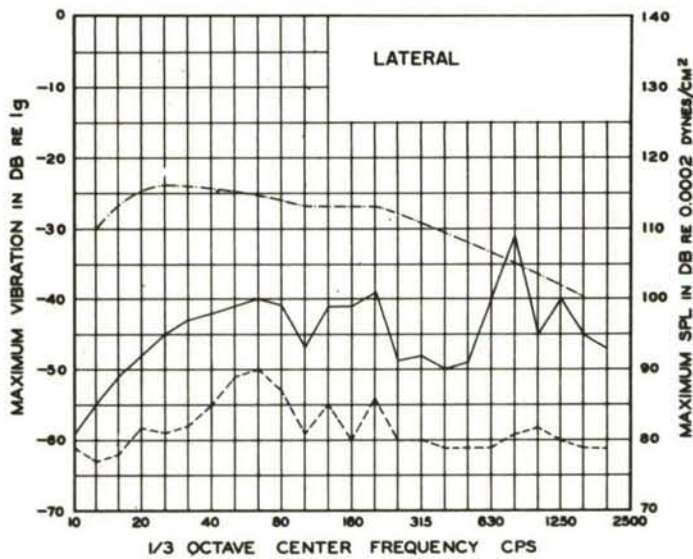


Figure 141.

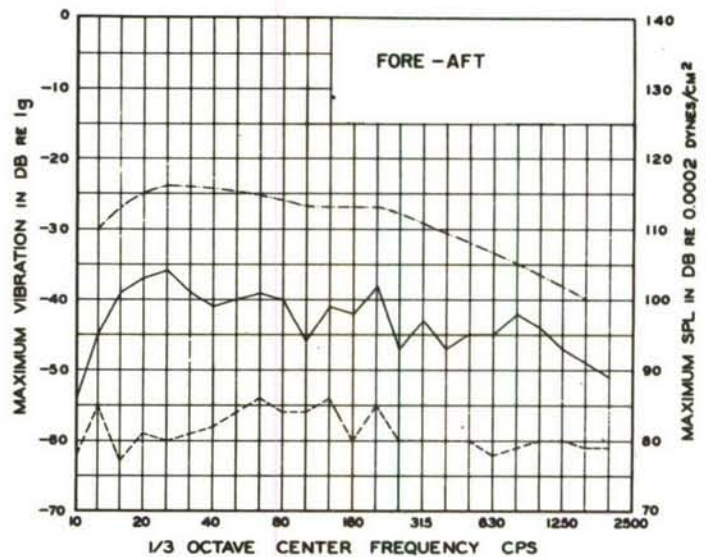


Figure 142.

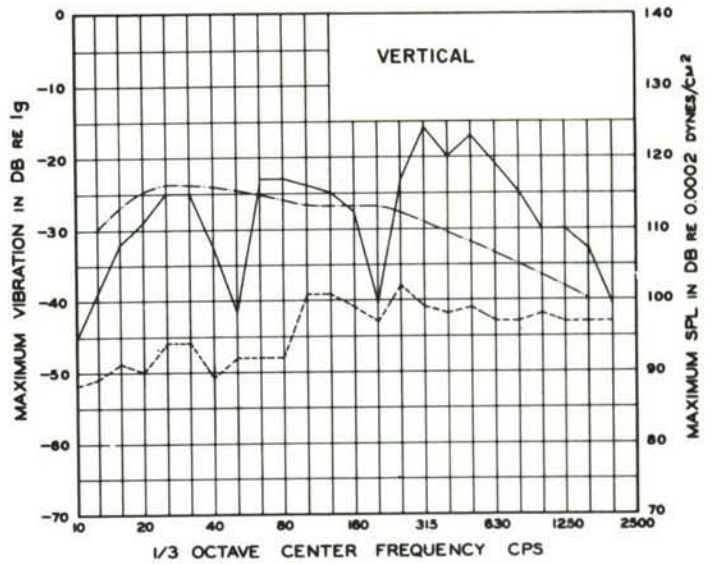


Figure 143.

Test No: 1804

Location: Azusa MKI, -On Dish of X<sub>C</sub>  
Receiving Antenna

--- Ambient Vibration  
— Noise Induced Vibration  
-.-.- Noise Level

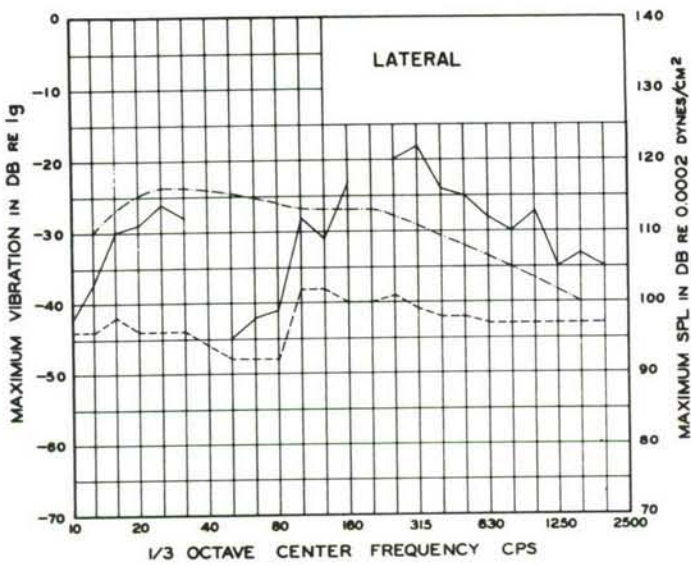


Figure 144.

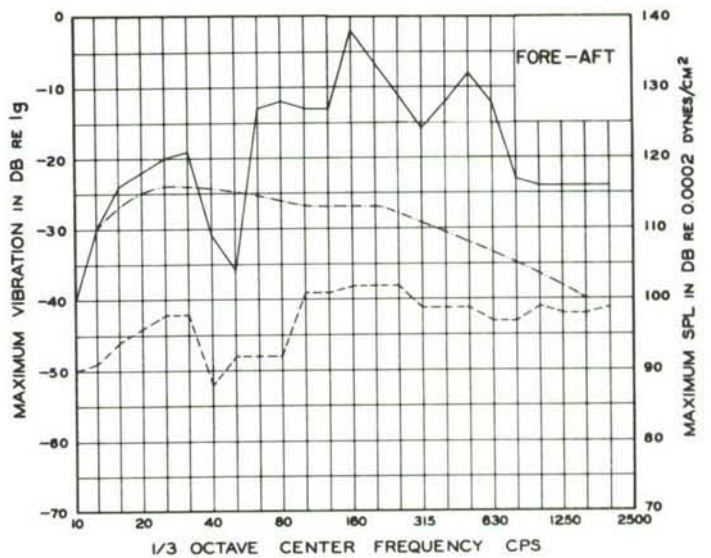


Figure 145.

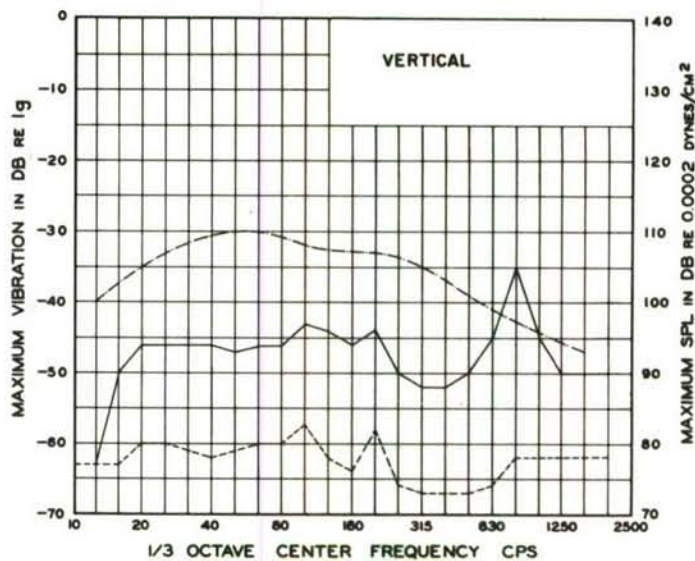


Figure 146.

Test No: 3764

Location: Azusa MKI, -On Pedestal  
of  $X_c$  Receiving Antenna

--- Ambient Vibration  
— Noise Induced Vibration  
-.- Noise Level

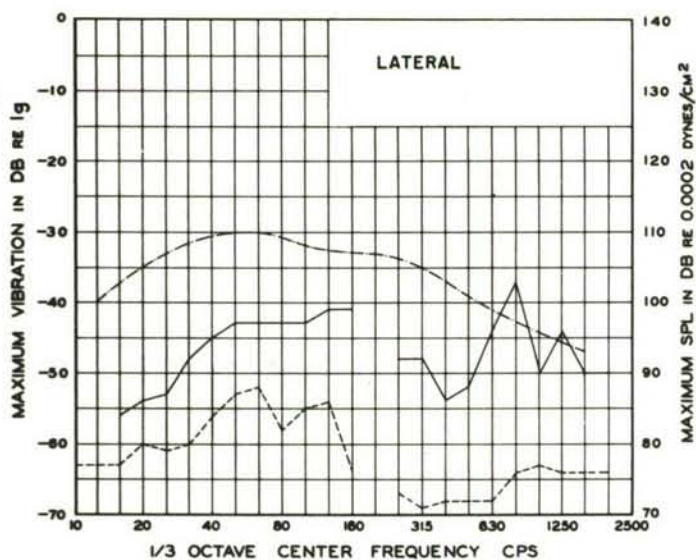


Figure 147.

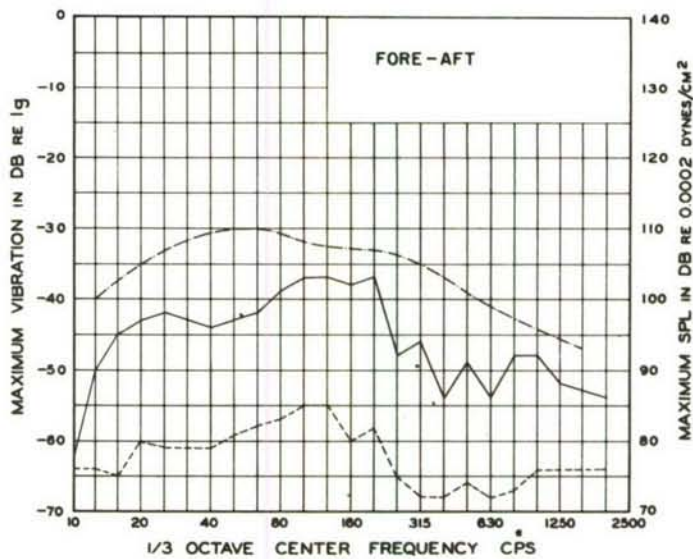


Figure 148.



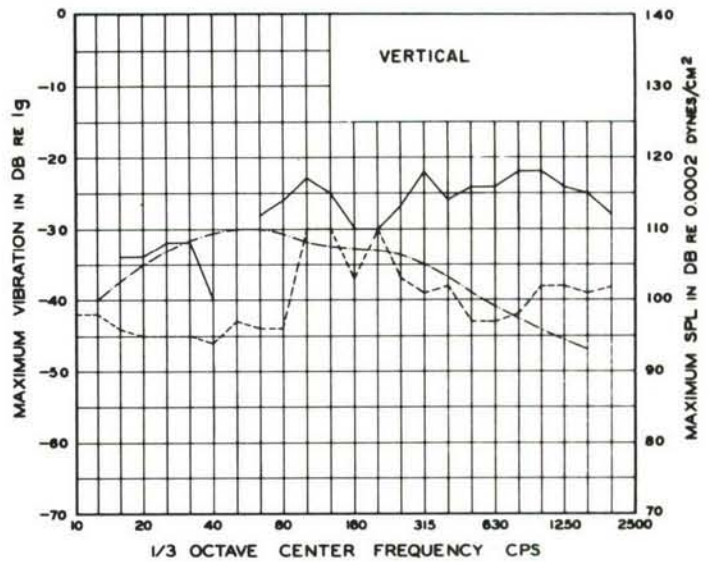


Figure 149.

Test No: 3764

Location: Azusa MKI, -On Dish  
of  $X_c$  Receiving Antenna

--- Ambient Vibration  
— Noise Induced Vibration  
-.-.- Noise Level

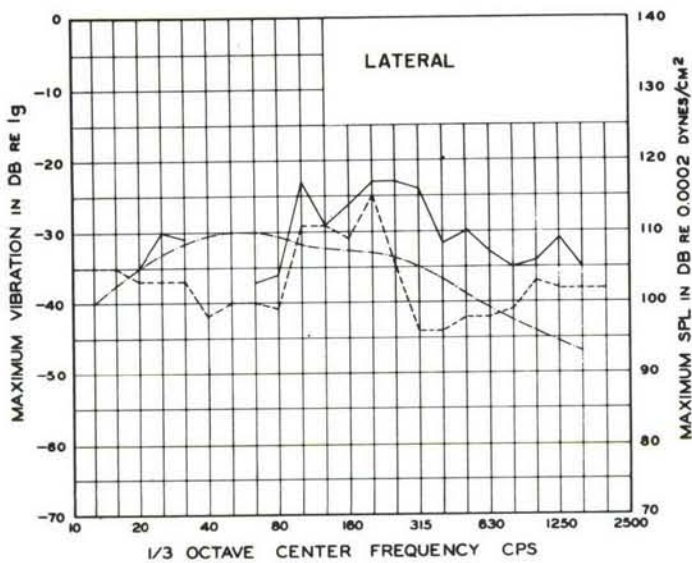


Figure 150.

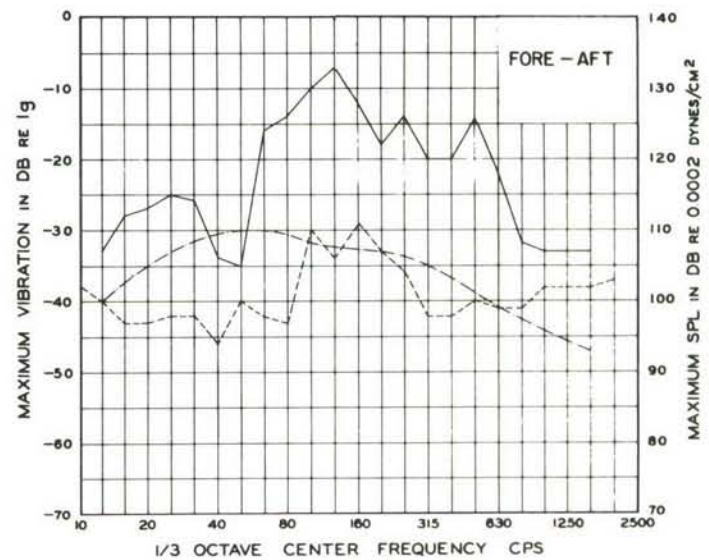


Figure 151.

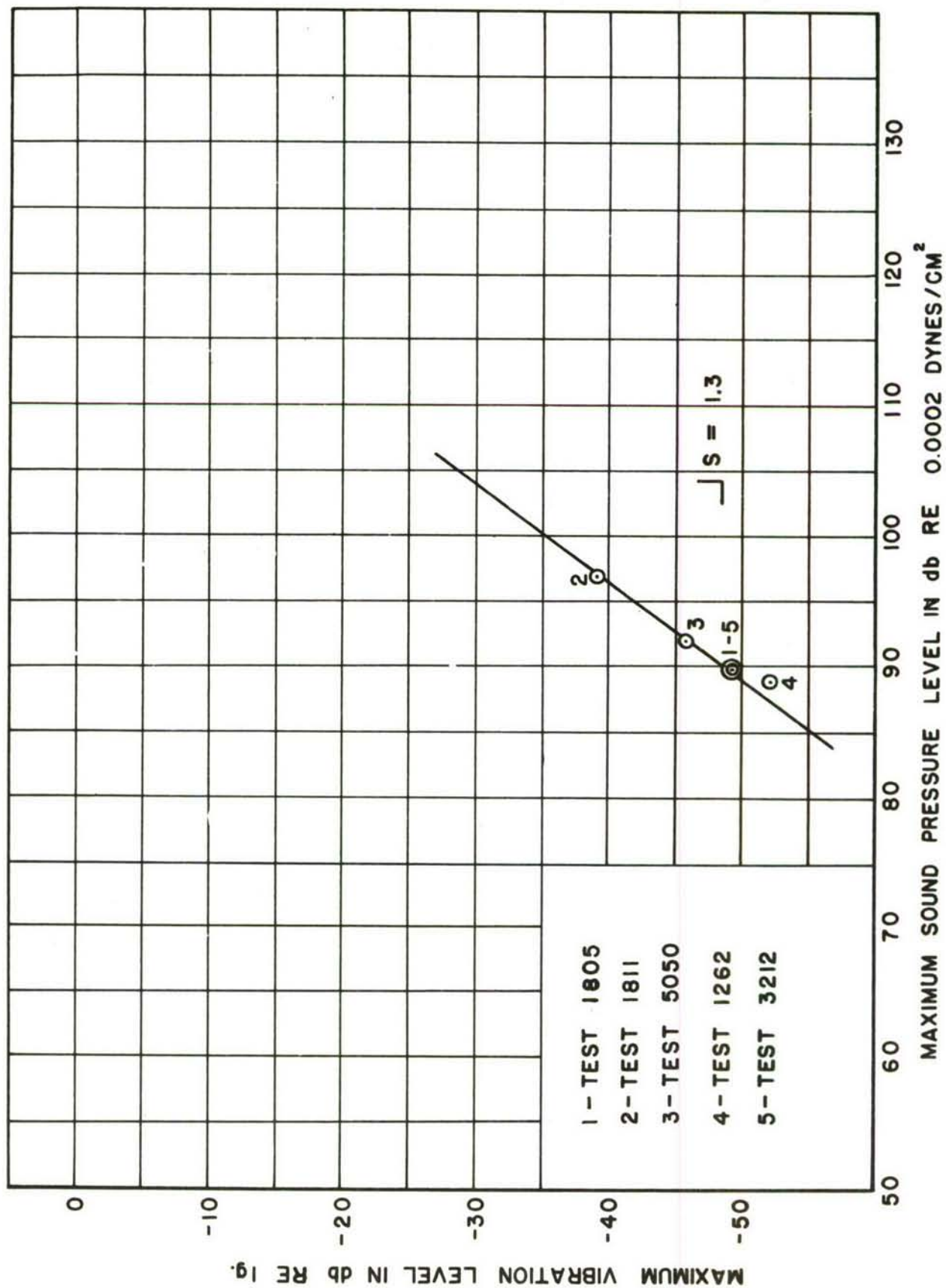


Figure 152. Maximum Vibration Level vs Maximum Sound Pressure Level, Steerable Tx Antenna Dish, 200 Cycle 1/3 Octave Center Frequency Band, Fore/Aft Direction.

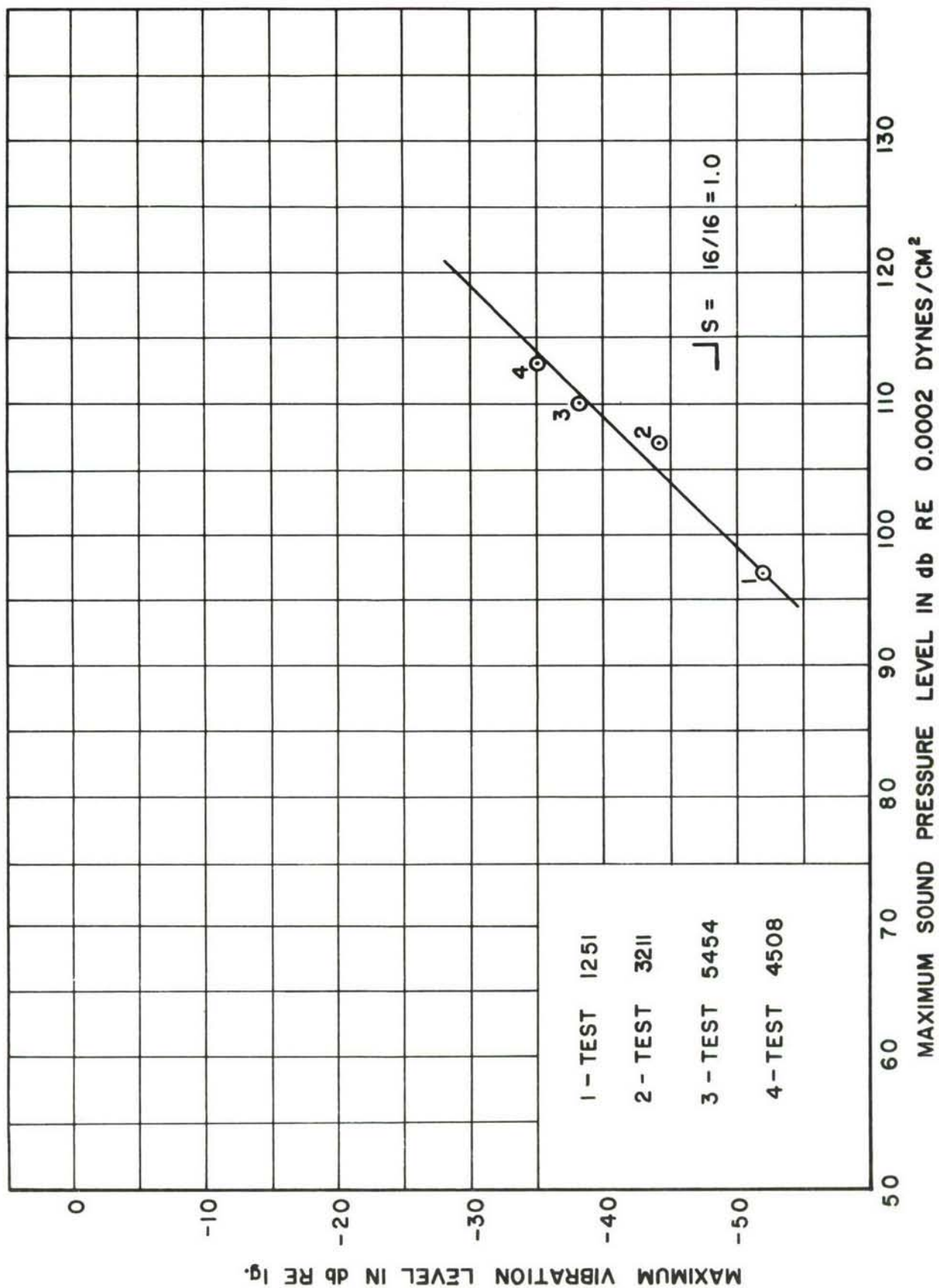


Figure 153. Maximum Vibration Level vs Maximum Sound Pressure Level, TLM 18 Antenna Dish, 100 Cycle 1/3 Octave Center Frequency Band, Lateral Direction.



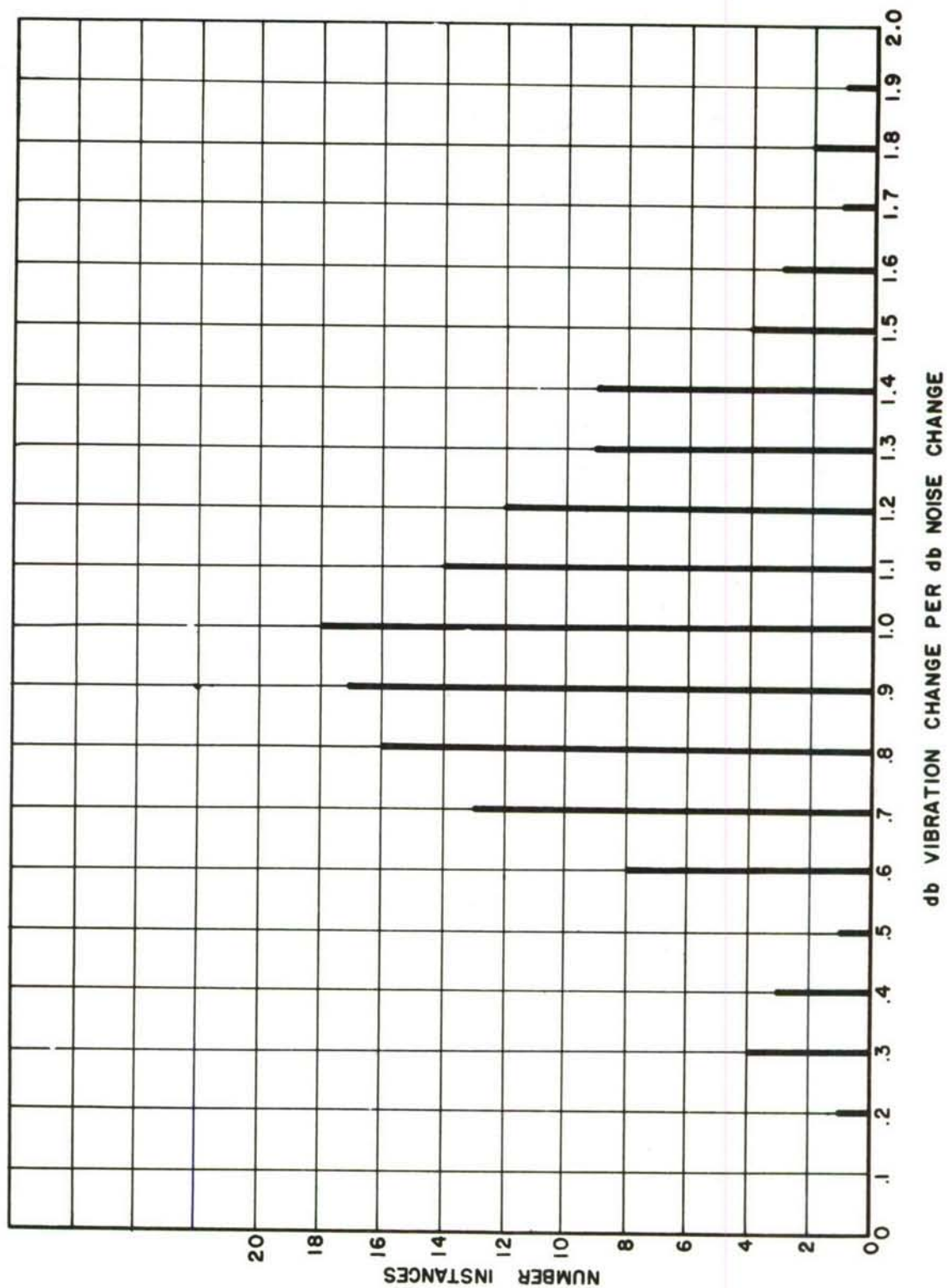


Figure 154. DB Vibration Change per db Noise Change: Results of 136 Measurements of the Maximum Vibration and Noise Produced at a Measurement Point During Various Missile Launches.

# TEST NO. 4508

## TEL 2, TRI-HELIX NO.4

### SOUND PRESSURE LEVEL vs. TIME

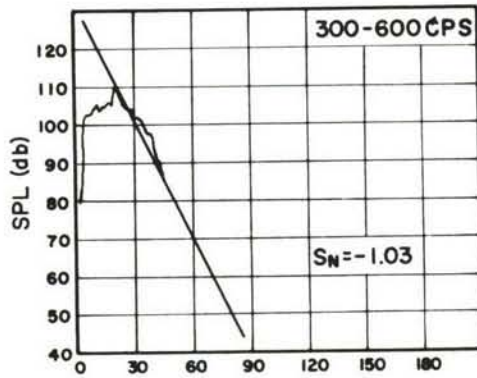


Figure 155.

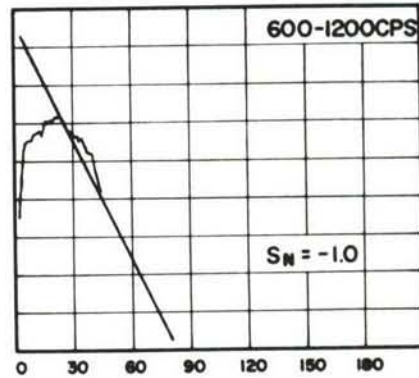
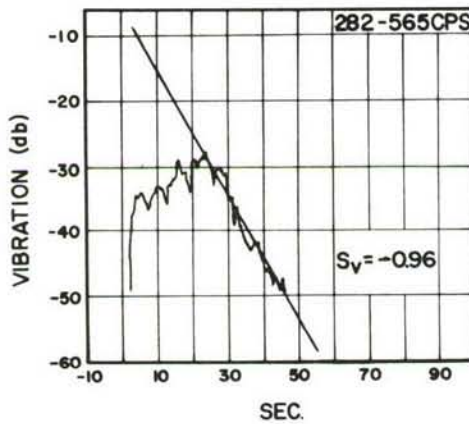


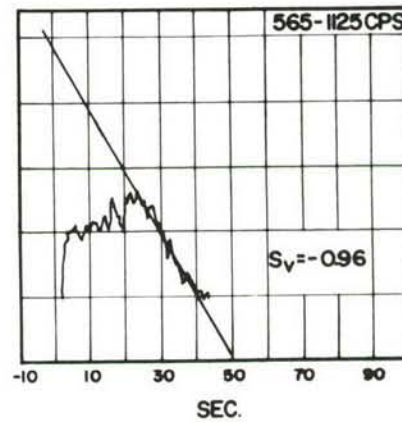
Figure 156.

### VIBRATION LEVEL vs. TIME



$$\frac{S_V}{S_N} = \frac{-0.96}{-1.03} = 0.93$$

Figure 157.



$$\frac{S_V}{S_N} = \frac{-0.96}{-1.0} = 0.96$$

Figure 158.

Typical Sound Pressure and Vibration Level Recordings  
vs. Time

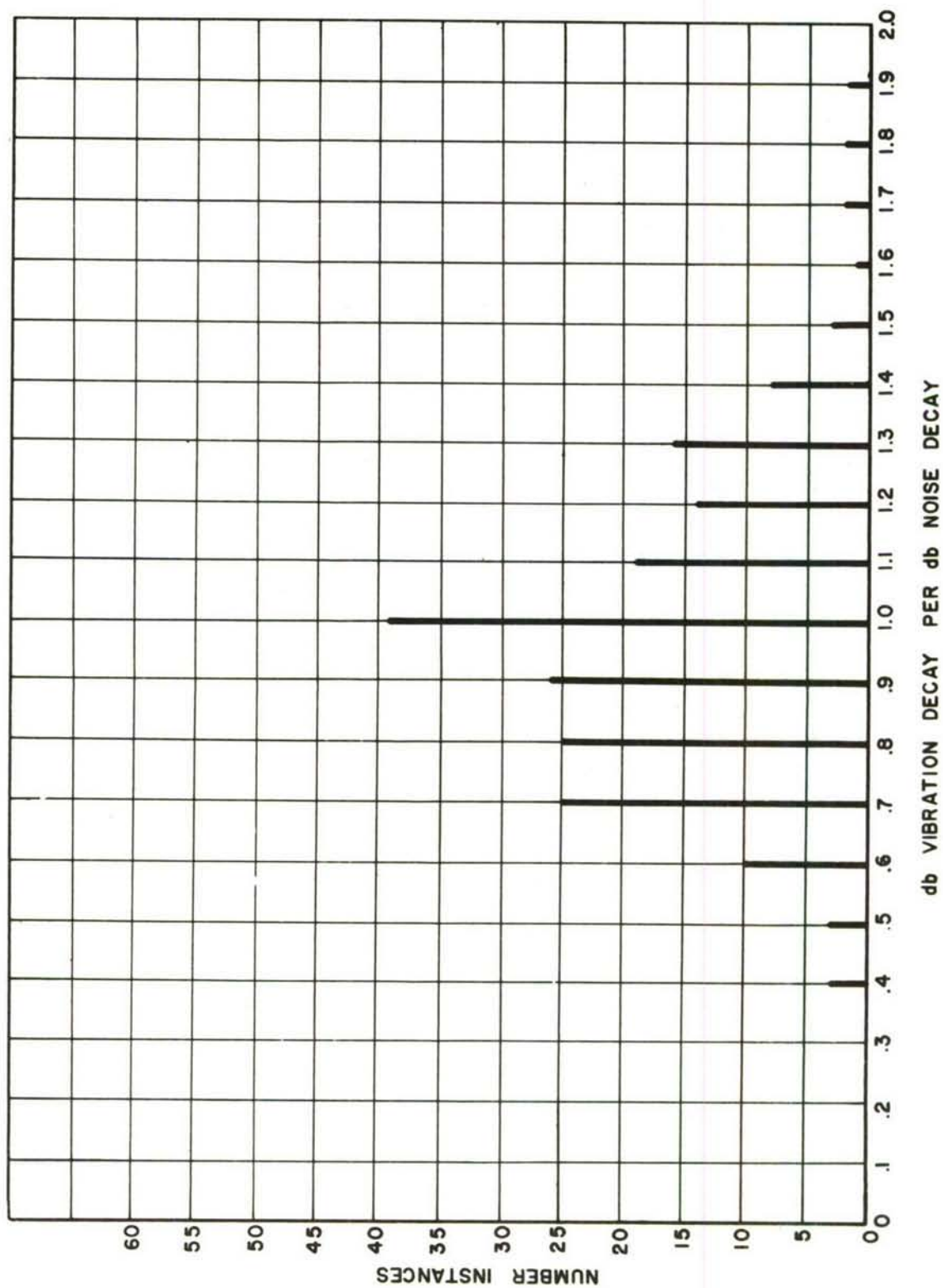


Figure 159. DB Vibration Decay per db Noise Decay: Results of 198 Measurements During Missile Launch.



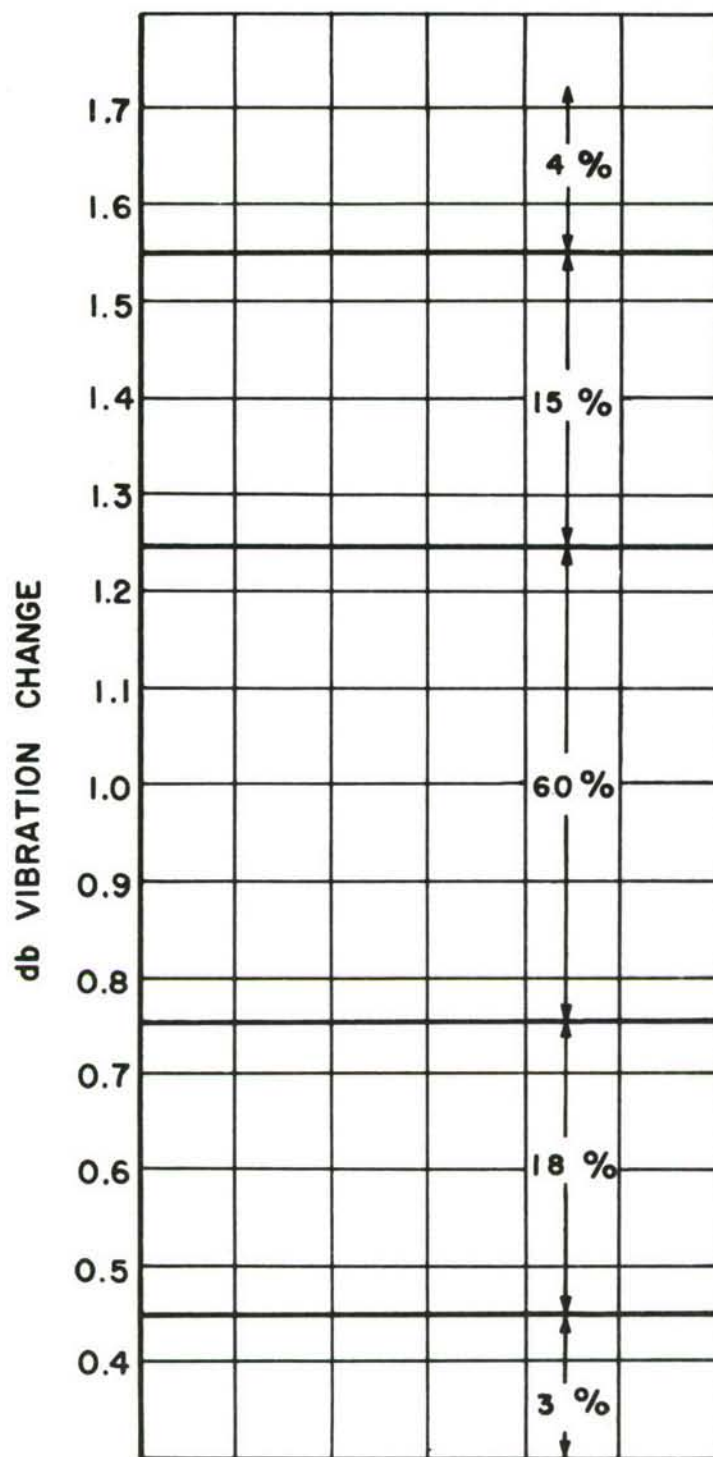


Figure 160. DB Vibration Level Change per db Noise Level Change: Accumulative Results of 334 Measurements Showing Percentage of Instances in Indicated Ranges.

Aeronautical Systems Division, Dir/Engineering  
Test, Environmental Criteria Br., Wright-  
Patterson AFB, Ohio.  
Rpt Nr ASD-TR-61-608, Vol II, ACOUSTIC NOISE  
AND VIBRATION STUDIES AT CAPE CANAVERAL  
MISSILE TEST ANNEX, VOLUME II, VIBRATION.  
Final report, Jan 63, 66 p., incl. illus.

Unclassified report

Acoustic-noise-induced vibrational effects  
upon seven antenna structures were recorded  
during fourteen missile launches at Cape  
Canaveral Missile Test Annex (CCMTA). Vibra-  
tional effects were recorded within the fre-  
quency range between 3 and 2000 cycles per

( over )

second. Maximum vibrations encountered per  
one-third octave frequency band are pre-  
sented in this report along with findings on  
the relationship of vibration levels to  
acoustic noise. All vibration levels measured  
in this test series were relatively low.  
changed in direct proportion to sound-pressure  
levels, and provided experimental sub-  
stantiation for predicting increases in  
structural acceleration levels based on pre-  
dicted increases in acoustic levels resulting  
from more powerful rocket engines.

1. Acoustic Noise &  
Vibration Effects  
during Missile  
Launches

- I. AFSC Project 1309  
Task 130905
- II. Robert P. Boyd
- III. Aval fr OTS
- IV. In ASTIA collection

Aeronautical Systems Division, Dir/Engineering  
Test, Environmental Criteria Br., Wright-  
Patterson AFB, Ohio.  
Rpt Nr ASD-TR-61-608, Vol II, ACOUSTIC NOISE  
AND VIBRATION STUDIES AT CAPE CANAVERAL  
MISSILE TEST ANNEX, VOLUME II, VIBRATION.  
Final report, Jan 63, 66 p., incl. illus.

Unclassified report

Acoustic-noise-induced vibrational effects  
upon seven antenna structures were recorded  
during fourteen missile launches at Cape  
Canaveral Missile Test Annex (CCMTA). Vibra-  
tional effects were recorded within the fre-  
quency range between 3 and 2000 cycles per

( over )

second. Maximum vibrations encountered per  
one-third octave frequency band are pre-  
sented in this report along with findings on  
the relationship of vibration levels to  
acoustic noise. All vibration levels measured  
in this test series were relatively low.  
changed in direct proportion to sound-pressure  
levels, and provided experimental sub-  
stantiation for predicting increases in  
structural acceleration levels based on pre-  
dicted increases in acoustic levels resulting  
from more powerful rocket engines.

1. Acoustic Noise &  
Vibration Effects  
during Missile  
Launches

- I. AFSC Project 1309  
Task 130905
- II. Robert P. Boyd
- III. Aval fr OTS
- IV. In ASTIA collection

Aeronautical Systems Division, Dir/Engineering  
Test, Environmental Criteria Br., Wright-  
Patterson AFB, Ohio.  
Rpt Nr ASD-TR-61-608, Vol II, ACOUSTIC NOISE  
AND VIBRATION STUDIES AT CAPE CANAVERAL  
MISSILE TEST ANNEX, VOLUME II, VIBRATION.  
Final report, Jan 63, 66 p., incl. illus.

Unclassified report

Acoustic-noise-induced vibrational effects  
upon seven antenna structures were recorded  
during fourteen missile launches at Cape  
Canaveral Missile Test Annex (CCMTA). Vibration  
effects were recorded within the frequency  
range between 3 and 2000 cycles per

( over )

second. Maximum vibrations encountered per  
one-third octave frequency band are presented  
in this report along with findings on  
the relationship of vibration levels to  
acoustic noise. All vibration levels measured  
in this test series were relatively low,  
changed in direct proportion to sound-pressure  
levels, and provided experimental substantiation  
for predicting increases in structural  
acceleration levels based on predicted  
increases in acoustic levels resulting  
from more powerful rocket engines.

1. Acoustic Noise &  
Vibration Effects  
during Missile  
Launches

- I. AFSC Project 1309  
Task 130905
- II. Robert P. Boyd
- III. Aval fr OTS
- IV. In ASTIA collection

Aeronautical Systems Division, Dir/Engineering  
Test, Environmental Criteria Br., Wright-  
Patterson AFB, Ohio.  
Rpt Nr ASD-TR-61-608, Vol II, ACOUSTIC NOISE  
AND VIBRATION STUDIES AT CAPE CANAVERAL  
MISSILE TEST ANNEX, VOLUME II, VIBRATION.  
Final report, Jan 63, 66 p., incl. illus.

Unclassified report

Acoustic-noise-induced vibrational effects  
upon seven antenna structures were recorded  
during fourteen missile launches at Cape  
Canaveral Missile Test Annex (CCMTA). Vibration  
effects were recorded within the frequency  
range between 3 and 2000 cycles per

( over )

second. Maximum vibrations encountered per  
one-third octave frequency band are presented  
in this report along with findings on  
the relationship of vibration levels to  
acoustic noise. All vibration levels measured  
in this test series were relatively low,  
changed in direct proportion to sound-pressure  
levels, and provided experimental substantiation  
for predicting increases in structural  
acceleration levels based on predicted  
increases in acoustic levels resulting  
from more powerful rocket engines.

1. Acoustic Noise &  
Vibration Effects  
during Missile  
Launches

- I. AFSC Project 1309  
Task 130905
- II. Robert P. Boyd
- III. Aval fr OTS
- IV. In ASTIA collection